ABSTRACT

Title of Thesis: FLAMMABILITY PROPERTIES OF CLAY-NYLON NANOCOMPOSITES

Xin Liu, M.S., 2004

Thesis Directed By: Professor James G. Quintiere
Department of Fire Protection Engineering

A Cone Calorimeter device has been used to measure the flammability properties of samples with different clay dispersion on the nanometer (molecular) scale. Specifically, chemical energy release rate, mass loss rate, and time to ignite (melt and char also) are measured. Samples consisting of pure Nylon 6 and Nylon with nano-clay additives up to 5 % are used in the study. In addition, the effect of thickness is considered for 1 to 24 mm. Data obtained over a range of radiant heat flux are analyzed to illustrate the effect of clay loading and thickness on heat of combustion, heat of gasification and ignition temperature.

FLAMMABILITY PROPERTIES OF CLAY-NYLON NANOCOMPOSITES

By

Xin Liu

Thesis submitted to the Faculty of the Graduate School of the
University of Maryland, College Park, in partial fulfillment
of the requirements for the degree of
Master of Science
2004

Advisory Committee:
Professor James G. Quintiere, Chair
Associate Professor James A. Milke
Associate Professor Andre Marshall

Acknowledgements

I would like to express my deepest thanks to Dr. James Quintiere, whose guidance and support made this research possible. Dr.Q is the greatest professor and advisor I've ever seen.

I would like to thank the Federal Aviation Administration for financial support of this project. I would like to thank Dr. Takashi Kashiwagi and the group at National Institute of Standards and Technology for all the samples, data and advice. They always gave me fast response and great help when I met trouble.

I would like to thank Dr. James A. Milke and Dr. Andre Marshall for being my committee member and correcting my thesis. I wish to thank all the faculty and staff of the Department of Fire Protection Engineering for the unending support during my two years study here.

Also, I would like to thank Joe for assistance in operating the equipment, Jonathan for correcting the grammar in my thesis, and Pock for always being patient and helping me whenever I met trouble. I would like to thank all the friends to give the support and happiness. I would like to thank my family for endless love. I would like to thank Haipeng for sharing every moment with me.

One page is not enough for expressing all my appreciation. I wish all of you a happy life and successful career.

Table of Contents

List of Tables

List of Figures

Nomenclature

a_p	pre-exponential factor
c_p	specific heat
d	sample thickness
E_a	activation energy
Δh_c	heat of combustion
k	thermal conductivity
$k\rho c$	thermal inertia
L	heat of gasification
m	mass
M	molecular weight
Q	heat release
t	time
T	temperature
X	mole fraction
X_c	char fraction
α	volumetric expansion factor
δ	vaporizing front
δ_T	thermal penetration depth
ε	emissivity
ρ	density
ϕ	oxygen depletion factor

Subscripts

a	air
ext	external
f	final
fl	flame
ig	ignition

int	initial
net	net
O_2	oxygen
p	pyrolysis
v	vaporization
peak	at the peak energy release rate
peak avg.	average of the peak energy release rate
overall avg.	average of the overall properties during steady, sustained burning

Superscripts

$\dot{X}$	per unit time
X''	per unit area
X'''	per unit volume
$\overline{X}$	average value

Chapter 1: Introduction

Composites consisting of organic polymer and small additives of inorganic aluminum silicate have shown significant improvements in many mechanical and physical properties. We are examining the additive montmorillonite (MMT) clay with nylon (PA-6). These samples have been formed as a nanocomposite in which there is a specific interaction between the clay platelet and the polymer. The objective of this study is to determine the effects of clay loading on flammability properties, and to address the effect of thickness that has been evident in previous work. For example, the study by Gilman et al. [1] at NIST, found that peak heat release rates (firepower) were reduced by adding clay, at a heat flux of 50 kW/m^2, for this nanocomposite. The NIST group found that the peak heat release rate dropped from about 2000 to 1200, 600, and 400 kW/m^2 with the addition of 2, 5 and 10% clay to the nylon (Fig.1.1).

However, these peaks were influenced by thickness (8 mm) with an insulated back-face. The insulated back-face caused heat to be stored in the sample and led to an increase in the firepower at the late burning stage. Other measurements of pure nylon, at 25 mm thickness, show a peak, (steady), heat release rate of about 600 kW/m^2 compared to 2000 kW/m^2 at 8 mm[2]. However, the data for the 8 mm specimens indicate a tendency to establish a plateau in their early burning also at about 600 kW/m^2. Therefore, thickness effects are interfering with an independent assessment

of the role of the clay agent. There is a need to sort out these effects and establish the direct influence of the clay.

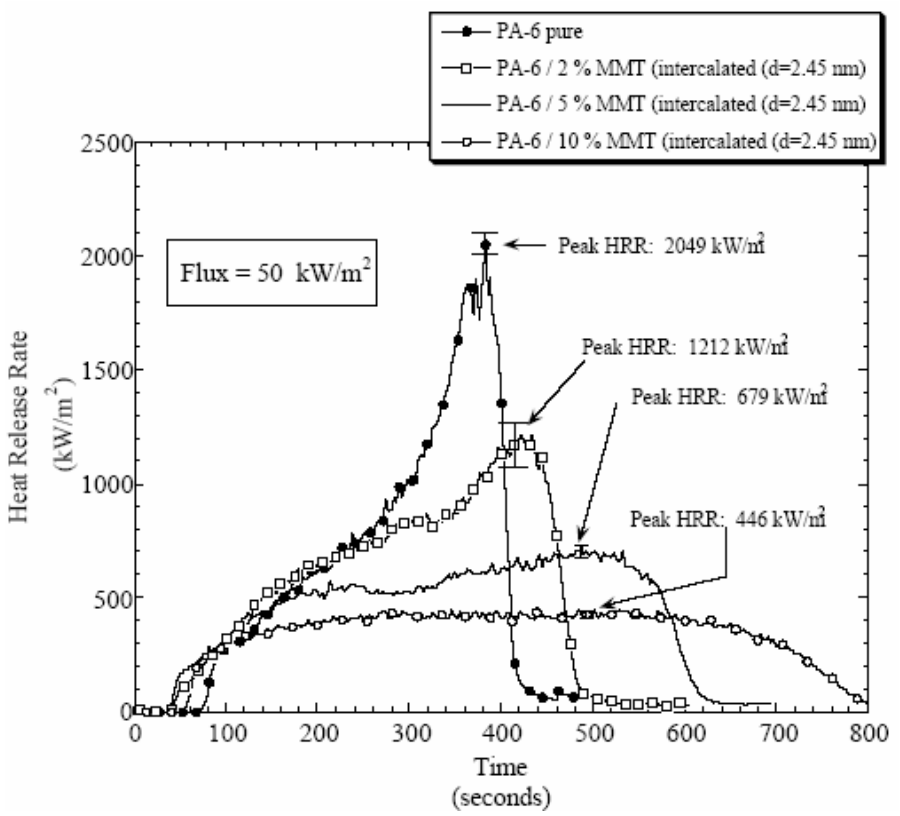

Fig. 1.1 Effects of clay content on heat release rate of 8 mm Nylon at 50 kW/m^2 [1]

It is clear that the clay affects the flammability characteristics of the nanocomposite. The measurement in this study will attempt to present these effects in terms of fire properties. These are the physical and chemical properties representative of the bulk polymer. In some cases they are approximate and are representative of idealized burning conditions. For example, they include the heat of combustion, Δh_c, – measured for the flaming state; the heat of gasification, L – representative of steady burning and ideally representing the enthalpies of phase change, and the heat capacity effect based on its supply temperature; thermal properties ($k\rho c$), the char fraction, X_c,

and the ignition temperature, T_{ig}. Gilman et al. [1] find the energy release rate decreases while there is no change in the heat of combustion, remaining at about 27 kJ/g. Giannelis [3] reports that an increase in thermal stability and a decrease in permeability can also be achieved by the addition of clay. Both of these characteristics can affect flammability by increasing the time to ignite and reducing the production of volatile fuel gases, accordingly. Indeed, this indicates that the clay additive is reducing the flow rate of volatiles while not affecting the combustion of the nylon. A Transmission Electron Microscopy (TEM) of a section of residue from PA-6-MMT shows 1 nm thick bands of carbonaceous-silicate char that were noticed to form on the burning samples[1]. Charring materials yield a lower mass loss rate due to the char left behind. Subsequently, this char will oxidize in a fire environment and yield additional energy.

For a thin burning sample, as it is depleted, its reduced thickness causes higher temperatures on its back surface. Thus, this reduced heat loss causes an increase in burning rate. This increase is not an inherent characteristic of the polymer, but an effect of thickness. On the other hand, the nanocomposites show a reduction of this tendency to increase burning at the end of the test, and this reduction appears to correlate with the MMT addition. The charring effects, induced by the MMT, are likely playing a role here. These are compensating actions between the tendency of the char to decrease burning, and the back-face insulation to increase burning. The general characteristic of thick charring materials to decrease in burning rate, falling as $1/t^{1/2}$ after an initial rise to a peak following ignition is not seen with the addition of

the MMT [4]. Hence, the effects of char in the 8 mm tests appear more complicated, or affected by thickness.

Another factor observed in the Gilman et al. study [1] is that as the MMT additive is increased, the overall total energy available to combustion appears invariant. Thus, the burning time is increased as the MMT is increased. For these same samples, the time to ignition is not necessarily changed. The ratio of the time to ignite (t_{ig}) and burn time (t_b) is significant in flame spread. Indeed, the burn time can be reduced in vertical spread by melting and dripping. This is a characteristic of Nylon and other thermoplastics. These factors may be influential in small-scale tests such as the vertical application of UL-94. It has been reported that PA-6 at 5% MMT receives a V-2 rating in UL-94 (meaning the cotton below was ignited from flaming drips), and PA-6 at 10 % MMT failed the UL-94 (meaning that it burned for more than 30 s). The latter could be explained by char inhibiting the drips, but holding more of the polymer in place and hence a longer burning time. The passing of this test by the pure nylon might be due to its increased tendency to melt. Hence, the addition of the MMT can have various flammability outcomes depending on the fire process: ignition, spread, or static burning.

This study will examine the flammability in the Cone Calorimeter for nylon-MMT samples of 0, 2 and 5 %. Thickness will range over 1.6, 3.2, 4 and 8 mm, but only the latter two sizes will be reported now. The burning data in the Cone will range over

heat fluxes from the minimum needed for ignition to about 60 kW/m^2. Properties will be reduced from these data by analysis, and will include

1. Heat of combustion, Δh_c: the energy released in combustion per unit mass lost.
2. Critical heat flux for ignition: the threshold of radiant heat flux for piloted ignition.
3. Ignition temperature, T_{ig}: the estimated surface temperature at ignition.
4. Thermal inertia, $k\rho c$: the effective thermal property for a "thick" material that indicates the ability to conduct heat into the material.
5. Heat of gasification, L: the energy required to gasify the material into fuel.

The ratio $\Delta h_c/L$ is a measure of the energy release rate of the material given equal flame heat flux. The parameter $k\rho c(T_{ig} - T_{initial})^2$ is proportional to the ignition time for the same applied heat fluxes. The flame spread rate is inversely proportional to this quantity for the same flame heating conditions. These properties terms relate to fire hazard potential, while the individual properties can give some indication of the mechanistic role of the MMT.

Chapter 2: Experimental Set-up and Procedure

2.1 Experimental Set-up

The Cone Calorimeter is a commonly used device utilized to measure the mass loss rate per unit area ($\dot{m}''$) and the heat release rate per unit area ($\dot{Q}''$) for a given constant external radiative heat flux. Experiments for the nanocomposites materials were performed using a radiant cone heater assembly. The apparatus, shown in Fig.2.1.1, consisted of a cone heater, a load cell, an electric arc igniter. A computer program built by Labview (Fig.2.1.2) was utilized as the data acquisition system.

2.2 Materials and sample preparation

Samples consisting of pure Nylon 6, Nylon with 2% and 5 % Nano-Clay additives were used in the study. Pure Nylon 6 is also called polyamide 6 (PA6). They are PA6 homopolymer (molecular mass $M_W \approx 15{,}000$ g/mol, UBE 1015B), PA6 ($M_W \approx 15{,}000$) with montmorillonite (MMT) of 2% by mass fraction (UBE 1015C2), and PA6 ($M_W \approx 18{,}000$) with MMT of 5% by mass fraction (UBE 1018C5). All samples were dried for 2h at 75 ^{o}C, and molded at 280 ^{o}C. The disks are 75 mm diameter with thickness of 1.6 mm, 3.2 mm, 4 mm, 8 mm [5]. This is obvious, given that 4 thicknesses are included.

Sample was wrapped by aluminum foil to prevent melting. The back side of the sample was insulated by 1 inch thick Kaowool board (Type M) to minimize heat loss effects.

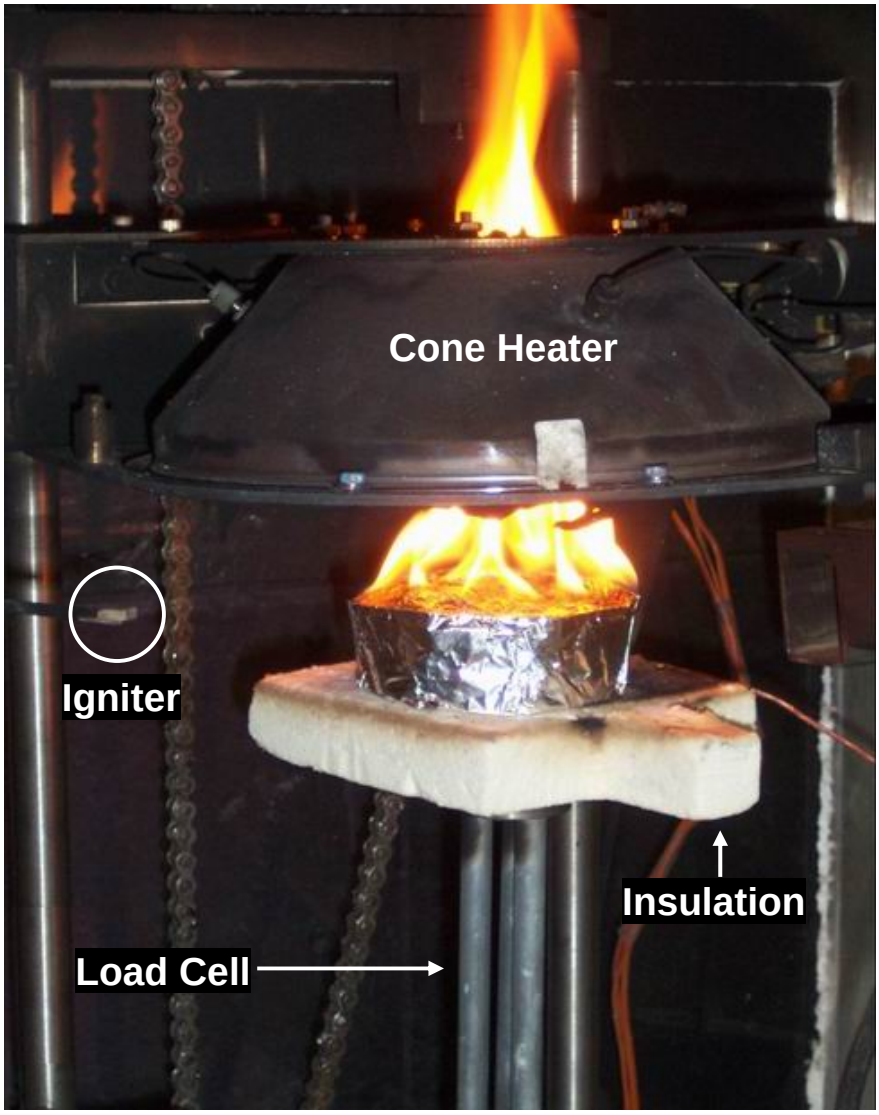

Fig. 2.1.1 Experimental system

2.3 Experimental Procedure

The experimental procedure consisted of exposing a sample, in the horizontal orientation, to a constant external irradiance from the cone heater. The initial incident heat flux was determined using a heat flux gauge. Each time before testing, the heat

flux was checked in the same location above the center of the sample. The experiment was not started until a constant heat flux recording was obtained.

The test procedure consisted of the following steps:

(1) Start data acquisition system.

(2) Cover the sample surface by an aluminum sheet.

(3) Put the sample onto the metal holder of the cone.

(4) Remove the aluminum sheet quickly and start timing. The aluminum sheet prevents the radiation heat to the sample before the timing starts.

Fig. 2.1.2 Data acquisition system built by Labview

In addition, the electric arc igniter was applied above the sample, when the sample surface started releasing fuel gas. The igniter, located approximately 1 cm above the surface of the sample, was used as a pilot ignition source.

The time to piloted ignition was measured by a stop watch. The ignition time is defined as the time at which a continuous flame is supported on the material surface. In some cases, flashing occurred on the surface before a sustained flame was observed. However, the ignition time was taken only at the time the entire surface was covered by flame.

The mass loss of the samples was measured by a load cell. The mass loss readings were recorded every second by the data acquisition program.

Chapter 3: Experiment Observations

3.1 Burning behavior

The clay loading for a sample affects the burning process. The external heat flux from the heater of the cone ranged from 18 kW/m^2 to 56 kW/m^2 for testing the samples.

3.1.1 Nylon

For high heat flux (above 30 kW/m^2), the pure Nylon sample exhibited a melting like behavior. When the heater is on, the sample surface starts bubbling. Evaporative fuel gas keeps coming out. When the concentration of fuel gas reaches the lower flammable limit, it is ignited by the electric arc igniter. The whole piece is swelling under the external heat flux from the Cone heater and the flame heat flux. The center part may rise due to the swelling (shown in Fig. 3.1.1), then recedes because of sample melting. It keeps melting until the whole piece turns to liquid phase. It burns like a liquid until all fuel is used up. After burning, nothing is left. The following pictures show the burning process of 4 mm nylon under 56 kW/m^2 external heat flux. The order is from early stage burning with the center part rising (Fig. 3.1.1) $\rightarrow$ Steady burning (Fig. 3.1.2) $\rightarrow$ Extinguished (Fig. 3.1.3).

Fig.3.1.1 4mm Nylon burning under 56 kW/m^2
Center rises due to swelling

Fig.3.1.2 4mm Nylon burning under 56 kW/m^2
Liquid-like steady burning

Under low heat flux, the decomposition is relatively slow. The surface will oxidize first, form a thin carbonaceous skin. Fig. 3.1.4 shows 3.2 mm Nylon under 16 kW/m^2 external heat flux. No ignition occurs at that heat flux, but oxidation still happens; a thin carbonaceous skin is formed.

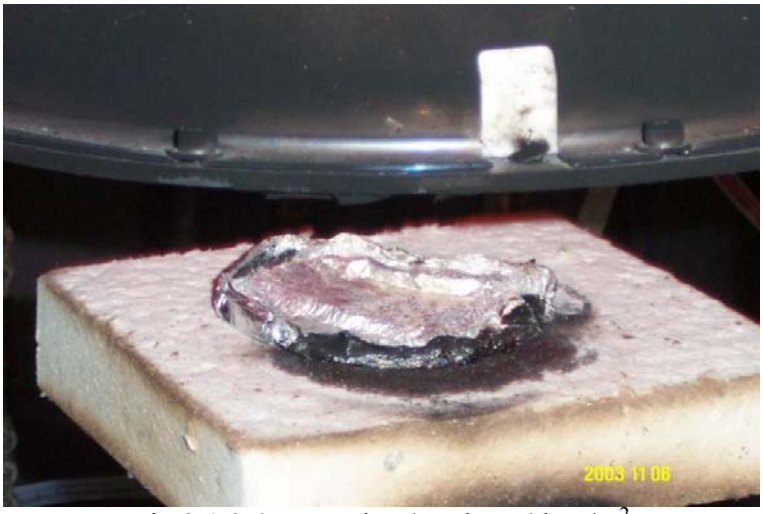

Fig.3.1.3 4mm Nylon6 under 56 kW/m^2
After burning

Fig.3.1.4 3.2mm Nylon under 16 kW/m^2
No ignition

3.1.2 Nylon+ clay (MMT)

For samples with clay, the time to ignite is increased as the clay loading is increased. The carbonaceous skin due to oxidation is always formed before ignition. For high heat flux, at about 50 kW/m^2, the char skin is relative thin and weak, evaporated fuel

gas can still go through the skin. When ignition occurs, the flame can cover the whole surface. The burning of 24 mm Nylon+2%clay under 50 kW/m^2 is shown in Fig.3.1.5.

Fig. 3.1.5 24mm Nylon+2%clay burning under 50 kW/m^2
Just after ignition

For lower heat fluxes (less than 30 kW/m^2), due to a longer ignition time, the char skin forms before ignition, and it is thicker and stronger. Before ignition, fuel gas cannot go through the char skin; it accumulates underneath the skin. A big bubble is formed. The whole sample looks like a "muffin". As the bubble keeps increasing, the char skin cannot cover the whole sample any more. There are leaks at the edge of skin. Dense fuel gas, due to its accumulation, is then released. It is sufficient to be ignited. Flame attachment at these leaks consumes fuel. The gas bubble shrinks. The char skin then falls back. Sometimes, it can seal the leaks. The same process will happen again until the gas evaporating rate is high enough for a flame at the edge to be supported. Flame heat flux also offers extra heating to the sample, which speeds up the melting and evaporating. The spreading flame will extend the leak along the edge or maybe to some part of the skin. The whole piece can be completely covered by

flame finally. But the carbonaceous skin is not flammable. It remains until all the fuel shielded under it is used up. Fig.3.1.6 shows the big bubble formed before ignition. Fig.3.1.7 shows the flame burning at edge. They are 8 mm Nylon+2%clay samples heated under 34 kW/m^2.

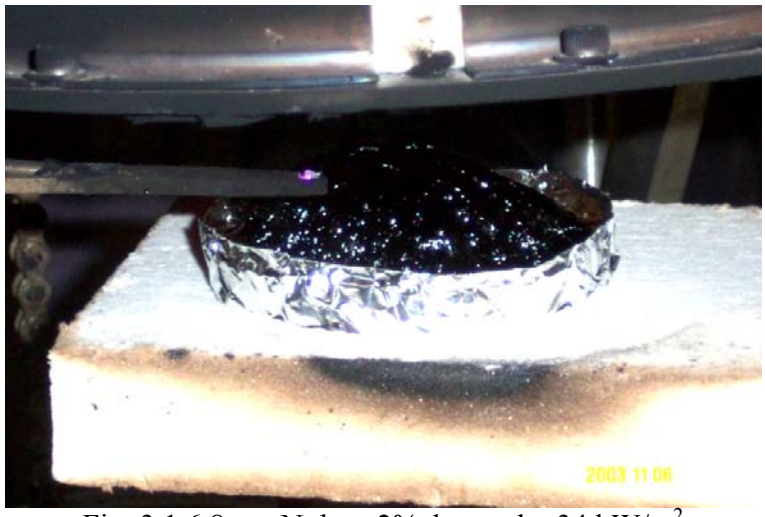

Fig. 3.1.6 8mm Nylon+2%clay under 34 kW/m^2
Before ignition

Fig. 3.1.7 8mm Nylon+2%clay under 34 kW/m^2
Burning at leaks of edge

3.2 Residue

Samples consisting of different clay additive have different amount of residue left. For pure Nylon, no residue is left after burning. A char skin may be formed under low heat fluxes, but it is very thin. The skin is consumed by the flame.

For Nylon with 2% clay, at the end of burning, the char skin remains. Under that skin, on the bottom of the aluminum cup containing the sample piece, only small pieces of char remain. It is nearly hollow between the top char skin and the bottom of the aluminum cup. A cut of the side of the aluminum cup shows the residue inside as clearly seen in Fig.3.2.1.

Fig. 3.2.1 24mm Nylon+2%clay under 50 kW/m^2
Residue after burning

For Nylon with 5% clay, char skin formed before ignition remains on top. But as the clay percentage is increased, more char is left. It fills the space between top skin and the bottom of the cup. To show the inside of the sample clearly, the cup was again cut and shown in Fig.3.2.2.

Fig. 3.2.2 24mm Nylon+5%clay under 50kW/m^2
Residue after burning

Chapter 4: Results and Analysis

4.1 Experimental Results

4.1.1 Specimen Mass (g)

The mass is measured by the load cell of the Cone and recorded by a Labview data acquisition program. Fig. 4.1.1 shows the sample mass changing with time.

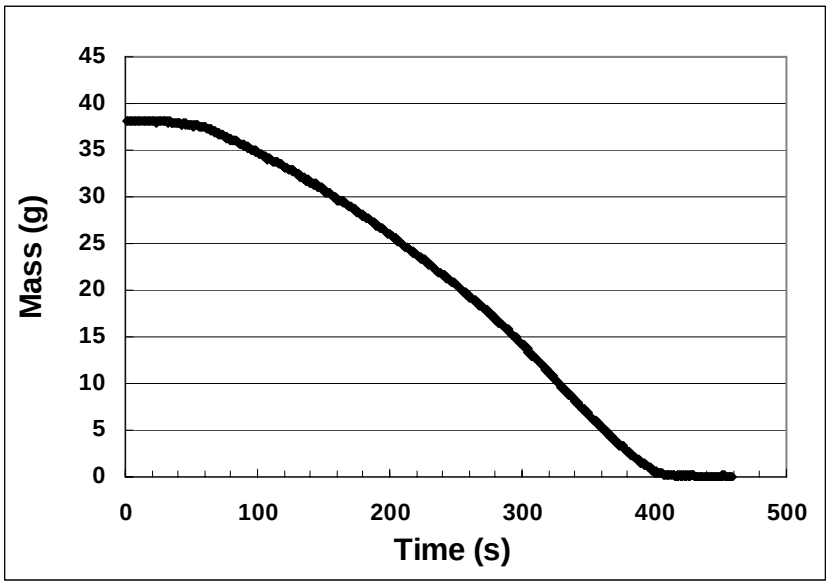

Fig. 4.1.1 Mass curve of 8mm Nylon+2%clay under 55kW/m^2

4.1.2 Mass Loss Rate (g/s)

In order to get mass loss rate $\dot{m} = \frac{dm}{dt}$, which is the numerical derivative of mass-time data, a 3-point interpolation formula (See Eq.(4.1)) is used [6].

$$\frac{dy}{dx} = \frac{1}{h}(\Delta y_n - \frac{1}{2}\Delta^2 y_n + \frac{1}{3}\Delta^3 y_n - \frac{1}{4}\Delta^4 y_n + \cdots)$$

$$\Delta y_n = y_{n+1} - y_n$$

$$\Delta^2 y_n = \Delta y_{n+1} - \Delta y_n = y_{n+2} - 2y_{n+1} + y_n$$

$$\Delta^3 y_n = \Delta^2 y_{n+1} - \Delta^2 y_n = y_{n+3} - 3y_{n+2} + 3y_{n+1} - y_n$$

… … … … … … …

3-point

$$\dot{m}_i = \frac{dm_i}{dt} = \frac{1}{t}(-0.5m_{i+2} + 2m_{i+1} - 1.5m_i) \tag{4.1}$$

t: time interval

Also 4-point and 5-point interpolation formulas were tried. Fig. 4.1.2 shows that the 3-point formula is smoother than the other two. Therefore, 3-point formula was used in the analysis.

4-point

$$\dot{m}_i = \frac{dm_i}{dt} = \frac{1}{t}(\frac{1}{3}m_{i+3} - \frac{3}{2}m_{i+2} + 3m_{i+1} - \frac{11}{6}m_i)$$

5-point

$$\dot{m}_i = \frac{dm_i}{dt} = \frac{1}{t}(-\frac{1}{4}m_{i+4} + \frac{4}{3}m_{i+3} - 3m_{i+2} + 4m_{i+1} - \frac{25}{12}m_i)$$

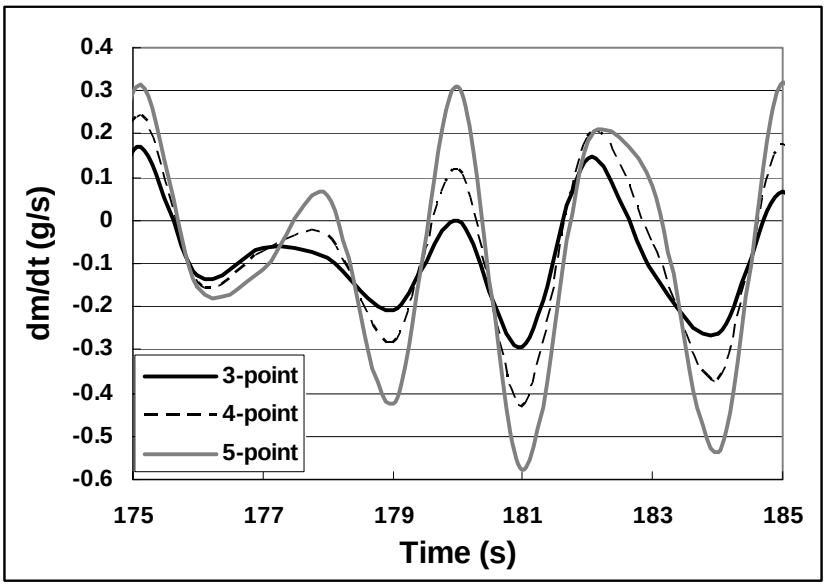

Fig. 4.1.2 Mass loss rate of 8mm Nylon+2%clay under 55kW/m^2
Comparison of different interpolation formulas

4.1.3 Mass Loss Rate per Unit Area (g/m^{2}s)

$$\dot{m}'' = \frac{\dot{m}}{Area} \tag{4.2}$$

Even though the 3-point interpolation formula was chosen to get the derivative, $\dot{m}''$ vs. time curve shown in Fig. 4.1.3 is still noisy. Therefore, a moving average value is needed to show the trend more clearly.

A comparison of a 5 points average, 9 points average and 19 points average are shown in Fig. 4.1.4. A 19 points moving average can clearly show the trend. Therefore, the 19 points average was used for all data.

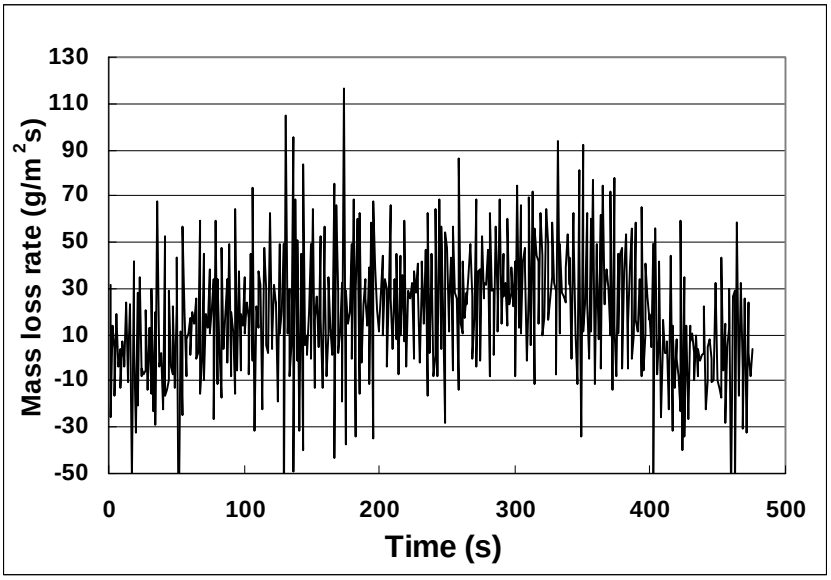

Fig. 4.1.3 Mass loss rate of 8mm Nylon+2%clay under 55kW/m^2
Before moving average

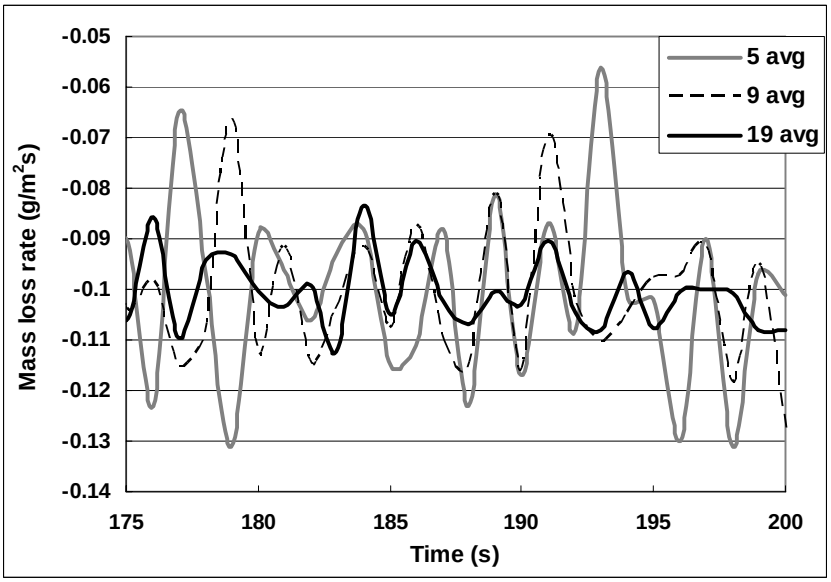

Fig. 4.1.4 Mass loss rate of 8mm Nylon+2%clay under 55kW/m^2
Moving average comparison

After using the 19 points moving average, the trend of the mass loss rate per unit area is relatively smooth (See Fig. 4.1.5).

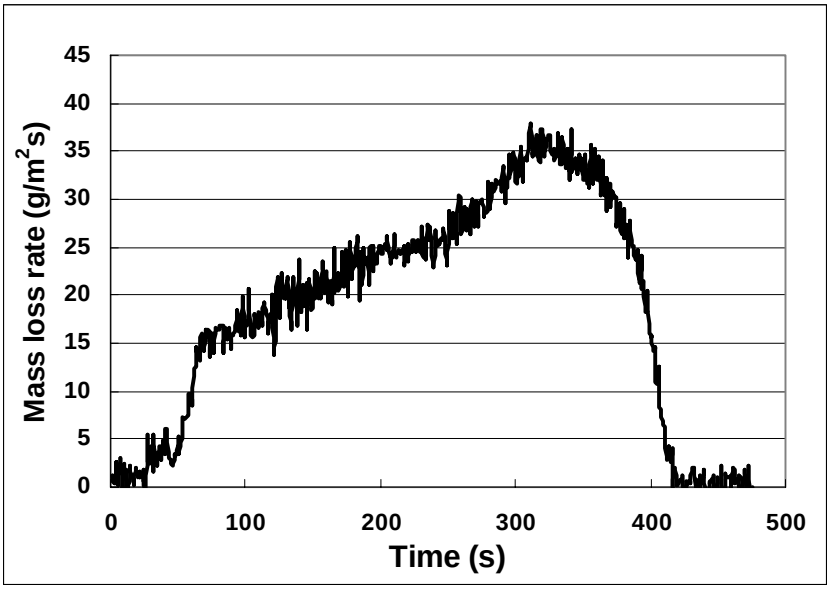

Fig. 4.1.5 Mass loss rate of 8mm Nylon+2%clay under 55kW/m^2

Fig. 4.1.6 shows mass loss rate per unit area of the Nylon+5%clay for different thickness under 53+/-3 kW/m^2. The peak value decreases with the increasing thickness.

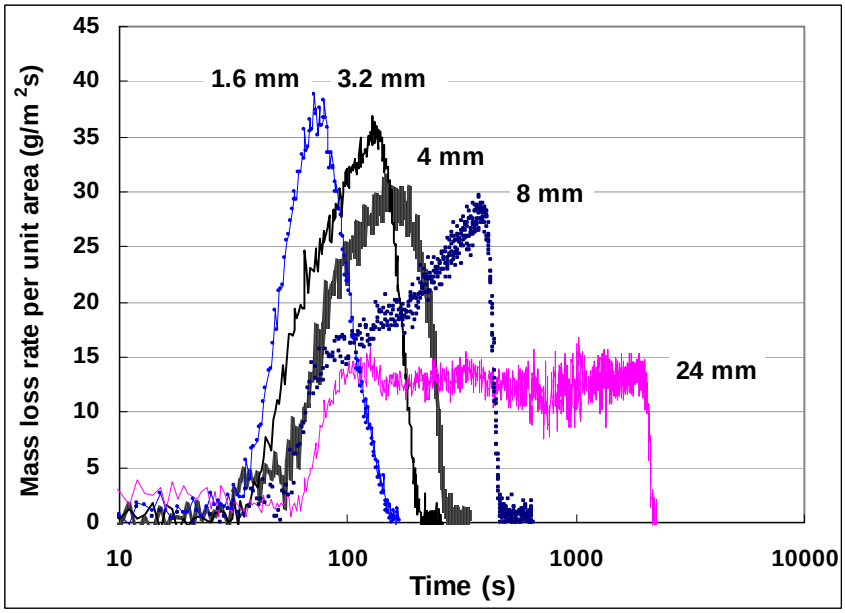

Fig. 4.1.6 Mass loss rate curves of Nylon+5%clay with different thickness under 53+/-3 kW/m^2

4.1.4 Oxygen Concentration (%)

The oxygen concentration is measured by a "Combi-Analyzer" oxygen sensor ULTRAMAT/OXYMAT 6 from SIEMENS.

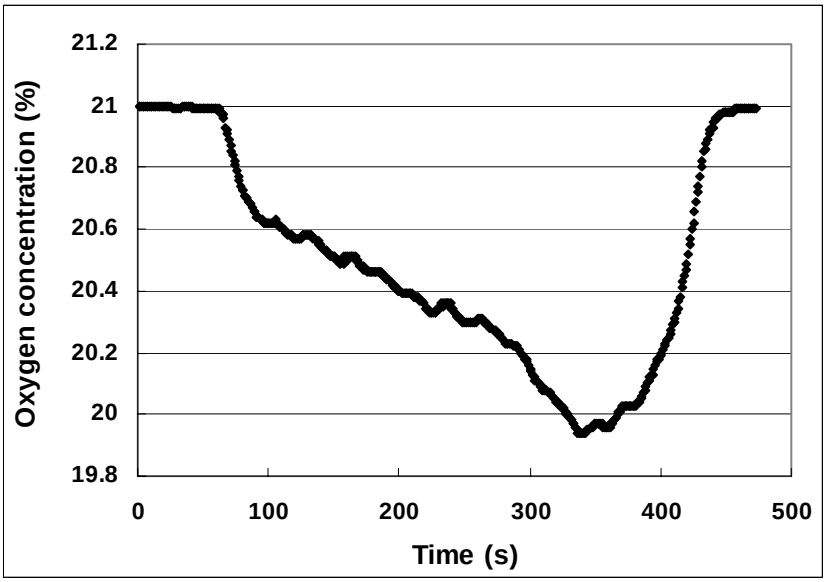

Fig. 4.1.7 Oxygen concentration curve of 8mm Nylon+2%clay under 55kW/m^2

4.1.5 Heat Release Rate per Unit Area (kW/m^2)

The rate of heat release is determined by measurement of the oxygen consumption as determined by the oxygen concentration and the flow rate in the exhaust product stream.

In the test, water vapor (removed by a cooling unit and a moisture sorbent) and CO_2 (removed by a chemical sorbent) must be removed from the exhaust gas sample stream before O_2 is measured at the sensor. The oxygen sensor is the "Combi-Analyzer" ULTRAMAT/OXYMAT 6 from SIEMENS. As shown in Fig. 4.1.8, all of

the combustion products are collected and removed through an exhaust duct. Both flow rate and composition of the gases are measured.

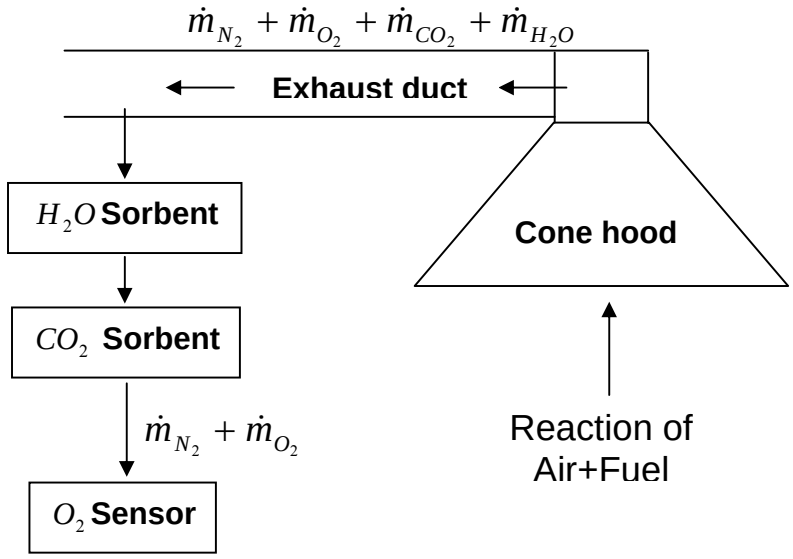

Fig. 4.1.8 Equipment arrangement for the O_2 measurement

Since the sample gas only consists of O_2 and N_2, the standard[7, 8] gives the heat release rate (firepower) as:

$$\dot{Q} = \Delta h_{O_2} \left[\frac{\phi}{1 + \phi(\alpha - 1)} \right] \dot{m}_e \frac{M_{O_2}}{M_a} X^0_{O_2} (1 - X^0_{H_2O} - X^0_{CO_2}) \tag{4.3}$$

$$\text{with } \phi = \frac{X^0_{O_2} - X_{O_2}}{(1 - X_{O_2}) X^0_{O_2}} \tag{4.4}$$

where ϕ=oxygen depletion factor

α=volumetric expansion factor

M_{O_2}=molecular weight of oxygen (28g/mol)

M_a =molecular weight of the combustion air (29g/mol for dry air)

$X_{O_2}^0$ = initial reading from the oxygen analyzer.

X_{O_2} = final reading from the oxygen analyzer.

$X_{H_2O}^0$ =mole fraction of H_2O in the incoming air

$X_{CO_2}^0$ =mole fraction of CO_2 in the incoming air

$X_{H_2O}^0$ and $X_{CO_2}^0$ are small and negligible.

After simplification:

$$\dot{Q} = \frac{\Delta h_c}{r_{O_2}} \dot{m}_e \left(\frac{M_{O_2}}{M_a}\right) \frac{X_{O_2}^0 - X_{O_2}}{\alpha - \left(1 + \frac{\alpha - 1}{X_{O_2}^0}\right) X_{O_2}} \tag{4.5}$$

Generally $\frac{\Delta h_c}{r_{O_2}}$ =13.1 kJ/g, $\frac{M_{O_2}}{M_a}$=1.10, $X_{O_2}^0 = 0.21$

In the literature such as ASTM E1354-99, the particular value for the expansion factor α is not specified, but the heat release equation is presented with an average value for the expansion factor ($\alpha = 1.105$).

In a more detailed analysis (See Appendix A), I used the same oxygen consumption measurement method to determine the heat release rate equation with consideration of stoichiometric chemical reactions for many materials. By comparing the new heat release equation with Eq.(4.5), I can show how the expansion factor, α, and how it varies for materials. The derivation is explained in the Appendix A, and the result is:

$$\dot{Q} = \frac{\Delta h_c}{r_{O_2}} \dot{m}_e \left(\frac{M_{O_2}}{M_a}\right) \frac{X_{O_2}^0 - X_{O_2}}{1 + \frac{Y_{O_2,\infty}}{r_{O_2}} - \frac{r_{CO_2} + r_{H_2O}}{r_{O_2}} \left(\frac{M_{O_2}}{M_a}\right) X_{O_2}} \tag{4.6}$$

Comparing Eq.(4.5) and Eq.(4.6) shows the only difference is the denominator. In the ASTM literature, α=1.105 and $(1+\frac{\alpha-1}{X_{O_2}^0})$=1.5. For my analysis of different fuels, it is shown that average values of the corresponding terms $\alpha \equiv 1 + \frac{Y_{O_2,\infty}}{r_{O_2}}$, and $1 + \frac{\alpha - 1}{X_{O_2}^0} \equiv \frac{r_{CO_2} + r_{H_2O}}{r_{O_2}} \left(\frac{M_{O_2}}{M_a}\right)$ for a range of materials is 1.08 and 1.44, respectively. Therefore there is not much difference. However, for a specific fuel, it is easy to get the chemical properties, and the second equation gives a more accurate result. For the current test, the samples are nylon with different clay distribution. Therefore, I used the standard heat release equation to be consistent with previous literature results for the nylon nanocomposites.

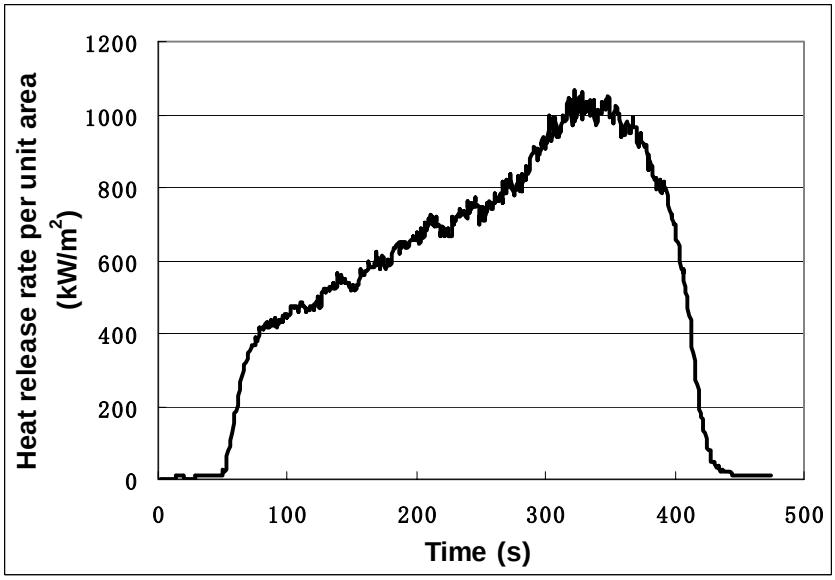

Fig. 4.1.9 Heat release rate per unit area of 8 mm Nylon+2%clay under 55 kW/m^2

Heat release rate per unit area curve of 8mm Nylon+2%clay under 55 kW/m^2 is shown in Fig. 4.1.9 as an example.

Under the same external heat, the curves for different thickness of Nylon+5%clay are shown in Fig. 4.1.10.

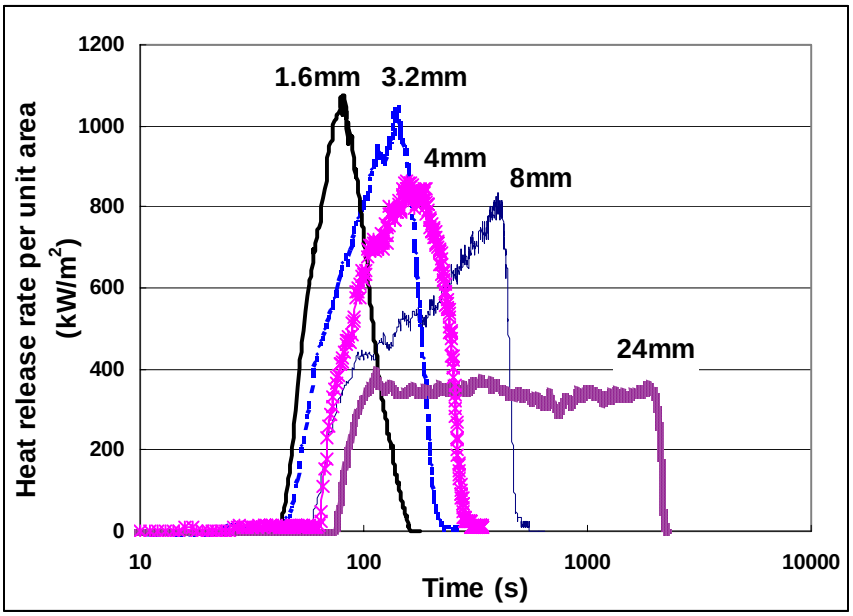

Fig. 4.1.10 Heat release rate per unit area of Nylon+5%clay with different thickness under 53+/-3 kW/m^2

4.1.6 Total Energy Release (MJ/m^2)

The total energy release is the amount of energy released over the duration of the test. It can be calculated by integrating the heat release rate over that period (See Eq.(4.7)).

$$Q''_{total} = \int \dot{Q}'' dt \tag{4.7}$$

Fig.4.1.11 shows the total energy release for each time of an 8mm Nylon+2%clay sample under 55kW/m^2. For each time, it is the integration of heat release rate from the beginning to that point.

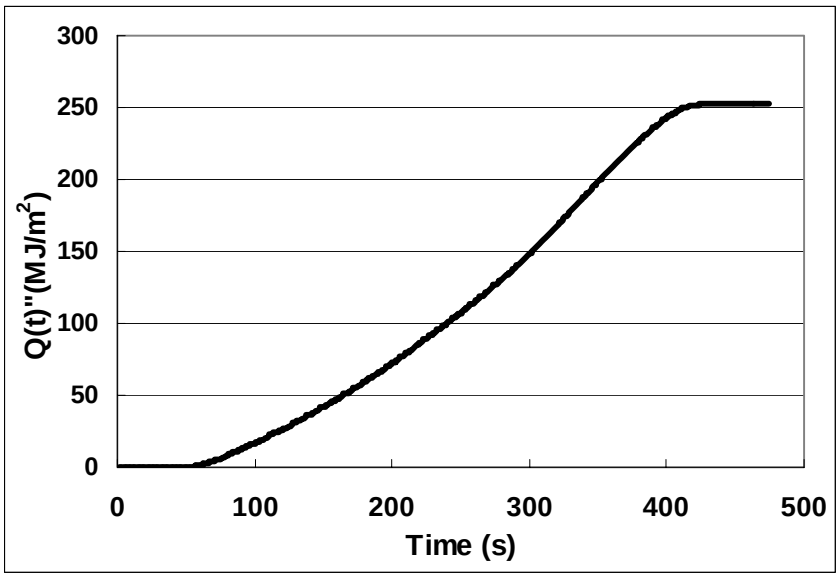

Fig. 4.1.11 Total energy release of 8mm Nylon+2%clay under 55kW/m^2

The samples have the same surface area, but the different thickness. Thicker sample means that more fuel can be burned and more energy can be released. In order to eliminate the thickness factor, it can be expressed in terms of a unit volume (Q''_{total}). The total energy per unit volume is calculated by

$$Q'''_{total} = \frac{Q''_{total}}{d}, \tag{4.8}$$

where d is the sample thickness.

AS shown in Fig.4.1.12, the total energy release per unit volume is independent of the incident heat flux. The addition of clay does not affect the total energy release much. It is nearly invariant.

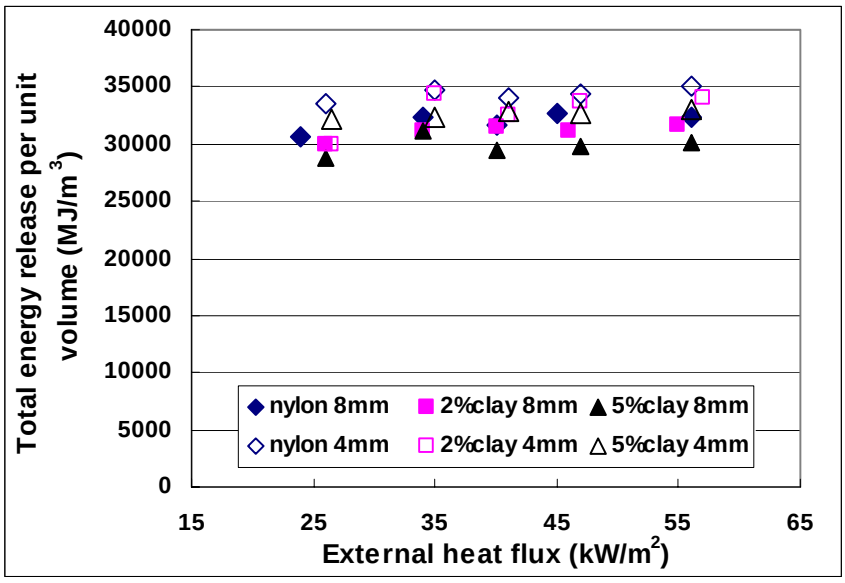

Fig. 4.1.12 Total energy release per unit volume of different samples under different external heat flux

4.2 Thermal properties

4.2.1 Heat of Combustion Δh_c

The heat of combustion is the amount of energy released as one mole of a given substance is burned in the presence of oxygen. It is defined as the positive value of enthalpy change per unit mass or mole of fuel reacted at 1 atm and in which the temperature of the system before and after the reaction is 25 ^{o}C[9].

The Cone Calorimeter standard [10] specifies the time-varying heat of combustion value to be calculated by $\Delta h_c = \frac{\dot{Q}''(t)}{\dot{m}''(t)}$, which is defined as the rate of energy produced divided by the sample mass loss rate.

$\dot{Q}''(t)$ Heat release rate per unit area (kW/m^2)

$\dot{m}''(t)$ Mass loss rate per unit area (g/m^{2}s)

Fig. 4.2.1 shows the heat of combustion, mass loss rate per unit area, heat release rate per unit area of 8 mm Nylon+2%clay under 55 kW/m^2.

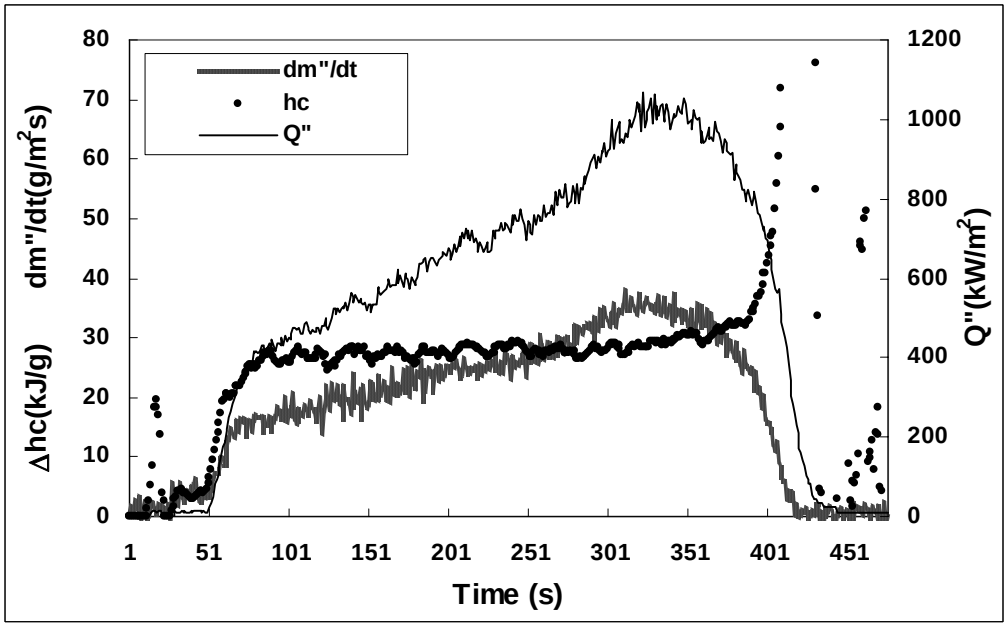

Fig. 4.2.1 Mass loss rate, heat of combustion and heat release rate of 8 mm Nylon+2% clay under 55 kW/m^2

4.2.2 Peak Average Heat of Combustion

The "peak average" value is intended to represent an energy release rate that is more consistent with steady burning as opposed to an instantaneous maximum value, or the

average of the entire burning process. Here, two "peaks" will be considered. The heat of combustion curve appears to reach a plateau (first peak), but may continue to increase due to the thickness effect (second peak). For some cases, two peaks are clearly seen. For the other cases, the first peak is not that clear. For this analysis, the *first peak average* value is the average over the perceived peak period. The *second peak average* value is estimated from an average peak energy release rate that occurs over a time period that continuously includes values 20% below the peak value of $\dot{Q}''$ [4]. The "peak average" is taken to be an integrated average of the measured values over this time period. This is illustrated, for the heat of combustion, by the Eq.(4.9)and Fig. 4.2.2.

$$\Delta\bar{h}_{c,peakavg} = \frac{1}{t_2 - t_1}\int_{t_1}^{t_2} \Delta h_c dt \tag{4.9}$$

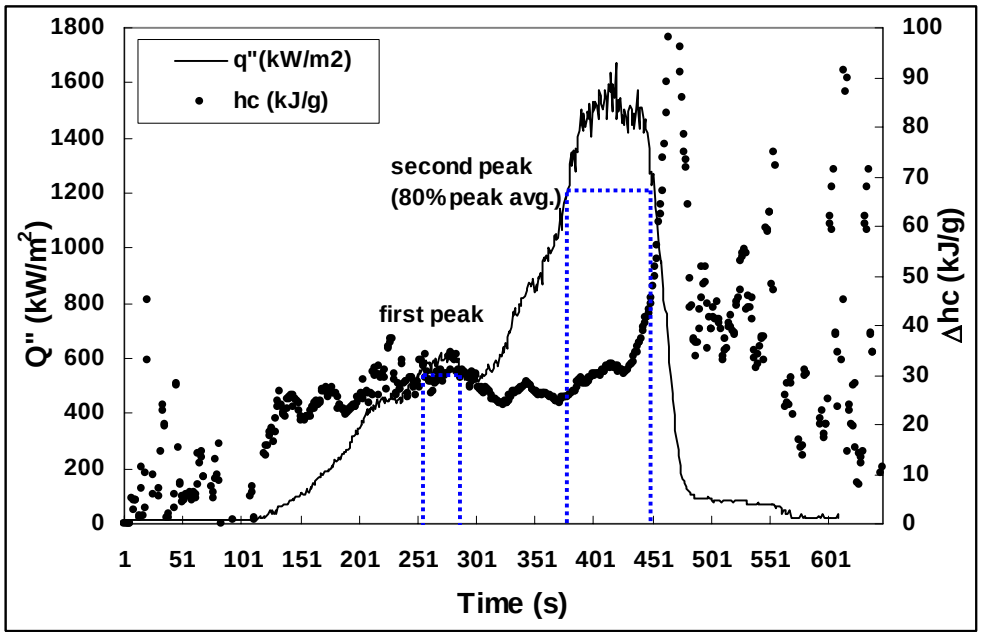

Fig. 4.2.2 Two peak averages of 8mm Nylon under 34kW/m^2

Fig. 4.2.3 gives the heat of combustion values as a function of heat flux, clay loading and thickness based on the second peak average. Table 4.2.1 shows the invariance of the heat of combustion with respect to the peaks, and samples, essentially 30 +/- 2 kJ/g.

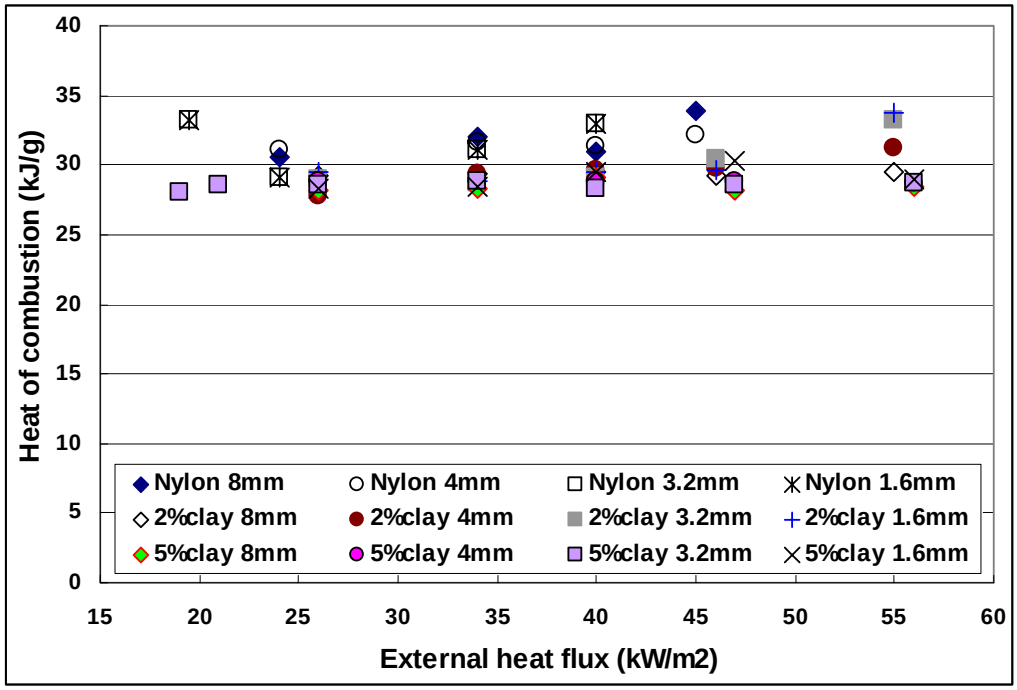

Fig. 4.2.3 Heats of combustion for different samples based on the second peak

4.2.3 Overall Heat of Combustion $\Delta h_{c,\,overall\ avg.}$

The *overall heat of combustion* is calculated by dividing the total heat release from each sample by the total specimen mass loss. This overall value represents an average of the burning characteristics over the entire test duration. The average values shown Fig. 4.2.4 are determined by taking the numerical average of the values calculated from each Cone test. There is a very light reduction due to clay addition.

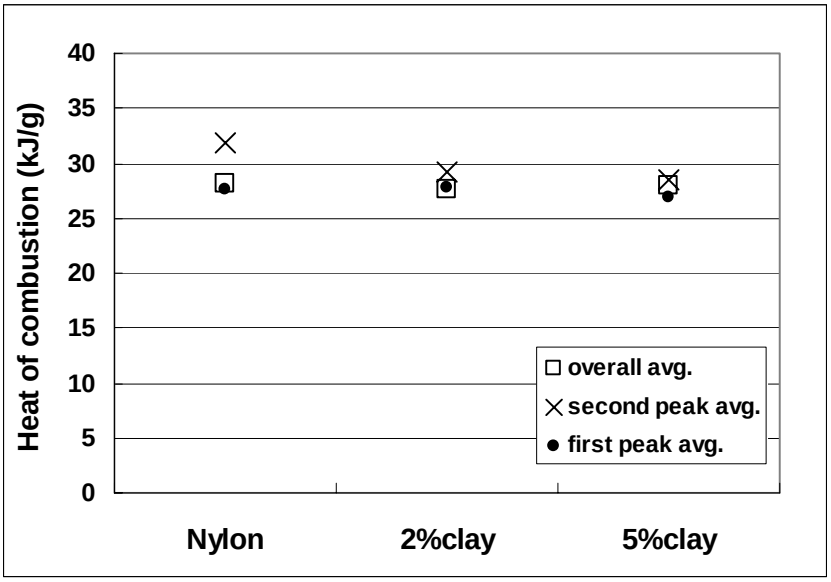

Fig. 4.2.4 Overall average heats of combustion for different samples

Table 4.2.1 Summary for the heat of combustion (kJ/g)

Additive	Thickness.(mm)	First peak	Second peak	Overall
0	24	29.2	29.8	28.6
	8	30.1	32.5	28.8
	4	26.8	33	28.6
	3.2	24.8	33.7	27.0
	1.6	--	30.1	27.7
2%Clay	24	27.3	27.4	26.4
	8	29.0	29.3	28.5
	4	26.2	29.6	28.2
	3.2	--	29.7	27.3
	1.6	--	30.2	27.3
5%Clay	24	27.2	27.0	26.4
	8	27.5	28.4	28.0
	4	26.2	28.8	28.1
	3.2	--	29.3	29.8
	1.6	--	29.0	27.5

4.2.4 Heat of Gasification, *L*

When exposed to a given heat flux, the material will vaporize at a certain rate. This rate can be expressed by the mass loss rate per unit area of material $\dot{m}''$ at a given net heat flux to the material $\dot{q}''_{net}$. The heat of gasification is the energy required to produce the fuel volatiles per unit mass of the material.

Materials may be approximated as vaporizing solids, in order to represent, on average, their ability to vaporize under heating. An exact solution for a thermally-thick, steadily vaporizing solid indicates the mass flux is proportional to the net heat flux:

$$\dot{m}'' = \frac{\dot{q}''_{net}}{L} \tag{4.10}$$

The heat of gasification represents the total energy needed to vaporize from its initial state. The net surface heat flux for the gasification period is

$$\dot{q}''_{net} = \varepsilon \dot{q}''_{ext} + \dot{q}''_{fl} - \varepsilon \sigma T_v^4 \tag{4.11}$$

For the following analysis, the surface emissivity ε of the burning material is approximated as being equal to 1, as to simplify the analysis. The formation of an oxidized skin or char justifies this approximation. If the flame heat flux in Eq.(4.11) is assumed to be constant, which has been shown to be the case for thermoplastic-like materials burning in the Cone Calorimeter[2], then the Eq.(4.10) can be written as

$$\dot{m}'' = (\frac{1}{L})\dot{q}''_{ext} + \frac{(\dot{q}''_{fl} - \varepsilon \sigma T_v^4)}{L}, \tag{4.12}$$

where $\dot{q}''_{fl}$ is the incident flame heat flux,

$\dot{q}''_{ext}$ is the external heat flux provided by the Cone heater (kW/m2),

T_v is the vaporization surface temperature.

Using the mass loss rate data from the Cone Calorimeter, estimations of the heat of gasification can be made. In order to use Eq.(4.12), we consider the flame heat flux and re-radiant heat loss for each material in the Cone Calorimeter to be constant. We can therefore assume that the $\dot{q}''_{net}$ is only linearly dependent on $\dot{q}''_{ext}$.

Plotting the peak-average mass loss rate data against the applied external flux will yield an average value for L as the slope represents the inverse of the heat of gasification, $1/L$. Fig. 4.2.5 indicates this theoretical interpretation for second peak regions. It should be noted that when the second peak occurs due to the insulated back, the material begins to act thermally thin with an internal temperature distribution approaching the vaporization temperature. This makes the effective L value smaller.

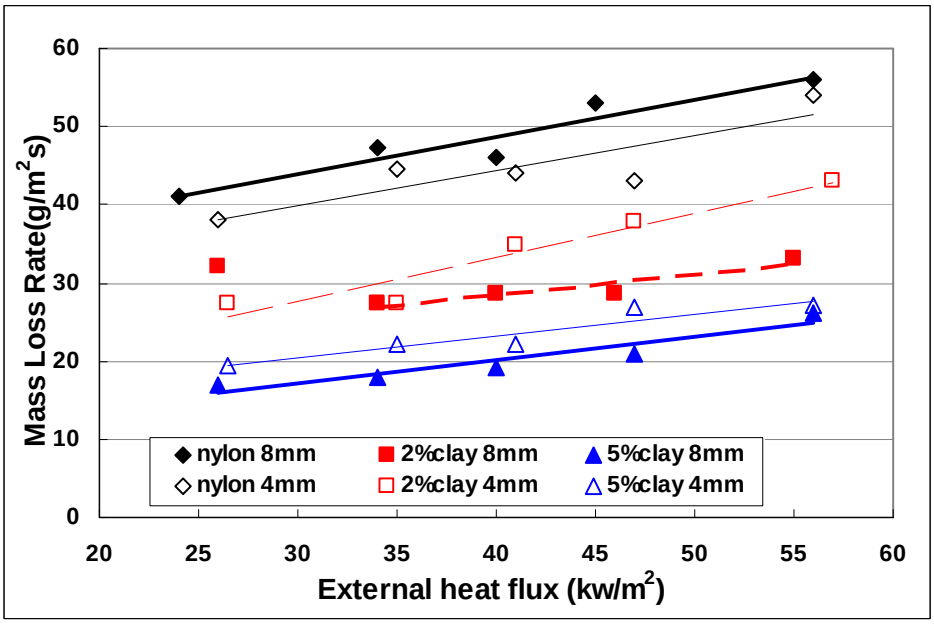

Fig. 4.2.5 Peak-average mass loss rate per unite area at the second peak for L calculation

The negative intercept of the straight lines on the $\dot{m}'' = 0$ line gives the net flame heat flux $\dot{q}''_{fl} - \sigma T_v^4$. It is seen in Fig. 4.2.6 that it decreases with the addition of clay.

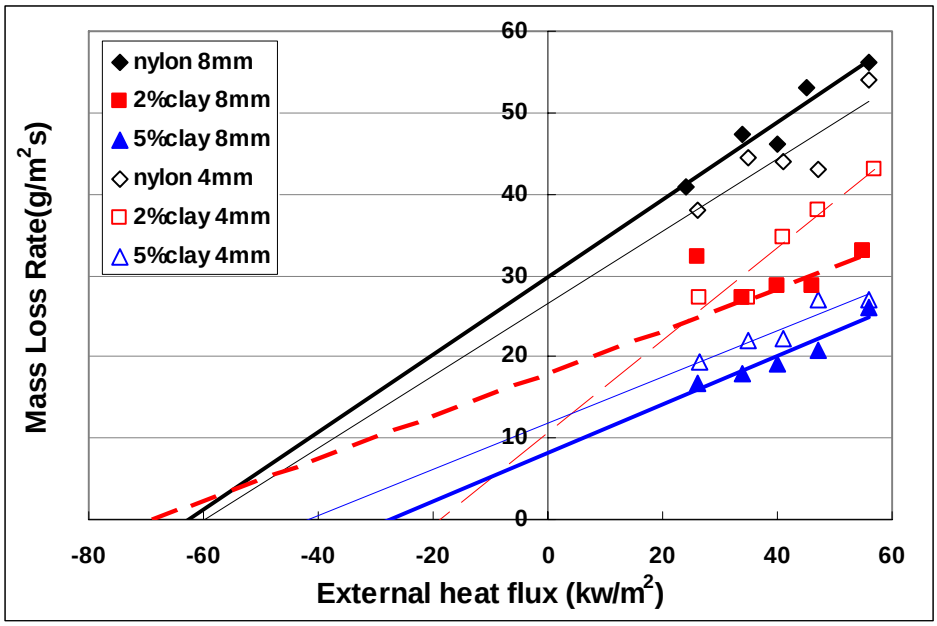

Fig. 4.2.6 Peak-average mass loss rate per unite area at the second peak for net flame heat flux

The heat of gasification also allows the heat release rate of a material to be predicted[4]. $\dot{Q}'' = \dot{m}'' \Delta h_c$, where $\dot{Q}''$ is the heat release rate per unit area (kW/m^2). Thus, from Eq. (4.10) and (4.12):

$$\dot{Q}'' = \dot{q}''_{net} \frac{\Delta h_c}{L}$$

$$\dot{Q}'' = (\frac{\Delta h_c}{L})\dot{q}''_{ext} + (\frac{\Delta h_c}{L})(q''_{fl} - \varepsilon\sigma T_v^4)\,. \qquad (4.13)$$

Plotting the peak-average heat release rate data against the applied external flux will yield an average value for L as the slope represents $\frac{\Delta h_c}{L}$. These results are shown in Fig. 4.2.7, and summarized in Table 4.2.2 for the first and second peaks. The first

peak L should not contain the effect of thickness. There is a tendency for the heat of gasification to increase with clay loading, but this is inconclusive. It would be expected that the first peak, if it was truly representative of a thermally thick steady state burning rate, to have a lower L that the second peak. But this is not seen, and a deeper analysis is needed to sort out these effects.

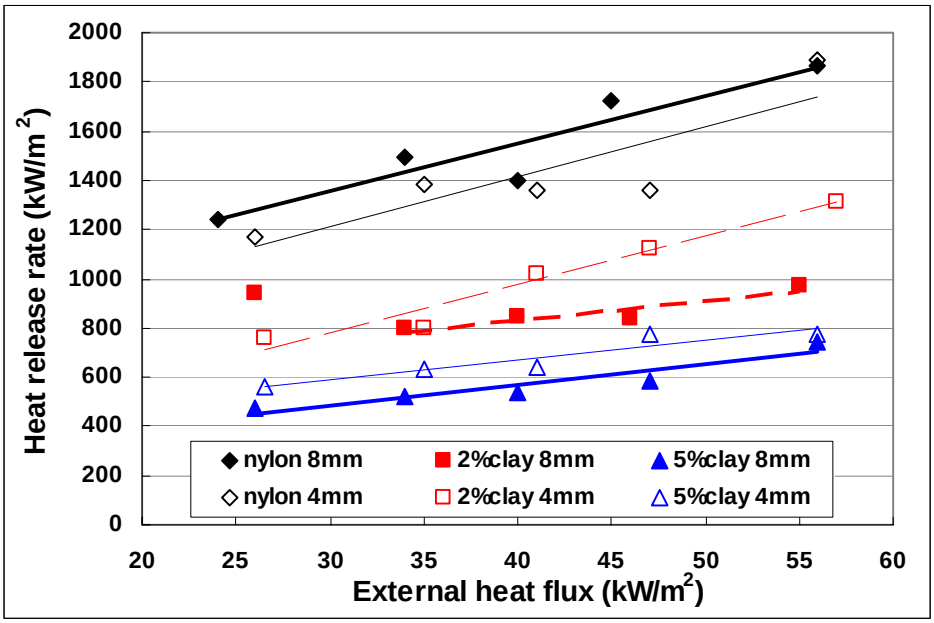

Fig. 4.2.7 Peak-average heat release rate for the second peak for L calculation

To see a general trend, for each thickness, all the L values are averaged. It is shown in Fig. 4.2.8. There are two factors affect L value:

1) Effect of char—A trend is not very clear.

2) Effect of thickness—L will increase with the thickness increase.

For steady burning,

for a thin sample $L = \Delta h_V$; and

for a thick sample $L = \Delta h_V + c_p \Delta T$

where Δh_V is the heat of vaporization, and

$c_p \Delta T$ is the energy needed to bring the material from its original temperature to its evaporation temperature.

For a thick sample, $\Delta T = T_{vap} - T_{back}$. For a thin sample, the temperature distribution becomes nearly uniform. So a thicker sample has a higher heat of gasification. This trend is shown in Fig. 4.2.8.

Table 4.2.2 Summary for heat of gasification for the first and second peaks.

Additive	Thickness (mm)	L from $\dot{m}'' = \frac{\dot{q}''_{net}}{L}$ (kJ/g)		L from $\dot{q}'' = \dot{q}''_{net} \frac{\Delta h_c}{L}$ (kJ/g)	
		First	Second	First	Second
0 %	8	3.47	2.08	4.18	1.68
	4	3.60	1.96	5.31	1.62
	3.2	2.63	1.43	3.7	1.23
	1.6	--	2.27	--	1.34
2%Clay	8	3.18	3.85	3.33	3.80
	4	1.34	1.79	1.51	1.52
	3.2	--	1.92	--	1.56
	1.6	--	1.69	--	1.46
5%Clay	8	3.55	2.33	3.64	3.40
	4	2.47	3.57	2.33	3.60

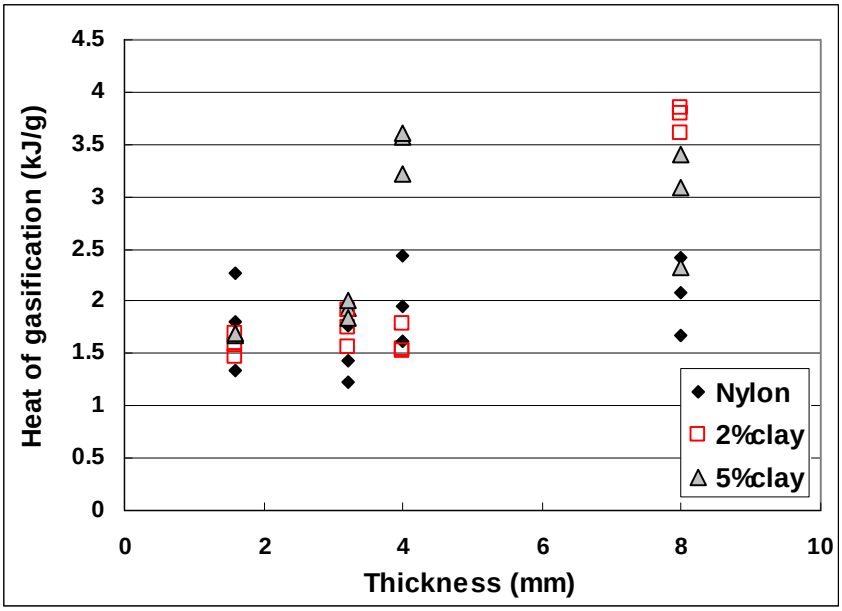

Fig. 4.2.8 Heat of gasification vs. thickness for different samples

4.2.5 Residue Fraction

The nominal residue fraction can be estimated from the initial and final mass of the sample $\frac{m_{final}}{m_{initial}}$.

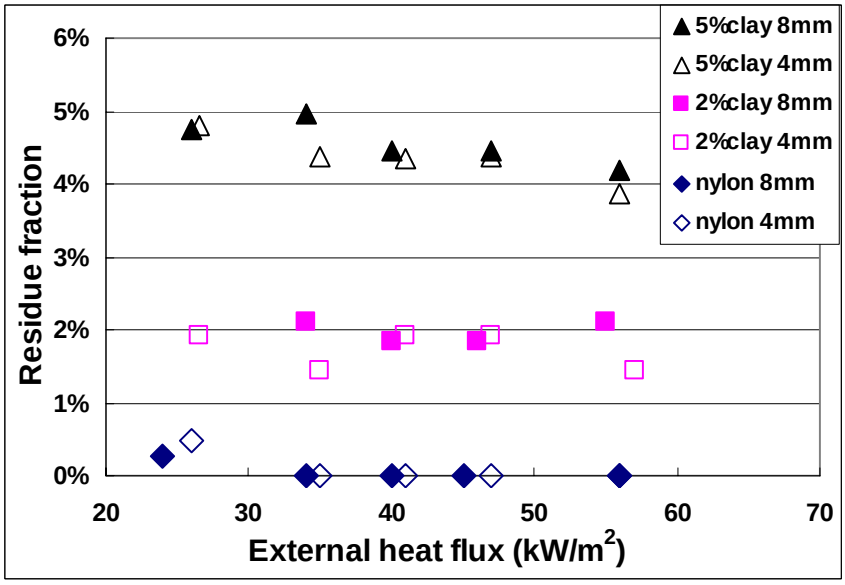

Fig. 4.2.9 Residue fraction vs. external heat flux

Sample is weighed before test as the initial mass. The weight of the aluminum cup is also measured before test. After burning, the residue with cup is weighed together. Then the aluminum cup weight is subtracted. The pure residue mass is the m_{final}.

Results are shown in the Fig. 4.2.9 for residue fraction. The results show residue fraction is primarily a function of loading from about 0.02 to 0.045 for 2 to 5 % clay.

4.3 Ignition characteristics and properties

4.3.1 Time to Ignite

The time to ignite can be computed by

$$t_{ig} = Ck\rho c \frac{(T_{ig} - T_{\infty})^2}{(\dot{q}''_{ext} - \dot{q}''_{cr})^2} \tag{4.14}$$

where the value C depends on $\dot{q}''_{ext}$, approaching π/4 for large $\dot{q}''_{ext}$ [2].

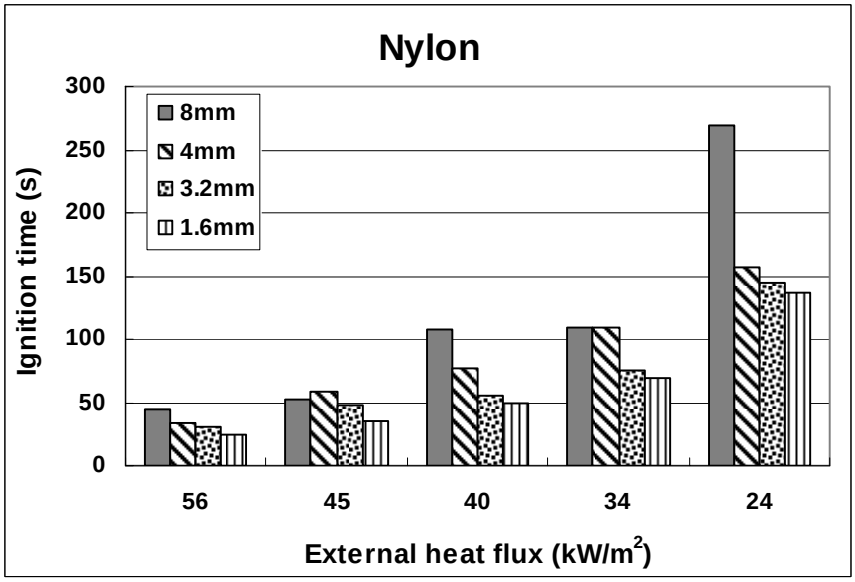

Fig. 4.3.1 Ignition time of Nylon with different thickness

By utilizing this theoretical expression, the data can be processed to derive ignition properties. Fig. 4.3.1 shows the general trends of the time to ignite as a function of thickness. Thick sample needs more time to be ignited. Fig. 4.3.2 shows the effect of clay loading. The addition of clay also tends to increase the time.

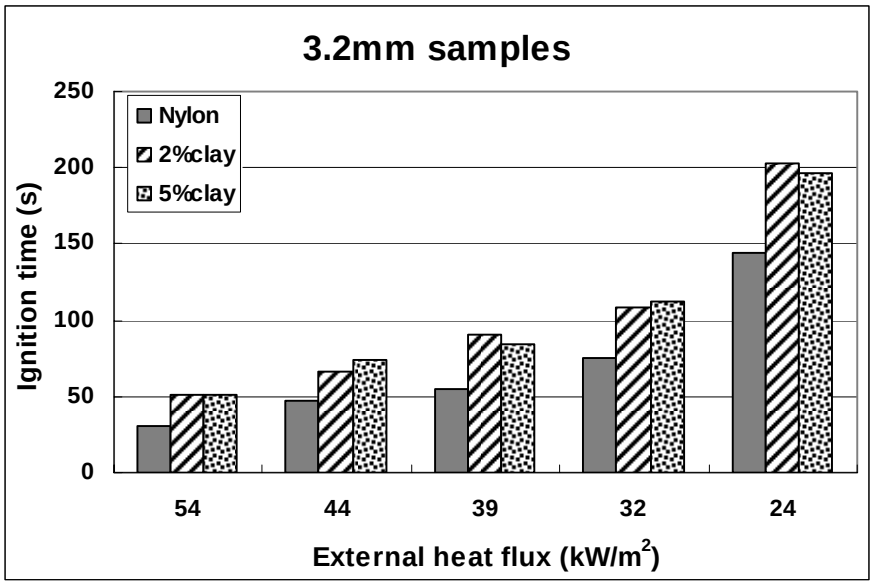

Fig. 4.3.2 Ignition time of 3.2mm samples with different clay loading

4.3.2 Critical Heat Flux

In order to predict the ignition temperature and thermal inertia, the critical flux for ignition must be determined. The critical heat flux for ignition occurs where $t_{ig} \to \infty$. Based on Eq.(4.14), a plot of ignition data as $t_{ig}^{-1/2}$ versus $\dot{q}''_{ext}$ is shown in Fig.4.3.4. The intercept at $t_{ig}^{-1/2} = 0$ gives $\dot{q}''_{ext} = \dot{q}''_{cr}$

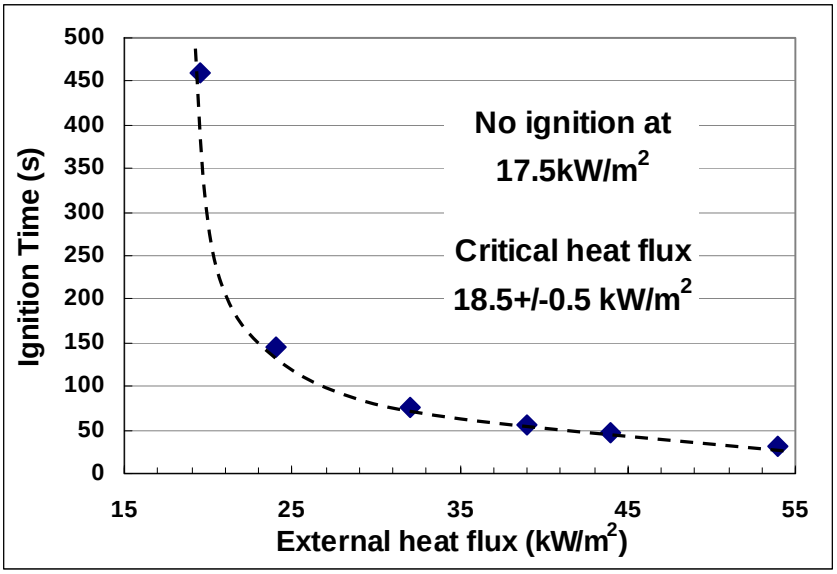

Fig. 4.3.3 3.2mm Nylon
Critical heat flux by $t_{ig} \rightarrow \infty$

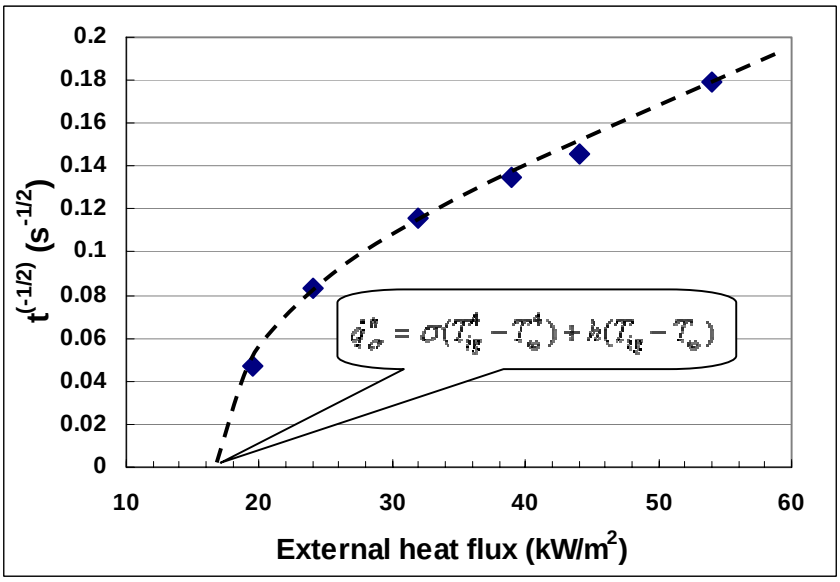

Fig. 4.3.4 3.2mm Nylon
Critical heat flux by intercept

4.3.3 Ignition Temperature

In general, the net heat flux at the surface can be expressed as:

$$\dot{q}''_{net} = \dot{q}''_{ext} - h(T_S - T_\infty) - \sigma(T_S^4 - T_\infty^4)$$

The critical heat flux for ignition was normally found by trial-and-error in the testing. It was found to be roughly 19 kW/m^2 for all samples, but this needs to be examined further, since we did not have enough samples to truly find this threshold. The ignition temperature is deduced from an energy balance at the surface when the heat flux into the material is theoretically zero. This is the limiting state under radiant heating. The equation becomes

$$\dot{q}''_{cr} = \sigma(T_{ig}^4 - T_\infty^4) + h(T_{ig} - T_\infty)\,. \tag{4.15}$$

For this analysis an average value of the convective coefficient of $h = 10$ W/m^{2}K, as indicated in [2] and confirmed by an extensive analysis given in Appendix B. The experimental value was based on an ambient temperature of $T_\infty = 23$ ºC, the average laboratory state. Generally, the ignition temperature was estimated at about 460+/-10 ^{o}C for all the samples.

4.3.4 Thermal Inertia, $k\rho c$.

From Eq. (4.14) ,

$$t_{ig}^{-1/2} = \frac{1}{(\frac{\pi}{4} k\rho c)^{1/2}(T_{ig} - T_\infty)} \dot{q}''_i \tag{4.16}$$

The slope for the plot $t_{ig}^{-1/2}$ versus $\dot{q}''_{ext}$ at high heat flux is $\left[(\frac{\pi}{4} k\rho c)^{1/2}(T_{ig} - T_\infty)\right]^{-1}$ (See Fig.4.3.5). With T_{ig} calculated from Eq. (4.15), $k\rho c$ can be determined.

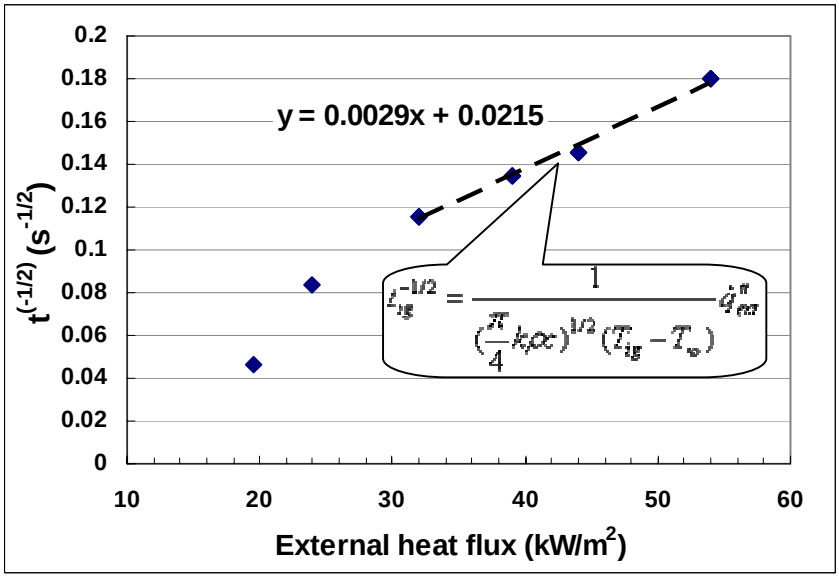

Fig. 4.3.5 3.2mm Nylon
Slope determines thermal inertia

Results for different samples are shown in Fig.4.3.6 and listed in Table 4.3.2.

Sample density can be calculated by $\frac{mass}{volume}$ as measured

Table 4.3.1 Density of samples (kg/m^3)

Thickness	Nylon	Nylon+2%Clay	Nylon+5%Clay
24mm	1103.1	1108.9	1108.9
8mm	1110.8	1108.0	1110.8

It appears in the table 4.3.1 that the sample density (ρ) is independent of small amount of clay loading, and specific heat (c_p) is also known to not change much due to the small amount of clay. Fig. 4.3.7 shows the thermal conductivity (k) data for Nylon and Nylon+5%clay from Kashiwagi [11]. There is not much difference too. If consider the three properties together as an thermal inertia ($k\rho c$), there is an increase in thermal inertia as clay additive is increased, which is clearly seen in Fig. 4.3.5.

The term $k\rho c$ derived from ignition time vs. external flux is so called "effective $k\rho c$ " or "apparent $k\rho c$ ". These values are quite different from the values derived from each value of k, ρ, and c_p. The reason is that the derivation from Eq.(4.16) is based on lumped approach solving thermal conduction equation with several assumptions. They are (1) external flux is absorbed at the surface (this may be not good for Nylon or at high flux); (2) each thermal property is assumed to be constant, not a function of temperature (c_p changes significantly with temperature); (3) radiative loss is approximated or not included.

During a sample burning, a dark skin was formed for samples with clay before ignition, but no such skin was formed for pure Nylon. Such skin could have significant effects and it might be one of reasons for the difference between the two samples.

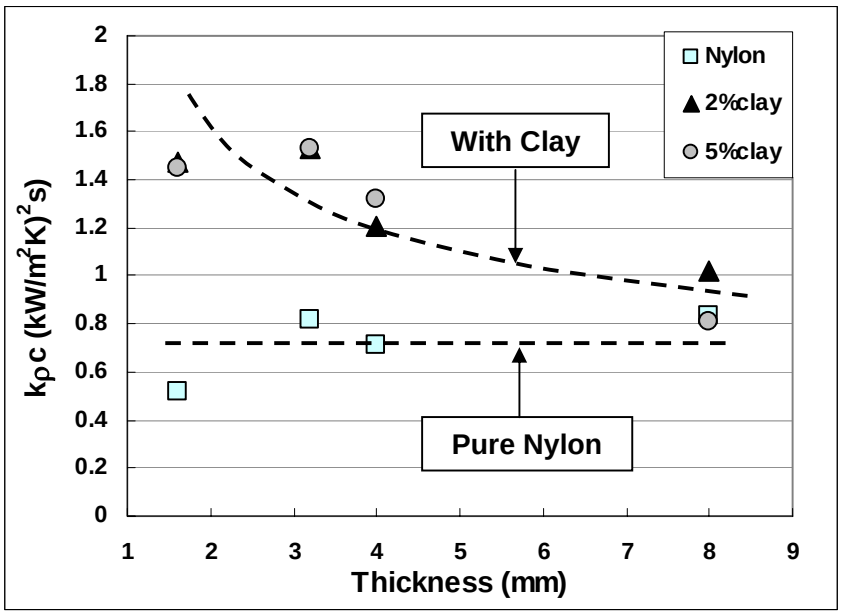

Fig. 4.3.6 $k\rho c$ vs. thickness

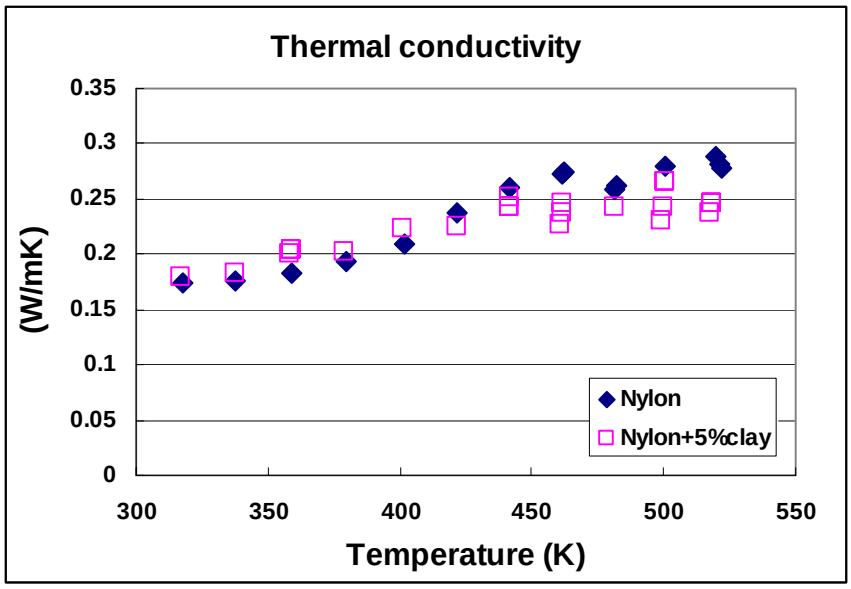

Fig. 4.3.7 Thermal conductivity of Nylon and Nylon+5%clay

Table 4.3.2 Ignition Tendency and Thermal Inertia

Additive	Thickness.(mm)	$\left[(\frac{\pi}{4}k\rho c)^{1/2}(T_{ig}-T_{\infty})\right]^{-1}$ ($s^{1/2}kW/m^2$)	$k\rho c(T_{ig}-T_{\infty})^2$ in 10^5 $(kW/m^2)^2s$)	$k\rho c$ $(kW/m^2K)^2s$)
0	8	0.0029	1.51	0.83
	4	0.003	1.42	0.71
	3.2	0.0029	1.51	0.82
	1.6	0.0038	0.88	0.52
2%Clay	8	0.0025	2.04	1.02
	4	0.0023	2.41	1.21
	3.2	0.0021	2.89	1.53
	1.6	0.0022	2.63	1.47
5%Clay	8	0.0028	1.63	0.81
	4	0.0022	2.63	1.32
	3.2	0.0021	2.89	1.53
	1.6	0.0023	2.41	1.45

4.4 Thickness Effect

4.4.1 Thermal Thickness

The thermal penetration depth can be estimated as $\delta_T = \sqrt{\alpha t}$

A thermally thin sample has its physical thickness d less than then thermal penetration depth δ_T. The internal temperature difference must be much smaller than the difference across the boundary layer.

$$d << \delta_T \approx \sqrt{\alpha t} \approx \frac{k(T_s - T_o)}{\dot{q}''} \tag{4.17}$$

Ignition time for a thermally thin material is

$$t_{ig} \approx \frac{\rho c d (T_{ig} - T_\infty)}{\dot{q}''_{ext}} \Rightarrow t_{ig} \sim \dot{q}''^{-1}_{ext} \tag{4.18}$$

A thermally thick material has a negligible back-face boundary condition. In other words, we might approximate the ignition of a solid as a semi-infinite medium.

$$d >> \delta_T \approx \sqrt{\alpha t_{ig}} \tag{4.19}$$

The ignition time is given as

$$t_{ig} \approx \frac{\pi}{4} k\rho c \frac{(T_{ig} - T_\infty)}{\dot{q}''_{ext}} \Rightarrow t_{ig} \sim \dot{q}''^{-2}_{ext}$$

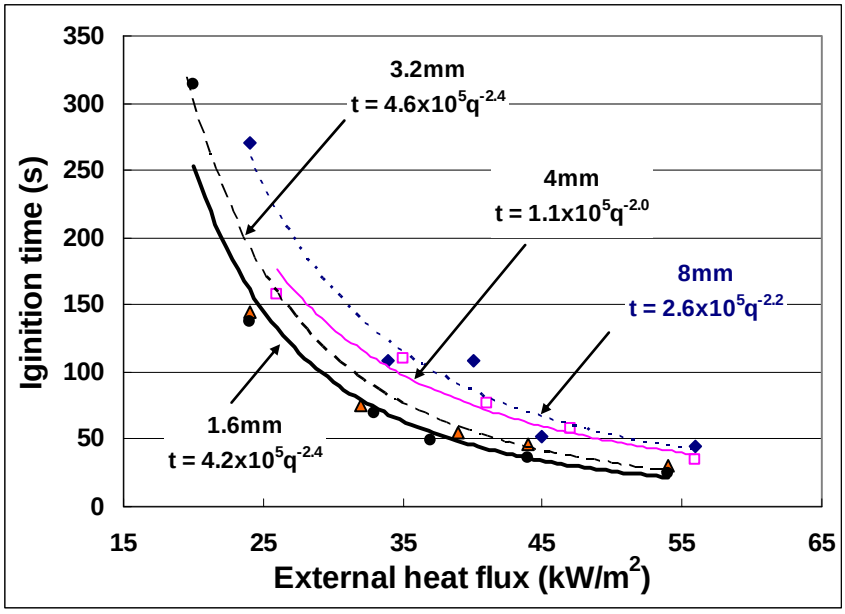

Fig. 4.4.1 Ignition of Nylon under different heat flux

Shown in Fig. 4.4.1, a plot of time to ignite with heat fluxes shows that even for the 1.6mm sample, the samples appear all thermally thick. This is due to the insulation effect for the thin materials and the fact that the thermal penetration is likely less than the physical thickness.

4.4.2 Vaporizing front

A burning sample consists of a char layer, which is left after ignition, and decomposition. The vaporizing front is at the surface where the melting sample is bubbling and releasing fuel gas vapor. For the vaporizing front defined at δ, depends on a power of time of the order of 1/2~1 [12].

$$\delta \sim (t - t_{ig})^{\frac{1}{2} \to 1} \quad \Rightarrow t \sim \delta^{1 \to 2} \tag{4.20}$$

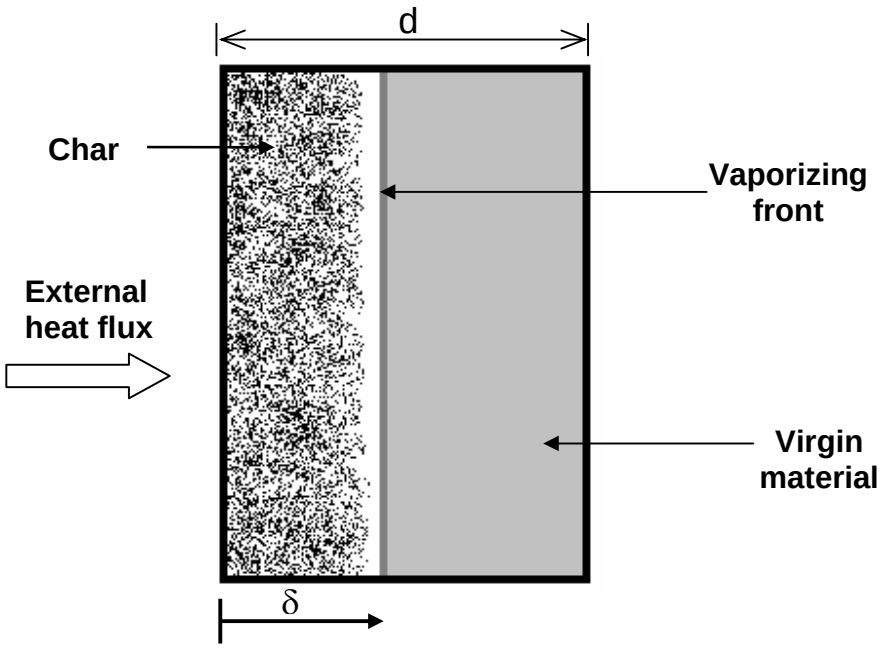

Fig. 4.4.2 Draft showing burning sample structure

Let $t - t_{ig}$ be the time to reach the maximum mass loss rate after ignition for a particular sample (See Fig.4.4.3). This gives the approximate δ as the back face sample depth (*d*) at that time. Hence, the array of sample data gives a general relationship for δ and $t - t_{ig}$. This correspondence is shown from the data in Fig. 4.4.4. The exponent for time varies from about 1.2 to 1.4, and suggests conformity to the theory.

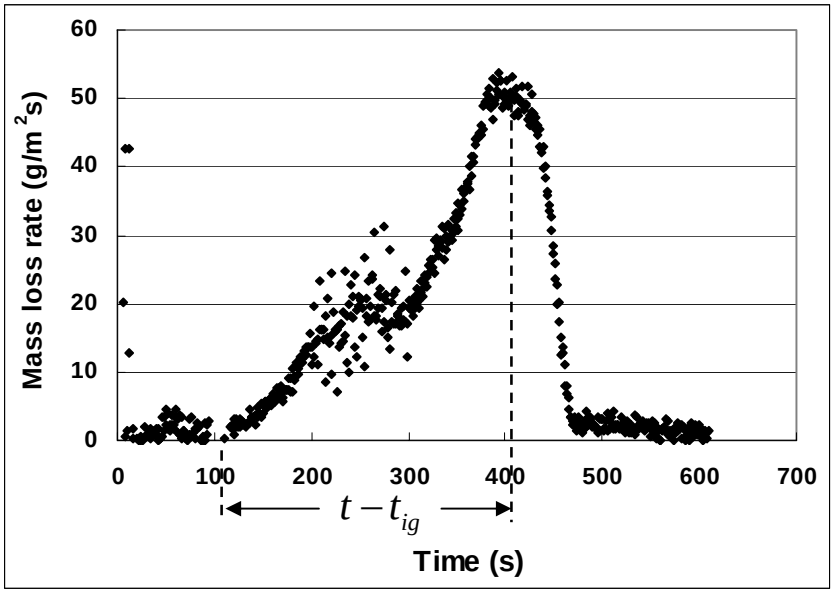

Fig. 4.4.3 Time to reach the maximum mass loss rate after ignition

Based on this thickness-time relationship, we can also determine the nominal or average mass loss rate per unit area, which is the "steady" burning part before reaching the back-face. This is by a sample mass balance.

$$\dot{m}'' = -\frac{1}{A}\frac{dm}{dt} = -\frac{1}{A}\left(\rho_c A\frac{d\delta}{dt} + \rho A\frac{d(d-\delta)}{dt}\right) = (\rho - \rho_c)\frac{d\delta}{dt} \tag{4.21}$$

Combining with Eq. (4.20) gives

$$\dot{m}'' \sim (t - t_{ig})^{-\frac{1}{2}\to 1}$$

The results are shown in Fig. 4.4.5 for the power law corresponding to the 0, 2 and 5% loadings. Departure of power law result values formed from the data is seen for small times or small thickness cases. While this data come from discrete specific times in a given test, they may be interpreted as a "thick" solution for all time at the loadings.

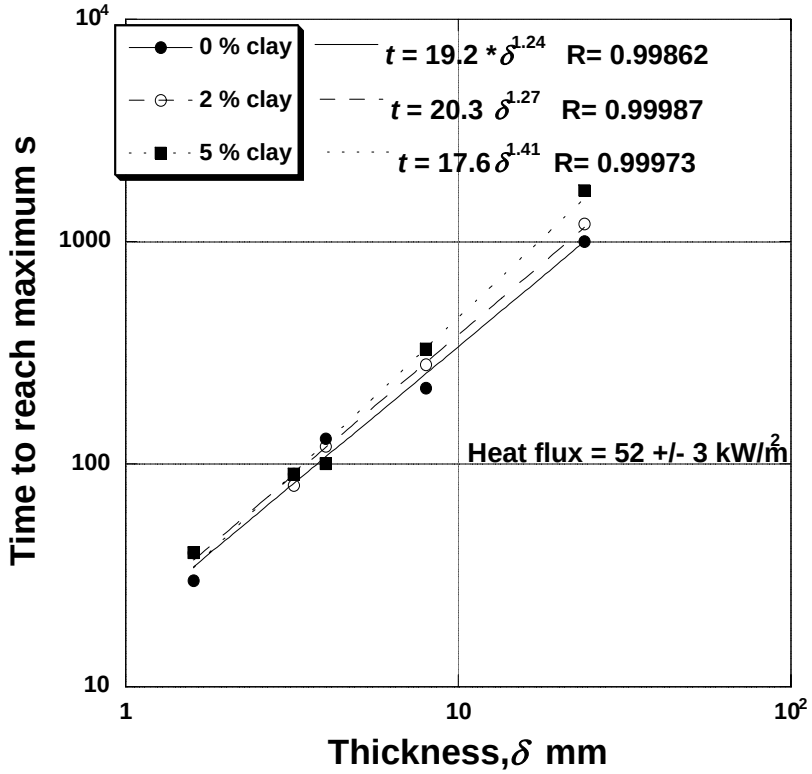

Fig. 4.4.4 Time reach the maximum mass loss rate after ignition

There are three factors affecting the mass loss rate.

(1) Effect of thickness

As mentioned in Section 4.2.4, the heat of gasification of a thick sample is higher than that of a thin sample. Mass loss rate is $\dot{m}'' = \frac{\dot{q}''_{net}}{L}$. So a thicker sample has a lower mass loss rate.

Thick: $$\dot{m}'' = \frac{\dot{q}''_{net}}{\Delta h_{vap} + c(T_{vap} - T_{back})} \tag{4.22}$$

Thin: $$\dot{m}'' = \frac{\dot{q}''_{net}}{\Delta h_{vap}} \tag{4.23}$$

where $$\dot{q}''_{net} = \dot{q}''_{ext} - h(T_S - T_\infty) - \sigma(T_S^4 - T_\infty^4) \tag{4.24}$$

This effect is also seen for each sample during burning. At the early stage of burning, the sample acts as a thick sample. Mass loss rate strives towards a steady state following Eq. (4.22). With the sample consumption, the unburned part becomes thinner and thinner. The thin piece left eventually has a nearly uniform temperature, which means a lower heat of gasification value as seen by Eq.(4.23). So both very thin samples and the burning in maximum burning period (second peak, due to back-face effect) act as a thin sample. Thick samples and the early sample burning tend to act like steady burning (see Fig.4.4.6).

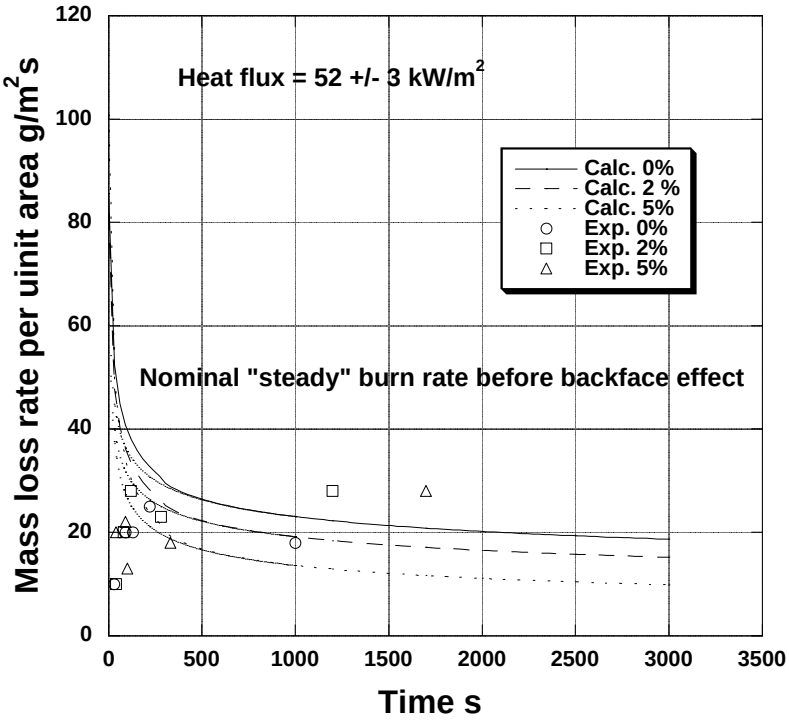

Fig. 4.4.5 Mass loss rate at steady burning (first peak)

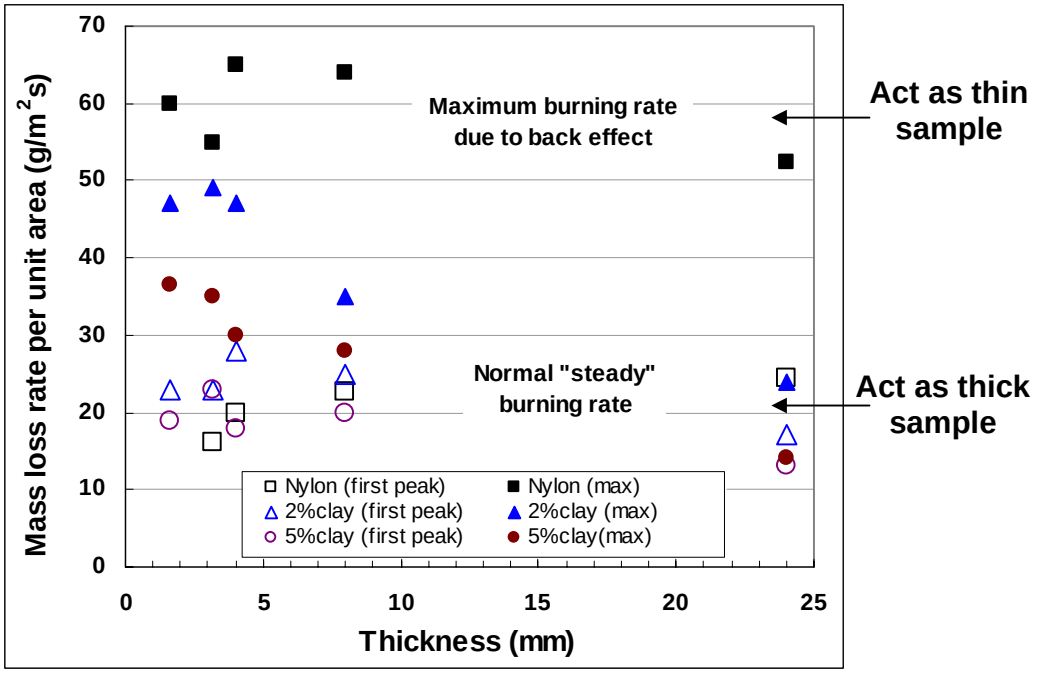

Fig. 4.4.6 Different thickness samples under 53+/-3 kW/m^2

(2) Effect of char

For the samples with clay, char layer forms before ignition occurs. It is like a film or a shell. It blocks the fuel gas from being released. It also blocks the external radiative heat flux to the gasifying surface. The net heat transfer to this surface changes from radiation (as shown in Eq. (4.24)) to conduction with the blockage (as shown in Eq. (4.25)). Clay additive will reduce the mass loss rate. The net heat flux decreases with the char thickness as

$$\dot{q}''_{net} = k_{char} \frac{(T_{sur} - T_{vap})}{\delta_{char}} \tag{4.25}$$

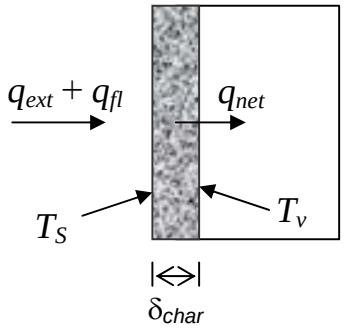

Fig. 4.4.7 Sketch of sample with char surface

(3) Back-face insulation effect

When the heat flux to the sample reaches the back face, the insulation layer causes the storage of energy, which can also increase mass loss rate. For pure Nylon, there will be a clear big jump at the final stage of burning (see the darkest curve in Fig. 4.4.8) . For a sample with clay inside, that jump may not be that obvious. The char, which is the left over from the clay, blocks the fuel gas from being released. Therefore the burning rate is reduced. This decrease in mass loss rate will lower the peak value. The curve for the sample with clay appears steadier. For example, as shown in Fig. 4.4.7, for pure Nylon, the jump at the final burning period is very obvious. For 2% clay curve, there is still a jump, but the peak value is lower than that of pure Nylon. For 5% clay curve, there is no jump because of the clay additive.

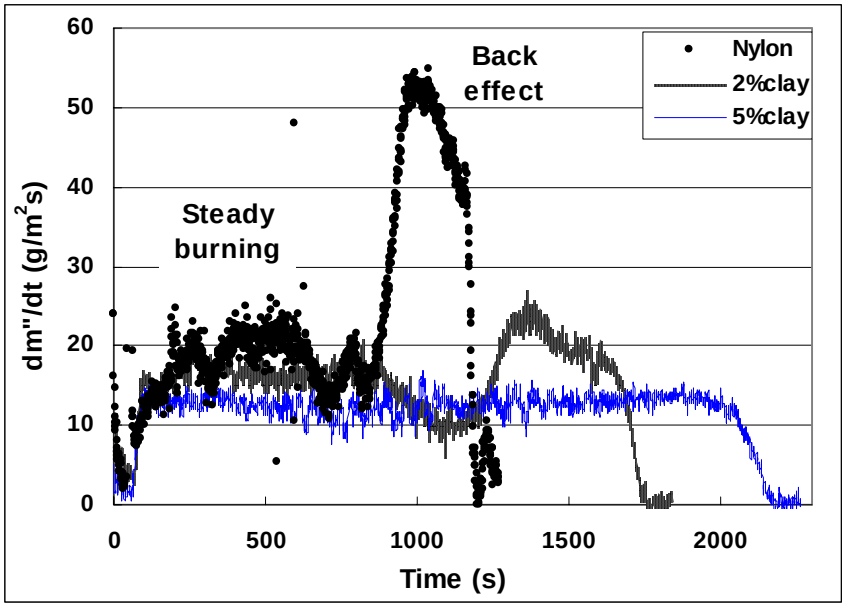

Fig. 4.4.8 24mm samples under 50kW/m^2

Chapter 5: Application of a Char Model for Nylon Nanocomposites

A theoretical solid phase model accounting for kinetic decomposition, and heat and mass transfer of subjected to a radiant heat source has been used[13]. The model includes variations of thermal properties of material and char.

In order to develop a theoretical model to describe the burning processes of the sample, kinetic parameters (the activation energy E_a and pre-exponential factor a_P) are needed for its decomposition. These were formed from Thermal gravimetric analysis (TGA) data.

Thermal gravimetric analysis is a standard technique for measuring the desorption or the decomposition properties of materials. In these tests, the sample is continuously weighed, while its temperature is increased.

5.1 Kinetic Parameters from Theory

In this section, methods to determine the kinetic parameters are discussed. This analysis follows from Boonmee[13].

5.1.1 Mass conversion fraction (α)

The total mass changes as it undergoes the pyrolysis process. A continuum representation for decomposition considers the sample with the char in a fixed volume. The mass conversion fraction (α) is defined as:

$$\alpha = \frac{m - m_{\text{int}}}{m_f - m_{\text{int}}} \tag{5.1}$$

m is the total mass of sample, which is changing with pyrolysis process.

m_{int} is the initial mass of sample.

m_f is the final mass of sample.

The value of α goes from zero to the final value (char fraction) as the total mass m goes from m_{int}, the initial mass of sample, to m_f, the final mass of sample. The rate of change of the conversion factor can be expressed in a general differential equation form as $\frac{d\alpha}{dt} = f(\alpha)k(T)$ (5. 2)

where $f(\alpha)$ is a reaction order function.

$k(T)$ can be expressed as the Arrhenius rate equation:

$$k(T) = a_p \exp(-E_a / RT) \tag{5.3}$$

where a_p is the pre-exponential factor

E_a is the activation energy

R is the universal gas constant $8.31 J / mol \cdot K$

Substitute Eq. (5.3) into (5.2):

$$\frac{d\alpha}{dt} = f(\alpha)a_p \exp(-E_a / RT) \tag{5.4}$$

5.1.2 Differential Method

Take the natural logarithms on both sides of Eq. (5.4)

$$\ln\left(\frac{d\alpha}{dt}\right) = \ln\left(f(\alpha)a_P\right) - \frac{E_a}{R}\left(\frac{1}{T}\right) \tag{5.5}$$

For one sample, pick $\ln\left(\frac{d\alpha}{dt}\right)$ at three different α_i, and plot against $1/T(\alpha_i)$ ($T(\alpha_i)$ is corresponding to α_i), the linear slope is $-E_a / R$, and the intercept is $\ln\left(f(\alpha_i)a_p\right)$.

$f(\alpha)$ is defined as

$$f(\alpha) = \frac{(1-\alpha)}{(1-X_C)}. \tag{5.6}$$

$X_C = \frac{m_f}{m_{\text{int}}}$ is the char fraction.

Then E_a and a_p are easily calculated.

$$E_a = -R \times slope \tag{5.7}$$

$$a_p = \frac{\exp(\text{intercept})}{f(\alpha)} \tag{5.8}$$

5.2 Kinetic Parameters from TGA Data

The TGA data of Nylon and Nylon+5%clay are from Kashiwagi, NIST[11]. The data are obtained from non-isothermal tests with a series of constant heating rates (β) of 1,

2 and 5 °C/min from NIST. At those low heating rate (<10 °C/min), the sample mass gradually decreases as the decomposition process is controlled by kinetics. For a given heating rate (e.g. 2 °C/min in Fig. 5.2.1), the sample mass decreases uniformly with one slope until its remaining mass reaches approximately 2% of the original mass.

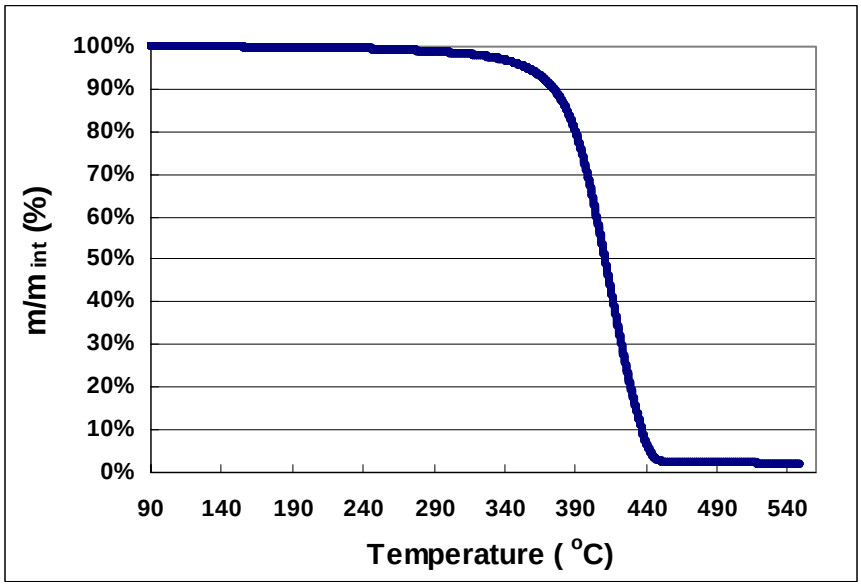

Fig. 5.2.1 Mass fraction of Nylon heated by 2 °C/min

In order to get activation energy E_a and pre-exponential factor a_p using Eq.(5.4), $\frac{d\alpha}{dt}$ is needed from TGA data.

Since α is defined as $\alpha = \frac{m - m_{\text{int}}}{m_f - m_{\text{int}}}$

$$\frac{d\alpha}{dt} = \frac{1}{m_f - m_{\text{int}}} \frac{dm}{dt}$$

TGA data shows mass fraction as a function of temperature, and temperature is a function of time.

$$\frac{dm}{dt} = \frac{dm}{dT}\frac{dT}{dt} = m_{\text{int}} \frac{d\dfrac{m}{m_{\text{int}}}}{dT}\frac{dT}{dt}$$

$\dfrac{dT}{dt}$ is the heating rate (e.g. 5 °C/min)

$\dfrac{d\dfrac{m}{m_{\text{int}}}}{dT}$ is the derivative of weight (%/°C), directly from TGA data as shown in Fig. 5.2.2

$$\frac{d\alpha}{dt} = \frac{m_{\text{int}}}{m_f - m_{\text{int}}} \frac{d\dfrac{m}{m_{\text{int}}}}{dT}\frac{dT}{dt} \tag{5.8}$$

Then following differential method, pick α =0.25, 0.5, 0.75, plot $\ln\left(\dfrac{d\alpha_i}{dt}\right)$ vs. $\dfrac{1}{T_i}$

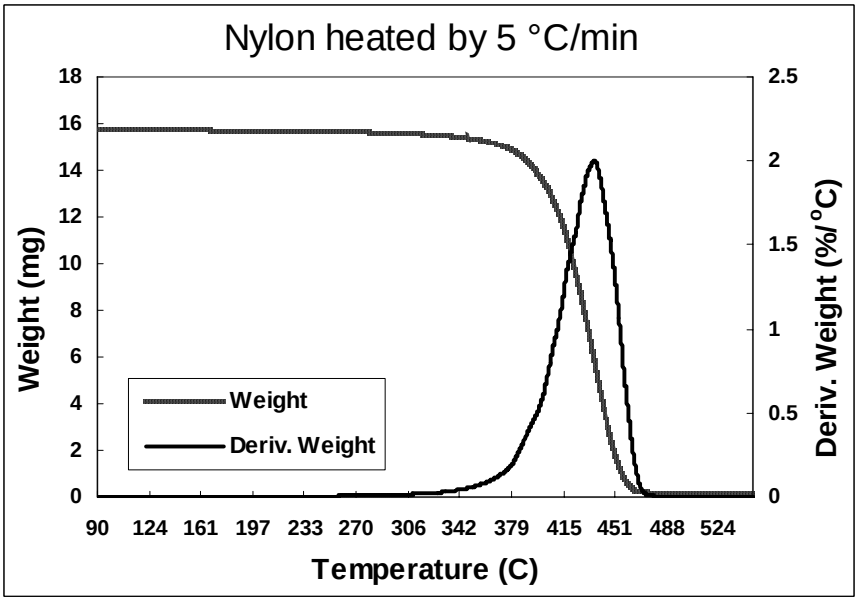

Fig. 5.2.2 TGA data
Nylon heated by 5 °C/min

Find the char fraction $X_C = \frac{m_f}{m_{\text{int}}}$ for each material, and substitute it into Eq. (5.6). Then $f(\alpha)$ is easy calculated for three different α values. Read slope and intercept in Fig. 5.2.3. Use slope in Eq.(5.7) to get E_a. Use intercept in Eq.(5.8) to get . Those values are listed in table 5.2.1

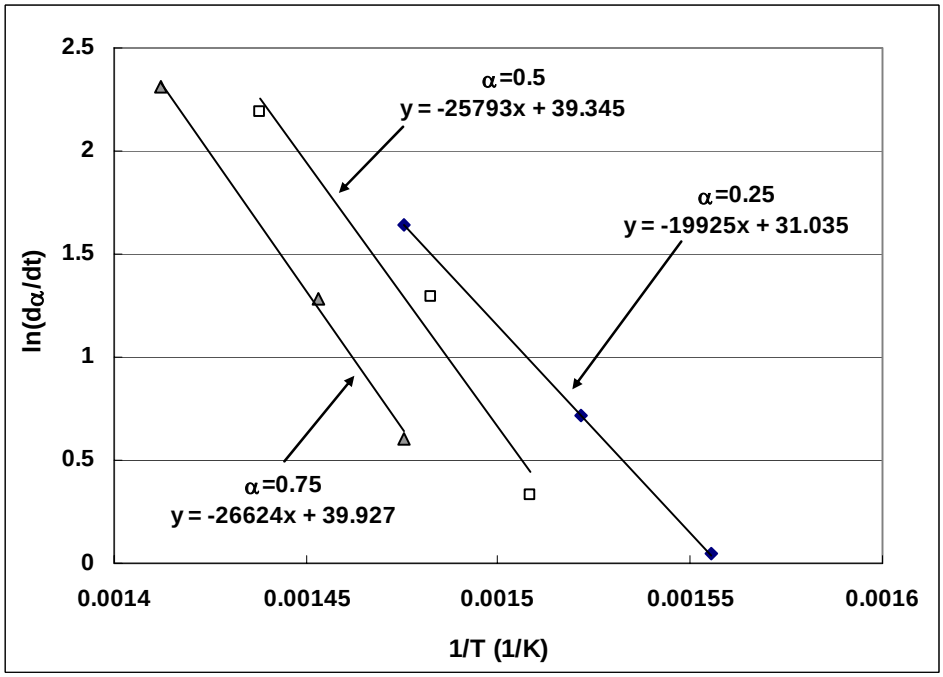

Fig. 5.2.3 Nylon + 5% clay

Table 5.2.1 Kinetic Parameters

Nylon *Xc*=0.017					
α	slope	intercept	*Ea* (J/mol)	$f(\alpha)$	a_p
0.25	-22282	34.209	185163.4	0.76297	9.4248E+14
0.5	-28752	43.188	238929.1	0.508647	1.12174E+19
0.75	-30770	45.233	255698.7	0.254323	1.73403E+20
Nylon+5%clay *Xc*=0.06					
α	slope	intercept	*Ea* (J/mol)	$f(\alpha)$	a_p
0.25	-19925	31.035	165576.8	0.797872	3.77E+13
0.5	-25793	39.345	214339.8	0.531915	2.3E+17
0.75	-26624	39.927	221245.4	0.265957	8.23E+17

Now there are three sets of E_a and a_p for each sample. Substitute each set back into Eq. (5.4), and combine with Eq. (5.6):

$$\frac{d\alpha}{dt} = \frac{1-\alpha}{1-X_C} a_p \exp(-E_a / RT) \tag{5.9}$$

In Eq.(5.9), X_C , E_a and a_p are fixed for each material, $\frac{d\alpha}{dt}$ is only a function of temperature (time).

$\frac{d\alpha}{dt}$ from TGA data calculation, from α=0.25, from α=0.5 and from α=0.75 are compared in Fig. 5.2.4.

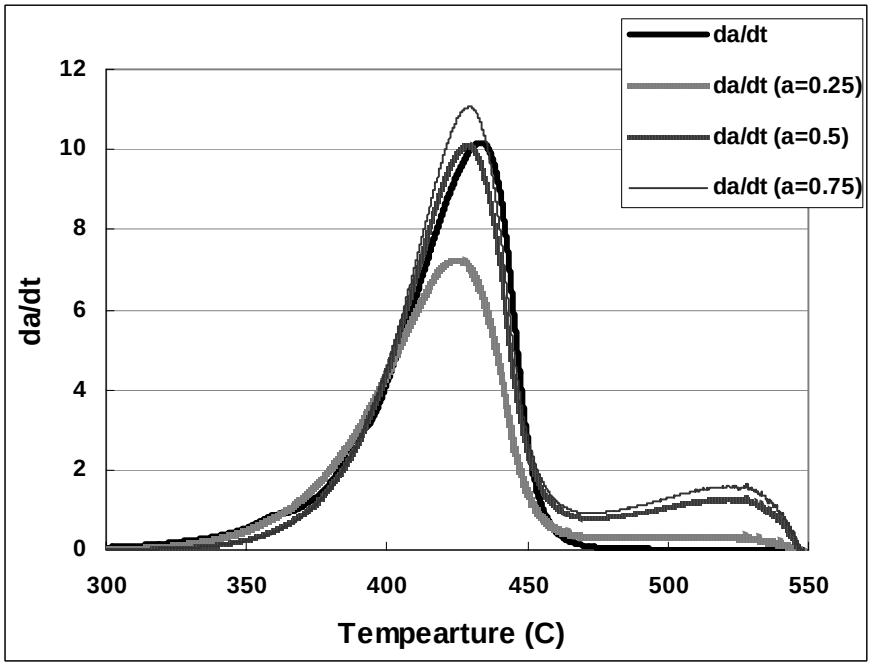

Fig. 5.2.4 Nylon6 +5%clay heated by 5 °C/min

Comparing these three sets values with the one calculated from TGA data (the darkest curve), the curve at $\alpha = 0.5$ matches the TGA data well. So X_C , E_a and a_p at $\alpha = 0.5$ are set to be the value used in the simulation model later.

5.3 Modeling for real samples

For a thermal gravimetric analysis, very small samples (milligram quantities) are heated in an inferior thermo-gravimetric analysis (TGA) instrument to find out whether or not thermal degradation will start at a given temperature. In this section, a FORTRAN program was used to simulate the combustion process of real size samples. This FORTRAN program was developed by Boonmee[13] for his wood material. I changed the input properties to best match my samples. Activation energy E_a and pre-exponential factor a_p were also used in the program, which was calculated in the former section.

The following assumptions are imposed in order to simplify the problem:

1. The problem can be formulated as a one-dimensional transient heat conduction problem.
2. The continuum volume of the sample consists of three species: active part, char, and gas.
3. Local thermal properties and density vary with temperature.
4. Convective and radiative heat losses are taken into account at the sample surface.
5. No heat or mass losses occur at the back of the sample.

The theoretical model involved the following equations.

Kinetics Decomposition $\frac{\partial \rho_j}{\partial t} = -\rho_{a,j} a_{P,j} \exp(-E_{a,j} / RT)$

Mass Conservation $\frac{\partial \rho}{\partial t} + \frac{\partial (\rho_a v_a)}{\partial x} + \frac{\partial (\rho_C v_C)}{\partial x} + \frac{\partial (\rho_g v_g)}{\partial x} = 0$

Energy Conservation $\frac{\partial(\rho_a h_a + \rho_c h_c)}{\partial t} = \frac{\partial}{\partial x}\left(k\frac{\partial T}{\partial x}\right) + \frac{\partial}{\partial x}\left(\dot{m}''_g h_g\right) - Q_P\left(-\frac{\partial \rho}{\partial t}\right)$

where Q_P is the heat of pyrolysis; positive for endothermic decomposition and negative for exothermic decomposition.

$\rho_a h_a = \sum_{j=1}^{3} X_j \rho_{a,j} h_{a,j}$ is the total enthalpy of the active part and

$\rho_C h_C = \sum_{j=1}^{3} X_j \rho_{C,j} h_{C,j}$ is the total enthalpy of char. The subscript "a" is for active part, "c" is for char, and "g" is for gas.

5.3.1 FORTRAN Model Input properties

Use input of Nylon as an example.

Ambient temperature (K)	298
Sample thickness (m)	0.024, 0.008, 0.004, 0.0016
Virgin density (kg/m3)	1136
Char fraction	0.017
Final density (kg/m3)	0.017x1136
Activation energy (J/mol)	2.4E+5
Pre-exponential factor (1/s)	1.1E+19
Incident heat flux (W/m2)	50×10^3
Flame heat flux (W/m2)	5×10^3
Heat transfer coefficient (W/m2K)	10
Emissivity	1.0

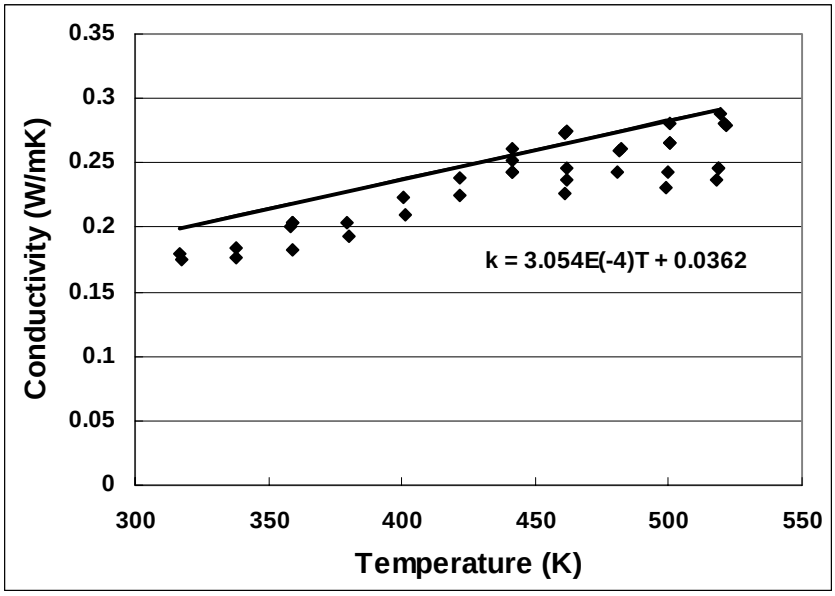

Fig. 5.3.1 Conductivity of Nylon

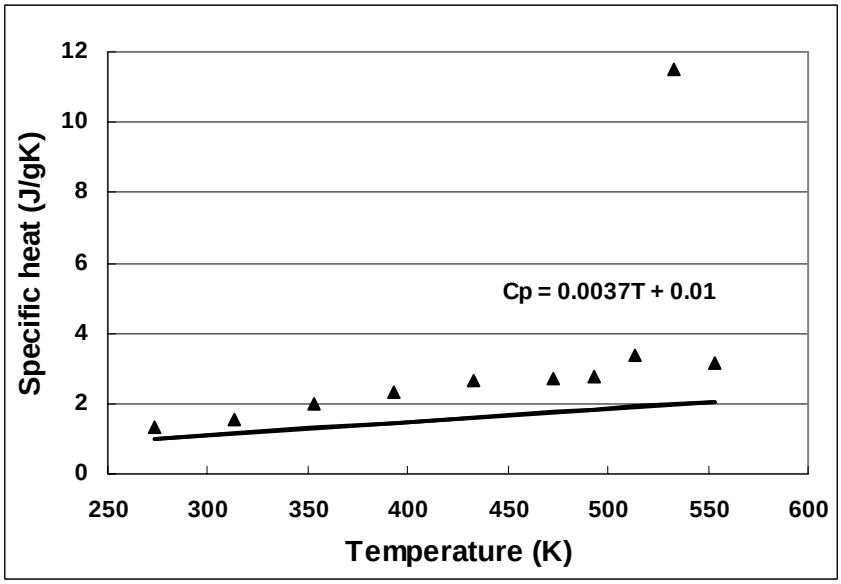

Fig. 5.3.2 Specific heat of Nylon

The other two thermal properties are thermal conductivity and specific heat. These are shown in Fig. 5.3.1 and Fig. 5.3.2, the dot data are from NIST [11]. A linear equation is used in the former FORTRAN program. Since the linear properties used in the FORTRAN program still match well with the data from NIST for Nylon, and

the aim of this simulation is to qualitatively show the thickness effect. I still used the linear properties written for former use.

5.3.2 Results analysis

Comparison of data from experiment and result from Fortran model. Use 8mm Nylon +5%clay under 50kW/m^2 as an example.

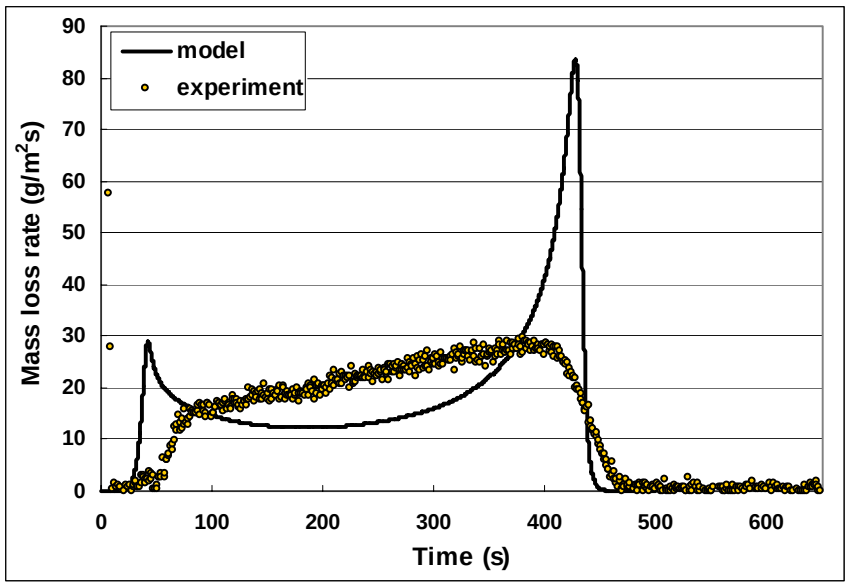

Fig. 5.3.3 8mm Nylon +5%clay under 50kW/m^2

There are three factors, which can affect the result.

(1) Thickness effect

Fig. 5.3.4 shows the mass loss rate of Nylon+5%clay with different thickness. They are the results of FORTRAN program simulation. Fig. 5.3.5 shows the experimental results for the same material. Comparing these two figures, the trend of thickness effect is the same. A thicker sample has a lower mass loss rate. The big jump for each

curve in Fig. 5.3.4 is from the back face insulation boundary condition. It is caused by the math simulation.

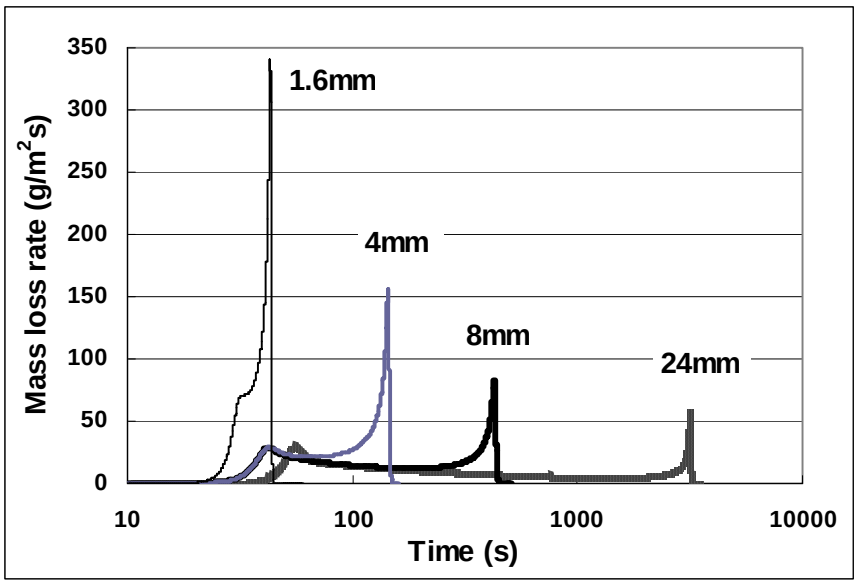

Fig. 5.3.4 Nylon+5%clay with different thickness from simulation

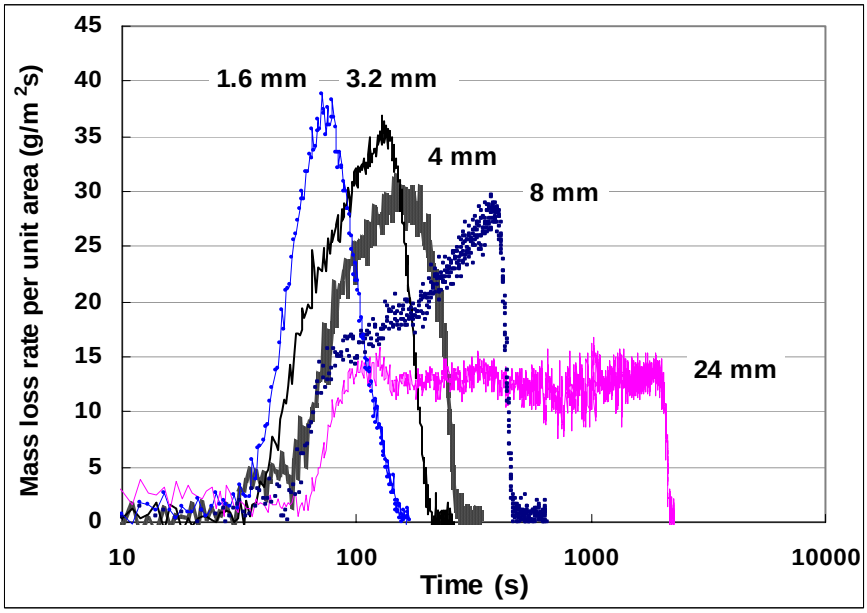

Fig. 5.3.5 Different thickness Nylon+5%clay under 53+/-3 kW/m^2 from experiments

(2) E_a and a_p effect

Since different α (0.25, 0.5 and 0.75) brings different set of E_a and a_p. The curve calculated by different E_a and a_p may be different too. Use the value of 8mm Nylon +5%clay under 50kW/m^2 as an example.

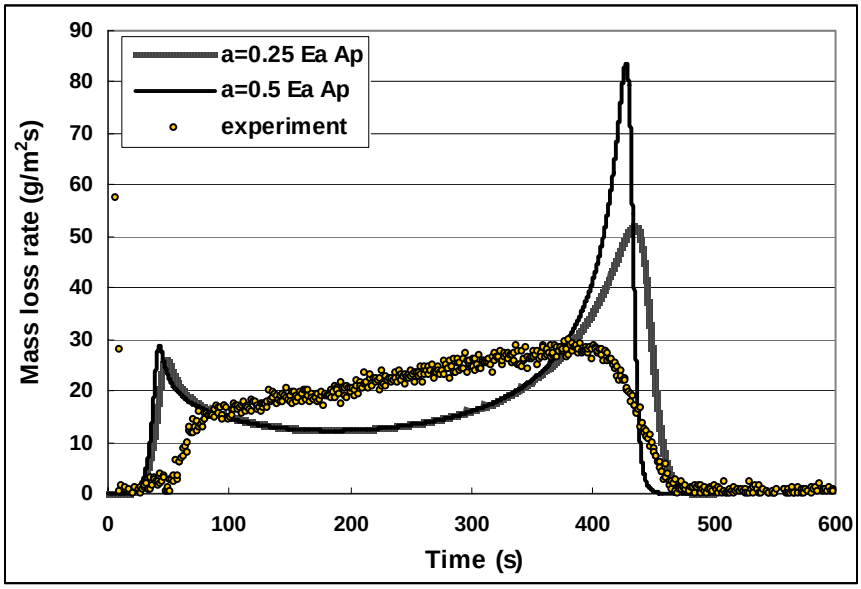

Fig. 5.3.6 Results comparison of different set of E_a and a_p
8mm Nylon +5%clay under 50kW/m^2

Shown in Fig. 5.3.6, smaller α has lower value of E_a and a_p, thus mass loss rate is smaller.

(3) Effect of heat of pyrolysis

Q_P is the heat of pyrolysis; positive for endothermic decomposition and negative for exothermic decomposition. It is an unknown for my samples. I changed this value from a large positive number to a large negative number to see if it could affect the final results.

Seen in Fig. 5.3.7, change the solid heat of pyrolysis setting in the program, with Q_P = 1500 J/kg (Endothermic), Q_P = 0 and Q_P = -1500 J/kg (Exothermic). The result doesn't show much difference. Therefore, I used Q_P = 0 for all simulations.

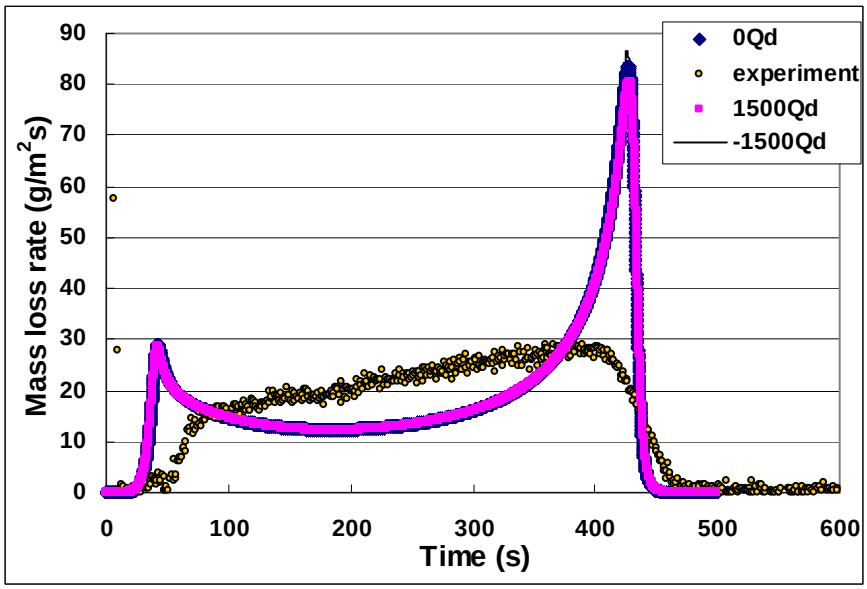

Fig. 5.3.7 Results comparison of different heat of pyrolysis
8mm Nylon+5%clay under 50kW/m^2

Chapter 6: Conclusions

Polymer layered-silicate (clay) nanocomposites have the unique combination of reduced flammability and improved physical properties. A summary of the properties is listed in Table 6.1. The heats of combustion and gasification pertain to heat release rate (fire power) potential, and the ignition temperature and thermal properties pertain to flame spread and ignition behavior.

1. Char yield will inhibit burning rate, but could enhance flame spread by providing a low-density matrix of fuel over a melted pool. It is clear from these properties that residue fraction is an important effect. It influences the heat of combustion slightly, but drops the peak burning rate or heat release rate considerably. For example, at a heat flux of about 40 kW/m^2, pure nylon peaks at about 1500 kW/m^2, at about 900 kW/m^2 for 2 % clay, and about 600 kW/m^2 at 5 %. However, the total energy available for a given thickness remains virtually unchanged.

2. The ignition characteristics remain virtually unchanged as the ignition temperature is insensitive to the additive, but the addition of clay shows that there is an effective increase for the $k\rho c$ despite the formation of char in the addition of clay.

3. The thickness of the sample also affects ignition behavior. A thicker sample needs a longer time to get ignited. The thick sample has a higher heat of gasification, because more energy is needed to bring the material from its original temperature

to its evaporation temperature. Due to the higher heat of gasification of the thicker sample, mass loss rate is reduced.

4. Insulation of the back face causes the storage of energy, which can suddenly increase the mass loss rate at the final stage of burning. The primary effect of the char is to provide a blockage to the heat flux, probably by the reduction of conduction and radiation, and this causes the second peak during the backing effect to be significantly reduced by the addition of clay.

5. A theoretical solid phase model accounting for kinetic decomposition, and heat and mass transfer of nanocomposites subjected to a radiant heat source has been used. The model includes variations of thermal properties of sample and char. Comparisons between the theoretical and experimental mass loss rate are given. The theoretical values agree reasonably well with the experiments.

From the point of view of a fire protection engineer, the improvements with the clay loading into this nanocomposite material is satisfied. First, the ignition time is increased, which means during a real fire, the escape time is increased. More people can get survived. Second, the total amount of energy is not changing by adding clay, but the peak heat release rate is greatly reduced. It can lower the risk of occurrence of flash over. This is an important factor of the safety of human during fire. No flash over, no sudden increase in fire growth. Small fire can be put out more easily than

large fire. Although the material ignition properties are not affected much by the clay loading, the fire proof ability is improved satisfactorily.

Table 6.1 Summary of the properties

	Nylon	Nylon +2%clay	Nylon +5%clay
8 mm samples			
Δh_c,sec.*peak avg.* (kJ/g)	32.5	29.3	28.4
$\dot{q}''_{cr}$ (kW/m^2)	<24	<26	<26
T_{ig} (°C)	447≈450	467≈470	467≈470
$k\rho c$ (kW/m^{2}K)^{2}s)	0.83	1.02	0.81
L (kJ/g), second peak	2.17	3.85	2.34
char fraction χ_c%	≈0	1.83~2.1	4.19~4.96
total HRR Q'' (MJ/m^3)	31.9	31.1	29.8
4 mm samples			
Δh_c,sec.*peak avg.* (kJ/g)	33	29.6	28.8
$\dot{q}''_{cr}$ (kW/m^2)	<26	<26.5	<26.5
T_{ig} (°C)	467 ≈470	472 ≈470	472 ≈470
$k\rho c$ (kW/m^{2}K)^{2}s)	0.71	1.21	1.32
L (kJ/g), second peak	2.25	1.77	3.6
char fraction χ_c	≈0	1.44~1.93	3.86~4.81
total HRR Q'' (MJ/m^3)	34.4	32.9	32.6
3.2 mm samples			
Δh_c,sec.*peak avg.* (kJ/g)	33.7	29.7	29.3
$\dot{q}''_{cr}$ (kW/m^2)	≤19	≤20	≤20
T_{ig} (°C)	452≈450	457≈460	457≈460
$k\rho c$ (kW/m^{2}K)^{2}s)	0.82	1.53	1.53
L (kJ/g),second peak	2.63	1.92	1.85
char fraction χ_c	0~1.2	0.6~1.9	4.0~4.8
total HRR Q'' (MJ/m^3)	31.2	30.2	34.5
1.6 mm samples			
Δh_c,sec.*peak avg.* (kJ/g)	30.1	30.2	29.0
$\dot{q}''_{cr}$ (kW/m^2)	≤19	≤19	≤17.5
T_{ig} (°C)	446.6≈450	446.6≈450	430
$k\rho c$ (kW/m^{2}K)^{2}s)	0.52	1.47	1.45
L (kJ/g),second peak	2.27	1.7	1.7
char fraction χ_c	0~1.0	1.0~3.0	4.0~5.0
total HRR Q'' (MJ/m^2)	33.5	37.5	37.7

Reference

1. J. W.Gilman, T.K., A. B. Morgan, R.H. Harris, L. Brassell, and a.C.L.J. M. VanLandingham, *Flammability of Polymer Clay Nanocomposites Consortium: Year One Annual Report*. 2000, National Institute of Standards and Technology: Gaithersburg, MD.
2. D. Hopkins, J.a.J.G.Q., *Material fire properties and predictions for thermoplastics.* Fire Safety Journal, 1996. **26**(3): p. 241-268.
3. Giannelis, E.P., *Polymer Layered Silicate Nanocomposites.* Advanced Materials, 1995.
4. S. E. Dillon, W.H.K.a.J.G.Q., *Determination of Properties and the Prediction of the Energy Release Rate of Materials in the ISO 9705 Room-Corner Test*. 1998, National Institute of Standards and Technology: Gaithersburg, MD.
5. T. Kashiwagi, R.H.H., X. Zhang, R. M. Briber, B. H. Cipreiano, S. R. Raghavan, W. H. Awad, J. R. Shields, *Flame retardant mechanism of polyamide 6-clay nanocomposites.* Polymer, 2004.
6. Henry Margenau, G.M.M., *The Mathematics of Physics and Chemistry*, ed. S. Edition.
7. Janssens, M., *Calorimetry*, in *SFPE Handbook of Fire Protection Engineering*.
8. Marc Jannssens, W.J.P., *Oxygen Consumption Calorimetry*, in *Heat Release in Fires*, V.B.a.S.J. Grayson, Editor, Elsevier Applied Science: London, New York.
9. Quintiere, J.G., *Fundamentals of Fire Phenomena*. 2002.
10. ASTME1354-90, *Standard Test Method for Heat and Visible Smoke Release Rates for Materials and Products Using and Oxygen Consumption Calorimeter*, in *Annual Book of ASTM Standards*, A.S.f.T.a. Materials, Editor. 1990: Philadelphia. p. 803-817.
11. Kashiwagi, T., *Private Communication: TGA data for Nylon and Nylon+5%clay with a series of constant heating rates*. 2004.
12. M.J. Spearpoint, J.G.Q., *Predicting the piloted ignition of wood in the cone calorimeter using an integral model - effect of species, grain orientation and heat flux.* Fire Safety Journal, 2000. **36**(2001): p. 391-415.
13. Boonmee, N., *Theoretical and Experimental Study of Autoignition of Wood*, in *Fire Protection Engineering*. 2004, University of Maryland: College Park. p. 88.
14. DeWitt, F.P.I.a.D.P., *Fundamentals of Heat and Mass Transfer.* p. 487.
15. Bohn, F.K.a.M.S., *Principles of Heat Transfer.* p. 314.
16. Bohn, F.K.a.M.S., *Principles of Heat Transfer.* p. 439.
17. DeWitt, F.P.I.a.D.P., *Introduction to Heat transfer.* 1990: p. Page524.

Appendix A Method for Measuring Heat Release Rate

Materials are exposed to controlled levels of radiant heating, with or without an external igniter. Products and responses of the materials are measured. This method is used to determine the ignitability, heat release rate, mass loss rate, and the effective heat of combustion of the materials. The rate of heat release is found by measurement of the oxygen consumption as determined from the oxygen concentration and the flow rate in the exhaust product stream. The effective heat of combustion is determined by combining the specimen's mass loss rate and its heat release rate. This method is called the oxygen consumption method.

In 1917 Thornton showed that, for a large number of organic liquids and gases, a more or less constant net amount of heat is released per unit mass of oxygen consumed for complete combustion. Thornton's rule implies that it is sufficient to measure the oxygen consumed in a combustion system in order to determine the net heat released [8] .

In the literature, such as ASTM E1354-99 and Section 3/Chapter 2 of the SFPE Handbook, the heat release equation based on oxygen consumption method is given:

$$\dot{Q} = \Delta h_{O_2} \left[\frac{\phi}{1 + \phi(\alpha - 1)} \right] \dot{m}_e \frac{M_{O_2}}{M_a} X_{O_2}^0 (1 - X_{H_2O}^0 - X_{CO_2}^0) \qquad \text{(A.1)}$$

$$\text{with } \phi = \frac{X_{O_2}^0 - X_{O_2}}{(1 - X_{O_2}) X_{O_2}^0}$$

where ϕ=oxygen depletion factor

α =volumetric expansion factor

These sources give the heat release equation with an average value for the expansion factor ($\alpha = 1.105$).

In the analysis below, the same oxygen consumption measurement method is used to determine the heat release rate equation but with a different analysis procedure. By comparing this heat release equation with Eq. (A.1) shown in the ASTM standard, one can find how the expansion factor α can vary by material.

In this method, only O_2 is measured. All water vapor (by a cooling unit and a moisture sorbent) and CO_2 (by a chemical sorbent) must be removed from the sample stream before O_2 is measured. This leads to the assumption that the sample gas only consists of O_2 and N_2. Another assumption is that CO production is negligible. These assumptions are consistent with the literature.

Heat release rate can be calculated either by fuel consumption or by oxygen consumption:

$$\dot{Q} = \dot{m}_F \Delta h_c = \dot{m}_{O_2,used} \Delta h_{O_2} \quad \text{(A.2)}$$

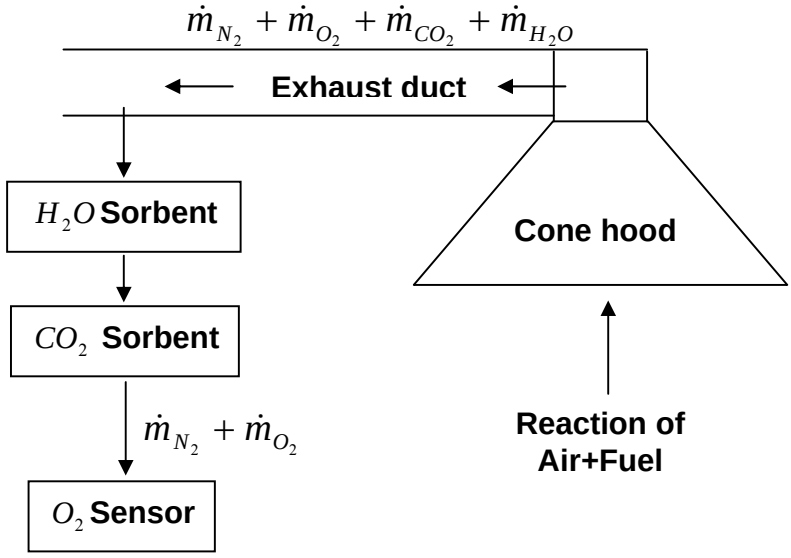

Fig.A.1 Equipment arrangement for O_2 measurement

Mass conservation:

$$\dot{m}_e = \dot{m}_a + \dot{m}_F$$

where $\dot{m}_a$ = Mass flow rate of the incoming air (kg/s)

$\dot{m}_F$ = Mass flow rate of the fuel gas (kg/s)

$\dot{m}_e$ = Mass flow rate in the exhaust duct (kg/s)

Oxygen conservation:

$$\dot{m}_{O_2,used} = \dot{m}^0_{O_2} - \dot{m}_{O_2} = \dot{m}_a Y_{O_2,\infty} - \dot{m}_e Y_{O_2}$$

$$= (\dot{m}_e - \dot{m}_F) Y_{O_2,\infty} - \dot{m}_e Y_{O_2} = \dot{m}_e (Y_{O_2,\infty} - Y_{O_2}) - \dot{m}_F Y_{O_2,\infty} \qquad \text{(A.3)}$$

$\dot{m}^0_{O_2}$ = Mass flow rate of O_2 in the incoming air (kg/s)

$\dot{m}_{O_2}$ = Mass flow rate of O_2 in the exhaust duct (kg/s)

$Y_{O_2,\infty}$ = Measured mass fraction of O_2 in the incoming air

Y_{O_2} = Measured mass fraction of O_2 in the exhaust gases

Chemical equation:

$$\nu_F F + \nu_{O_2} O_2 \rightarrow \nu_{H_2O} H_2O + \nu_{CO_2} CO_2$$

The exhaust gas is a mixture, including CO_2, H_2O, N_2, O_2 etc.

Exhaust gas: $\dot{m}_{CO_2} = \dot{m}_e Y_{CO_2}$ (A.4)

$$\dot{m}_{H_2O} = \dot{m}_e Y_{H_2O} \quad \text{(A.5)}$$

$\dot{m}_{CO_2}$ = Mass flow rate of CO_2 in the exhaust duct (kg/s)

$\dot{m}_{H_2O}$ = Mass flow rate of H_2O in the exhaust duct (kg/s)

Y_{CO_2} = Measured mass fraction of CO_2 in the exhaust gases

Y_{H_2O} = Measured mass fraction of H_2O in the exhaust gases

CO_2 and water vapor are absorbed before the O_2 in the exhaust gas is measured:

$$\dot{m}_e Y_{O_2} = (\dot{m}_e - \dot{m}_{CO_2} - \dot{m}_{H_2O}) Y'_{O_2} \quad \text{(A.6)}$$

Y'_{O_2} is the mass fraction in the oxygen analyzer after CO_2 and H_2O are removed from the exhaust gas. The gas going through oxygen analyzer only consists of O_2 and N_2.

Substitute Eq.(A.4) and (A.5) into Eq.(A.6)

$$Y_{O_2} = (1 - Y_{CO_2} - Y_{H_2O}) Y'_{O_2} \quad \text{(A.7)}$$

For the stoichiometric chemical reaction:

$$\nu_F F + \nu_{O_2} O_2 \rightarrow \nu_{H_2O} H_2O + \nu_{CO_2} CO_2$$

$$\frac{\nu_F}{\nu_{CO_2}} = \frac{\frac{\dot{m}_F}{M_F}}{\frac{\dot{m}_{CO_2}}{M_{CO_2}}} \qquad \Rightarrow \dot{m}_{CO_2} = \frac{\nu_{CO_2} M_{CO_2}}{\nu_F M_F} \dot{m}_F \tag{A.8}$$

$$\frac{\nu_F}{\nu_{H_2O}} = \frac{\frac{\dot{m}_F}{M_F}}{\frac{\dot{m}_{H_2O}}{M_{H_2O}}} \qquad \Rightarrow \dot{m}_{H_2O} = \frac{\nu_{H_2O} M_{H_2O}}{\nu_F M_F} \dot{m}_F \tag{A.9}$$

where M is the molecular weight.

Eq.(A.4) and (A.5) show the composition of the exhaust gas :

$$\dot{m}_{CO_2} = \dot{m}_e Y_{CO_2}$$

$$\dot{m}_{H_2O} = \dot{m}_e Y_{H_2O}$$

Consequently, Eq.(A.8) and (A.9) become:

$$\dot{m}_{CO_2} = \dot{m}_e Y_{CO_2} = \frac{\nu_{CO_2} M_{CO_2}}{\nu_F M_F} \dot{m}_F \qquad \Rightarrow Y_{CO_2} = \frac{(\frac{\nu_{CO_2}}{\nu_F})(\frac{M_{CO_2}}{M_F})}{\dot{m}_e} \dot{m}_F \tag{A.10}$$

$$\dot{m}_{H_2O} = \dot{m}_e Y_{H_2O} = \frac{\nu_{H_2O} M_{H_2O}}{\nu_F M_F} \dot{m}_F \qquad \Rightarrow Y_{H_2O} = \frac{(\frac{\nu_{H_2O}}{\nu_F})(\frac{M_{H_2O}}{M_F})}{\dot{m}_e} \dot{m}_F \tag{A.11}$$

Combining Eq.(A.2) and (A.3)

$$\dot{Q} = [\dot{m}_e (Y_{O_2,\infty} - Y_{O_2}) - \dot{m}_F Y_{O_2,\infty}] \Delta h_{O_2}$$

$$\xrightarrow{Eq.(A.7)}$$

$$\dot{Q} = [\dot{m}_e Y_{O_2,\infty} - \dot{m}_e (1 - Y_{CO_2} - Y_{H_2O}) Y'_{O_2} - \dot{m}_F Y_{O_2,\infty}] \Delta h_{O_2}$$

$$= [\dot{m}_e (Y_{O_2,\infty} - Y'_{O_2}) + \dot{m}_e Y_{CO_2} Y'_{O_2} + \dot{m}_e Y_{H_2O} Y'_{O_2} - \dot{m}_F Y_{O_2,\infty}] \Delta h_{O_2}$$

$$\xrightarrow{Eq.(A.10)Eq(A.11)}$$

$$\dot{Q} = [\dot{m}_e (Y_{O_2,\infty} - Y'_{O_2}) + (\frac{\nu_{CO_2}}{\nu_F})(\frac{M_{CO_2}}{M_F}) \dot{m}_F Y'_{O_2} + (\frac{\nu_{H_2O}}{\nu_F})(\frac{M_{H_2O}}{M_F}) \dot{m}_F Y'_{O_2} - \dot{m}_F Y_{O_2,\infty}] \Delta h_{O_2}$$

(A.12)

The stoichiometric ratio is defined as

$$r_{CO_2} = \frac{m_{CO_2}}{m_F} = \frac{\nu_{CO_2}}{\nu_F} \frac{M_{CO_2}}{M_F} \tag{A.13}$$

$$r_{H_2O} = \frac{m_{H_2O}}{m_F} = \frac{\nu_{H_2O}}{\nu_F} \frac{M_{H_2O}}{M_F} \tag{A.14}$$

$$\Delta h_{O_2} = \frac{\Delta h_c}{r_{O_2}} \tag{A.15}$$

Substitute Eq.(A.13), (A.14) and (A.15) into (A.12), and the heat release equation becomes:

$$\dot{Q} = [\dot{m}_e (Y_{O_2,\infty} - Y'_{O_2}) + (r_{CO_2} + r_{H_2O}) \dot{m}_F Y'_{O_2} - \dot{m}_F Y_{O_2,\infty}] \frac{\Delta h_c}{r_{O_2}}$$

All of the mass fractions (Y) are converted to mole fractions in the heat release equation because oxygen sensor can only output the mole fraction of oxygen.

$$Y_{O_2,\infty} = \frac{X^0_{O_2}}{M_a} \qquad\qquad Y'_{O_2} = \frac{X_{O_2}}{M_e}$$

$X^0_{O_2}$ Measured mole fraction of O_2 in the incoming air

X_{O_2} Measured mole fraction of O_2 in the exhaust gases

$$\dot{Q} = \dot{m}_e (\frac{X_{O_2}^0}{M_a} - \frac{X_{O_2}}{M_e}) M_{O_2} \frac{\Delta h_c}{r_{O_2}} + \dot{m}_F (r_{CO_2} + r_{H_2O}) \frac{X_{O_2} M_{O_2}}{M_e} \frac{\Delta h_c}{r_{O_2}} - \dot{m}_F Y_{O_2,\infty} \frac{\Delta h_c}{r_{O_2}}$$

(A.16)

Because $\dot{m}_F \Delta h_c = \dot{Q}$, with the assumption $M_e \approx M_a$, Eq. (A.16) becomes

$$\dot{Q} = \frac{\Delta h_c}{r_{O_2}} \dot{m}_e (\frac{M_{O_2}}{M_a})(X_{O_2}^0 - X_{O_2}) + \dot{Q} \frac{r_{CO_2} + r_{H_2O}}{r_{O_2}} (\frac{M_{O_2}}{M_a}) X_{O_2} - \dot{Q} \frac{Y_{O_2,\infty}}{r_{O_2}}$$

$$\Downarrow$$

$$\dot{Q}[1 - \frac{r_{CO_2} + r_{H_2O}}{r_{O_2}} (\frac{M_{O_2}}{M_a}) X_{O_2} + \frac{Y_{O_2,\infty}}{r_{O_2}}] = \frac{\Delta h_c}{r_{O_2}} \dot{m}_e (\frac{M_{O_2}}{M_a})(X_{O_2}^0 - X_{O_2})$$

$$\Downarrow$$

$$\dot{Q} = \frac{\Delta h_c}{r_{O_2}} \dot{m}_e (\frac{M_{O_2}}{M_a}) \frac{X_{O_2}^0 - X_{O_2}}{1 + \frac{Y_{O_2,\infty}}{r_{O_2}} - \frac{r_{CO_2} + r_{H_2O}}{r_{O_2}} (\frac{M_{O_2}}{M_a}) X_{O_2}}$$

(A.17)

In the heat release rate Eq. (A.17), for a given fuel, the molecular weights and stoichiometric ratios are known. The mole fraction of O_2 in the incoming air $X_{O_2}^0$ and the mole fraction of O_2 in the exhaust gases X_{O_2} can be measured by the oxygen sensor. The only unknown is the mass flow rate in the exhaust duct $\dot{m}_e$.

Flow Rate Measurements

The exhaust mass flow rate can be measured via the pressure drop across and temperature at an orifice plate in the exhaust duct:

$$\dot{m}_e = C \sqrt{\frac{\Delta P}{T_e}}$$

(A.18)

where $\dot{m}_e =$ Mass flow rate in the exhaust duct ($kg \cdot s^{-1}$)

C = Orifice plate coefficient ($kg^{1/2} \cdot m^{1/2} \cdot K^{1/2}$)

$\Delta p =$ Pressure drop across the orifice plate (Pa)

$T_e =$ Gas temperature at the orifice plate (K)

Substitute Eq. (A.18) into (A.17) and the heat release equation becomes

$$\dot{Q} = \frac{\Delta h_c}{r_{O_2}} \left(C \sqrt{\frac{\Delta P}{T_e}} \right) \left(\frac{M_{O_2}}{M_a} \right) \frac{X_{O_2}^0 - X_{O_2}}{1 + \frac{Y_{O_2,\infty}}{r_{O_2}} - \frac{r_{CO_2} + r_{H_2O}}{r_{O_2}} \left(\frac{M_{O_2}}{M_a} \right) X_{O_2}} \tag{A.19}$$

In ASTM E1354 P836, an average value of expansion factor is used (α=1.105) for Eq.(A.1), and the heat release equation is simplified with $\frac{M_{O_2}}{M_a} \approx 1.10$, $X_{O_2}^0 = 0.21$.

The final version of this equation found in ASTM E1354 P836 is:

$$\dot{Q} = \frac{\Delta h_c}{r_{O_2}} \left(C \sqrt{\frac{\Delta p}{T_e}} \right) 1.10 \frac{X_{O_2}^0 - X_{O_2}}{1.105 - 1.5 X_{O_2}} \tag{A.20}$$

In reference [8], heat release rate is shown as

$$\dot{Q} = \Delta h_{O_2} \left[\frac{\phi}{1 + \phi(\alpha - 1)} \right] \dot{m}_e \frac{M_{O_2}}{M_a} X_{O_2}^0$$

$$\text{with } \phi = \frac{X_{O_2}^0 - X_{O_2}}{(1 - X_{O_2}) X_{O_2}^0}$$

After simplification of ϕ and $\frac{M_{O_2}}{M_a} \approx 1.10$, the equation becomes:

$$\dot{Q} = \left[\frac{\Delta h_c}{r_{O_2}} \left(C \sqrt{\frac{\Delta p}{T_e}} \right) 1.10 \right] \frac{X_{O_2}^0 - X_{O_2}}{\alpha - \left[1 + \frac{(\alpha - 1)}{X_{O_2}^0} \right] X_{O_2}} \tag{A.21}$$

Comparison of Eq. (A.21) and (A.20) with Eq. (A.19) shows only differences in the denominator. From this comparison, the expansion factor can be defined as $\alpha = 1 + \frac{Y_{O_2,\infty}}{r_{O_2}}$.

Calibration constant C

In order to use Eq. (A.19), (A.20) or (A.21), one must know the calibration constant C. The calibration constant C can be calculated from the heat release equation (A.19) based on methane.

$$\frac{M_{O_2}}{M_a} \approx 1.10$$

$$c = \frac{\dot{Q}}{(\frac{\Delta h_c}{r_{O_2}})} \sqrt{\frac{T_e}{\Delta P}} \frac{\left(\alpha - 1.10 \frac{r_{CO_2} + r_{H_2O}}{r_{O_2}} X_{O_2} \right)}{1.10(X_{O_2}^0 - X_{O_2})}$$

For methane,

$$\frac{\Delta h_c}{r_{O_2}} = 12.54 \times 10^3 \, kW / kgO_2$$

$$\frac{r_{CO_2} + r_{H_2O}}{r_{O_2}} = 1.25$$

$$\alpha = 1 + \frac{Y_{O_2,\infty}}{r_{O_2}} = 1 + \frac{0.233}{4} = 1.05825$$

The specification $\dot{Q} = 5.0$ is then made, based on ASTM E1354, where 5.0 corresponds to 5.0 kW methane supplied.

$$c = \frac{5.0}{12.54 \times 10^3} \sqrt{\frac{T_e}{\Delta P}} \frac{1.05825 - 1.375 X_{O_2}}{1.10(X_{O_2}^0 - X_{O_2})}$$

ASTM E1354 also suggests that the methane calibration be performed daily in order to check for the proper operation of the instrument and to compensate for minor changes in mass flow determination.

Proof of the definition for the expansion factor α

To get the definition of the expansion factor α, a stoichiometric chemical reaction is used in the above analysis to get the heat release rate equation. To prove the validity of the definition of expansion factor α, the same oxygen consumption method is used. Instead of the analysis of the stoichiometric chemical reaction, the heat release rate equation is found from the conservation of mass. The definition of α is also used in the analysis. If the final heat release equation appears the same as Eq.(20) in ASTM E1354 P836 or Eq.(21) in reference [8], then the definition for the expansion factor α given above is reasonable.

Start with the oxygen consumption method. Changes in the oxygen concentration found in the combustion gases can be used to determine the heat release rate

$$\dot{Q} = \Delta h_{O_2} \dot{m}_{O_2,used} = \Delta h_{O_2} (\dot{m}_{O_2}^0 - \dot{m}_{O_2}) .$$

Only O_2 is measured. All water vapor and CO_2 must be removed from the sample stream before this measurement is taken. The sample gas only consists of O_2 and N_2.

Before combustion: $$X_{O_2}^0 = \frac{\frac{\dot{m}_{O_2}^0}{M_{O_2}}}{\frac{\dot{m}_{O_2}^0}{M_{O_2}} + \frac{\dot{m}_{N_2}^0}{M_{N_2}}}, \quad \text{(A.22)}$$

$X_{O_2}^0$ = Initial reading from the oxygen analyzer before combustion

$\dot{m}_{O_2}^0$ = Mass flow rate of O_2 in the incoming air (kg/s)

$\dot{m}_{N_2}^0$ = Mass flow rate of the N_2 in the incoming air (kg/s)

After combustion: $$X_{O_2} = \frac{\frac{\dot{m}_{O_2}}{M_{O_2}}}{\frac{\dot{m}_{O_2}}{M_{O_2}} + \frac{\dot{m}_{N_2}}{M_{N_2}}}, \quad \text{(A.23)}$$

X_{O_2} = Reading during test from the oxygen analyzer.

$\dot{m}_{O_2}$ = Mass flow rate of the O_2 in the exhaust duct (kg/s)

$\dot{m}_{N_2}$ = Mass flow rate of the N_2 in the exhaust duct (kg/s)

As N_2 is conserved and does not participate in the combustion reactions, $\dot{m}_{N_2}^0$ is equal to $\dot{m}_{N_2}$. Rearranging Eq. (A.22) and (A.23) while subtracting Eq.(A.23) from Eq. (A.22) leads to:

$$\dot{m}_{O_2}^0 - \dot{m}_{O_2} = \left[\frac{X_{O_2}^0 - X_{O_2}}{\left(1 - X_{O_2}^0\right)\left(1 - X_{O_2}\right)} \right] \dot{m}_{N_2} \frac{M_{O_2}}{M_{N_2}} \quad \text{(A.24)}$$

Because all water vapor and CO_2 has been removed from the sample stream before O_2 is measured, the component of the sample gas (in terms of mole fraction) before combustion becomes:

$$X^0_{N_2} + X^0_{O_2}$$

$$X^0_{N_2} + X^0_{O_2} = \left(\frac{\dot{m}_a}{M_a}\right)\left(1 - X^0_{H_2O} - X^0_{CO_2}\right) = \frac{\frac{\dot{m}_{N_2}}{M_{N_2}}}{(1 - X^0_{O_2})} \tag{A.25}$$

$\dot{m}_a$ = Mass flow rate of the incoming air (kg/s)

$X^0_{O_2}$ = Mole fraction of O_2 in the incoming air

$X^0_{H_2O}$ = Mole fraction of H_2O in the incoming air

$X^0_{CO_2}$ = Mole fraction of CO_2 in the incoming air

Combining the right hand sides of Eq.(A.24) and Eq.(A.25) to cancel the $\frac{\frac{\dot{m}_{N_2}}{M_{N_2}}}{(1 - X^0_{O_2})}$ term, transforms Eq.(A.24) into the following:

$$\dot{m}^0_{O_2} - \dot{m}_{O_2} = \left[\frac{X^0_{O_2} - X_{O_2}}{\left(1 - X_{O_2}\right)}\right]\dot{m}_a \frac{M_{O_2}}{M_a}(1 - X^0_{H_2O} - X^0_{CO_2}) \tag{A.26}$$

According to the oxygen consumption principle, combining with Eq.(A.26), the heat release rate then becomes:

$$\dot{Q} = \Delta h_{O_2}\dot{m}_{O_2,used} = \Delta h_{O_2}(\dot{m}^0_{O_2} - \dot{m}_{O_2}) = \Delta h_{O_2}\left[\frac{X^0_{O_2} - X_{O_2}}{\left(1 - X_{O_2}\right)}\right]\dot{m}_a \frac{M_{O_2}}{M_a}(1 - X^0_{H_2O} - X^0_{CO_2}) \tag{A.27}$$

The mole fractions of H_2O ($X^0_{H_2O}$) and of CO_2 ($X^0_{CO_2}$) in the incoming air are both negligible.

The heat release rate equation is then shown as:

$$\dot{Q} = \Delta h_{O_2} \left[\frac{X^0_{O_2} - X_{O_2}}{\left(1 - X_{O_2}\right)} \right] \dot{m}_a \frac{M_{O_2}}{M_a} \tag{A.28}$$

The oxygen depletion factor ϕ is defined as in reference [8]

$$\phi = \frac{\dot{m}^0_{O_2} - \dot{m}_{O_2}}{\dot{m}^0_{O_2}} = \frac{X^0_{O_2} - X_{O_2}}{(1 - X_{O_2}) X^0_{O_2}}$$

An assumption is required regarding the expansion due to combustion of the fraction of the air that is fully depleted of its oxygen (See ASTM E1354 Page 838 and "Heat Release in Fires", Chapter 3). This expansion depends on the composition of the fuel and the actual stoichiometry of the combustion.

The expansion factor is defined as $\alpha = 1 + \frac{Y_{O_2,\infty}}{r_{O_2}}$ (As gained from former analysis)

For the stoichiometric reaction, the stoichiometric ratio is

$$r_{O_2} = \frac{m_{O_2}}{m_F} = \frac{\dot{m}_{O_2,used}}{\dot{m}_F}$$

Substituting r_{O_2} into α

$$\alpha = 1 + \frac{Y_{O_2,\infty} \dot{m}_F}{\dot{m}_{O_2,used}} = 1 + \frac{Y_{O_2,\infty} \dot{m}_F}{\dot{m}^0_{O_2} - \dot{m}_{O_2}} = \frac{\dot{m}^0_{O_2} + Y_{O_2,\infty} \dot{m}_F - \dot{m}_{O_2}}{\dot{m}^0_{O_2} - \dot{m}_{O_2}}$$

Mass conservation: $\dot{m}_e = \dot{m}_a + \dot{m}_F$

$$\dot{m}^0_{O_2} = \dot{m}_a Y_{O_2,\infty}$$

$$\alpha = \frac{\dot{m}_a Y_{O_2,\infty} + Y_{O_2,\infty}\dot{m}_F - \dot{m}_{O_2}}{\dot{m}^0_{O_2} - \dot{m}_{O_2}} = \frac{Y_{O_2,\infty}(\dot{m}_a + \dot{m}_F) - \dot{m}_{O_2}}{\dot{m}^0_{O_2} - \dot{m}_{O_2}} = \frac{Y_{O_2,\infty}\dot{m}_e - \dot{m}_{O_2}}{\dot{m}^0_{O_2} - \dot{m}_{O_2}}$$

$$\alpha - 1 = \frac{Y_{O_2,\infty}\dot{m}_e - \dot{m}_{O_2}}{\dot{m}^0_{O_2} - \dot{m}_{O_2}} - 1 = \frac{Y_{O_2,\infty}\dot{m}_e - \dot{m}^0_{O_2}}{\dot{m}^0_{O_2} - \dot{m}_{O_2}} \tag{A.29}$$

Multiplying each side of Eq.(A.29) by $\frac{\dot{m}^0_{O_2} - \dot{m}_{O_2}}{\dot{m}^0_{O_2}}$ and substituting $\dot{m}^0_{O_2} = \dot{m}_a Y_{O_2,\infty}$

$$(\alpha - 1)\frac{\dot{m}^0_{O_2} - \dot{m}_{O_2}}{\dot{m}^0_{O_2}} = \frac{Y_{O_2,\infty}\dot{m}_e - \dot{m}^0_{O_2}}{\dot{m}^0_{O_2}} = \frac{Y_{O_2,\infty}\dot{m}_e - \dot{m}_a Y_{O_2,\infty}}{\dot{m}_a Y_{O_2,\infty}} \tag{A.30}$$

Canceling $Y_{O_2,\infty}$ from the right hand side of Eq.(A.30)

$$(\alpha - 1)\frac{\dot{m}^0_{O_2} - \dot{m}_{O_2}}{\dot{m}^0_{O_2}} = \frac{\dot{m}_e - \dot{m}_a}{\dot{m}_a} \tag{A.31}$$

Substituting $\phi = \frac{\dot{m}^0_{O_2} - \dot{m}_{O_2}}{\dot{m}^0_{O_2}}$ into Eq.(A.31)

$$(\alpha - 1)\dot{m}_a\phi = \dot{m}_e - \dot{m}_a \tag{A.32}$$

Rearranging Eq.(A.32)

$$\dot{m}_a = \frac{\dot{m}_e}{1 + (\alpha - 1)\phi} \tag{A.33}$$

This relationship between $\dot{m}_a$ and $\dot{m}_e$ is important, because the mass flow rate of the incoming air can not be measured; however one can measure the exhaust flow rate in the exhaust duct.

Substituting Eq.(A.33) into Eq. (A.28)

$$\dot{Q} = \Delta h_{O_2}\left[\frac{\phi}{1 + \phi(\alpha - 1)}\right]\dot{m}_e \frac{M_{O_2}}{M_a} X^0_{O_2} \tag{A.34}$$

Substituting the measured mass flow rate $\dot{m}_e = C\sqrt{\frac{\Delta p}{T_e}}$ into Eq.(A.34)

The heat release rate equation becomes:

$$\dot{Q} = \Delta h_{O_2}\left[\frac{\phi}{1+\phi(\alpha-1)}\right]\left(C\sqrt{\frac{\Delta p}{T_e}}\right)\frac{M_{O_2}}{M_a}X_{O_2}^0 \tag{A.35}$$

For the stoichiometric reaction, $\Delta h_{O_2} = \frac{\Delta h_c}{r_{O_2}}$

Rearranging Eq.(A.35) with $\phi = \frac{X_{O_2}^0 - X_{O_2}}{(1-X_{O_2})X_{O_2}^0}$

$$\dot{Q} = \left[\frac{\Delta h_c}{r_{O_2}}\left(C\sqrt{\frac{\Delta p}{T_e}}\right)\frac{M_{O_2}}{M_a}\right]\frac{\phi X_{O_2}^0}{1+\phi(\alpha-1)}$$

$$= \left[\frac{\Delta h_c}{r_{O_2}}\left(C\sqrt{\frac{\Delta p}{T_e}}\right)\frac{M_{O_2}}{M_a}\right]\frac{\frac{X_{O_2}^0 - X_{O_2}}{1-X_{O_2}}}{1+\frac{X_{O_2}^0 - X_{O_2}}{(1-X_{O_2})X_{O_2}^0}(\alpha-1)}$$

$$= \left[\frac{\Delta h_c}{r_{O_2}}\left(C\sqrt{\frac{\Delta p}{T_e}}\right)\frac{M_{O_2}}{M_a}\right]\frac{X_{O_2}^0 - X_{O_2}}{1-X_{O_2}+(1-\frac{X_{O_2}}{X_{O_2}^0})(\alpha-1)}$$

$$\Downarrow$$

$$\dot{Q} = \left[\frac{\Delta h_c}{r_{O_2}}\left(C\sqrt{\frac{\Delta p}{T_e}}\right)\frac{M_{O_2}}{M_a}\right]\frac{X_{O_2}^0 - X_{O_2}}{\alpha - \left[1+\frac{(\alpha-1)}{X_{O_2}^0}\right]X_{O_2}} \tag{A.36}$$

In ASTM E1354 P836, an average value of α =1.105 is used.

With $\frac{M_{O_2}}{M_a} \approx 1.10$, $X_{O_2}^0 = 0.21$, Eq.(A.36) becomes

$$\dot{Q} = \frac{\Delta h_c}{r_{O_2}} \left(C \sqrt{\frac{\Delta p}{T_e}} \right) 1.10 \frac{X_{O_2}^0 - X_{O_2}}{1.105 - 1.5 X_{O_2}}$$

This form is identical to the equation found on ASTM E1354 Page 836.

In conclusion, the definition for the expansion factor $\alpha = 1 + \frac{Y_{O_2,\infty}}{r_{O_2}}$ is reasonable.

In Table A, values of α and $1 + \frac{(\alpha - 1)}{X_{O_2}^0}$ are listed for different fuels. These values come from Eq.(A.19) with the stoichiometric ratios.

$$\alpha = 1 + \frac{Y_{O_2,\infty}}{r_{O_2}}$$

$$1 + \frac{(\alpha - 1)}{X_{O_2}^0} = \frac{r_{CO_2} + r_{H_2O}}{r_{O_2}} \left(\frac{M_{O_2}}{M_a} \right)$$

Table A Coefficient for different fuel

Fuel	**Formula**	α	$1+\frac{(\alpha-1)}{X_{O_2}^0}$
Normal Alkanes			
Methane	CH4	1.05825	1.375
Ethane	C2H6	1.062411	1.394643
Propane	C3H8	1.064075	1.4025
Butane	C4H10	1.064971	1.406731
Pentane	C5H12	1.065531	1.409375
Hexane	C6H14	1.065914	1.411184
Heptane	C7H16	1.066193	1.4125
Octane	C8H18	1.066405	1.4135
Nonane	C9H20	1.066571	1.414286
Decane	C10H22	1.066706	1.414919
Undecane	C11H24	1.066816	1.415441
Dodecane	C12H26	1.066909	1.415878
Tridecane	C13H28	1.066988	1.41625
Kerosene	C14H30	1.067055	1.41657
Hexadecane	C16H34	1.067166	1.417092
	AVG	1.065464	1.409058
Normal Alkenes			
Ethylene	C_2H_4	1.06793	1.4207
Propylene	C_3H_6	1.06793	1.4207
Butylene	C_4H_8	1.06793	1.4207
Pentene	C_5H_{10}	1.06793	1.4207
Hexene	C6H12	1.06793	1.4207
Heptane	C7H14	1.06793	1.4207
Octene	C8H16	1.06793	1.4207
Nonene	C9H18	1.06793	1.4207
Decene	C10H20	1.06793	1.4207
Dodecene	C12H24	1.06793	1.4207
Tridecene	C13H26	1.06793	1.4207
Tetradecene	C14H28	1.06793	1.4207
Hexadecene	C16H32	1.06793	1.4207
Octadecene	C18H36	1.06793	1.4207
	AVG	1.06793	1.4207
Normal Alkynes			
Acetylene	C2H2	1.075725	1.4575
Heptyne	C7H12	1.0699	1.43
Octyne	C8H14	1.069647	1.428804

Decyne	C10H18	1.069297	1.427155
Dodecyne	C12H22	1.069068	1.426071
	AVG	1.070727	1.433906
Arenes			
Benzene	C6H6	1.075725	1.4575
Toluene	C7H8	1.074431	1.451389
Ethylbenzene	C8H10	1.073506	1.447024
Xylene	C8H10	1.073506	1.447024
Propylbenzene	C9H12	1.072813	1.44375
Trimethylbenzene	C9H12	1.072813	1.44375
Cumene	C9H12	1.072813	1.44375
Butylbenzene	C10H14	1.072273	1.441204
Diethylbenzene	C10H14	1.072273	1.441204
p-Cymene	C10H14	1.072273	1.441204
Pentylbenzene	C11H16	1.071842	1.439167
Triethylbenzene	C12H18	1.071489	1.4375
	AVG	1.07298	1.444539
Polycarbonate	CH0.88O0.19	1.103097	1.586726
Polypropylene	CH	1.075649	1.453571
Polyvinylchloride	CH1.5Cl0.50	1.302597	1.411429
Nylon	CH1.8O0.17N0.17	1.119487	1.528718
GM21	CH1.8O0.30N0.05	1.113659	1.60439
Polyethylene	CH2	1.06793	1.4207

Appendix B Convective Heat Transfer Coefficient of the Cone Calorimeter

1. Theoretical Value

1) Combined Free and Forced Convection:

For such cases an external flow is superposed on the buoyancy-driven flow, and there exists a well-defined forced convection velocity. Generally, the combined effects of free and forced convection must be considered when $(Gr_L / \mathrm{Re}_L^2) \approx 1$. If the inequality $(Gr_L / \mathrm{Re}_L^2) << 1$ is satisfied, free convection effects may be neglected and $Nu_L = f(\mathrm{Re}_L, \mathrm{Pr})$. Conversely, if $(Gr_L / \mathrm{Re}_L^2) >> 1$, forced convection effects may be neglected and $Nu_L = f(Gr_L, \mathrm{Pr})$.[14]

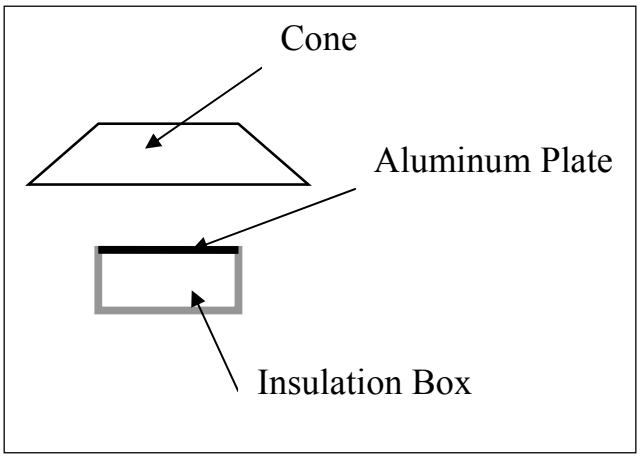

Fig. B.1 Sketch of the experimental assembly

2) Properties

✶ Air:

T_S =500 ºC $T_\infty = 26$ºC $T = \frac{T_S + T_\infty}{2} = 263$ºC=536 K

Air properties @ 550 K

$\rho = 0.6329 kg/m^2$ $\nu = 45.57 \times 10^{-6} m^2/s$

Pr = 0.683 $k = 43.9 \times 10^{-3} w/mK$

✶ Aluminum Plate:

L=7.7cm

$Area$= $7.7cm \times 7.7cm$

$Mass$=7.4g

✶ Exhaust duct

Diameter = 0.1106m

3) Analysis:

- *Grashof Number:*

$$Gr = \frac{g\beta(T - T_\infty)L^3}{\nu^2} = \frac{9.8 \times (7.7 \times 10^{-2})^3 (T - T_\infty)}{(45.57 \times 10^{-6})^2 T_\infty} = 2.154 \times 10^6 \frac{T - T_\infty}{T_\infty}$$

- U_∞ air flow velocity

Air flow rate is not easily measured, however utilization of the conservation of mass allows for a much more tangible measurement of the mass flow rate in the exhaust duct of the cone $\dot{m}_e$ to suffice.

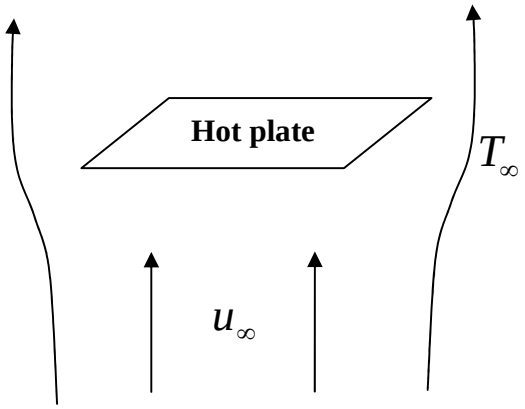

Mass conservation: $\dot{m}_e = \rho A_{duct} U_{duct} = \rho A_{test} U_\infty$

$\dot{m}_e$ = Mass flow rate in the exhaust duct (kg/s)

A_{duct} = Cross sectional area of exhaust duct

U_{duct} = Flow rate in the exhaust duct (m/s)

A_{test} = Bottom area of the small test compartment of the cone. Air comes into the small compartment vertically through the bottom.

$$A_{test} = 23in. \times 17in. = (23 \times 2.54)cm \times (17 \times 2.54)cm = 0.252m^2$$

U_∞ = Air flow velocity around the plate

From the mass conservation equation, air flow velocity can be calculated as:

$$U_\infty = \frac{\dot{m}_e}{\rho A_{test}}$$

- Reynold's Number

$$\mathrm{Re} = \frac{U_\infty L}{\nu}$$

- Nusselt Number

$$Nu_L = \frac{h_c L}{k}$$

Since there exists both free and forced convection, natural convection due to buoyancy and forced convection due to the exhaust fan will each effect the convection condition.

a) Natural Convection

For the hot upper surface case [15]

$$Nu_L = 0.54 Ra_L^{1/4} \qquad (10^5 \le Ra_L \le 10^7)$$

$$Nu_L = 0.15 Ra_L^{1/3} \qquad (10^7 \le Ra_L \le 10^{10})$$

$$Ra = Gr \,\mathrm{Pr}$$

b) Forced Convection

Normal flat plate [16]

$$Nu_L = 0.20 \,\mathrm{Re}_L^{2/3}$$

Combined Natural and Forced Convection [17]:

$$Nu_{combined}^n = Nu_{natural}^n + Nu_{forced}^n$$

+ sign applies when the flows are in the same direction.

n=7/2 may be better suited for transverse flows involving horizontal plates.

With this combined Nusselt Number, the combined convective heat transfer coefficient is easy calculated:

$$h_c = \frac{Nu \cdot k}{L}$$

Plot h_c versus $T_s - T_{amb}$ on log-log scale

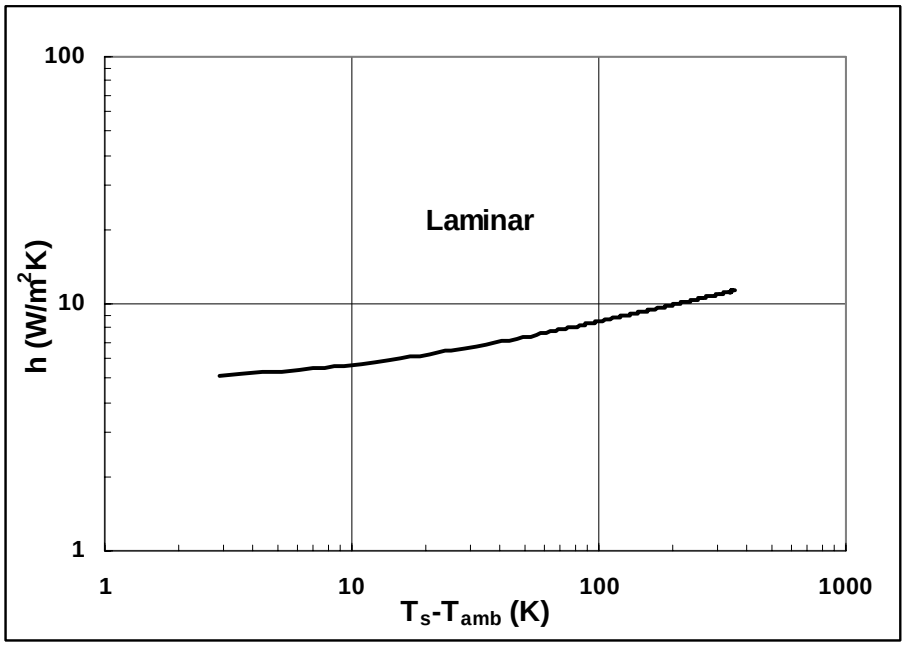

Fig. B.2 Theoretical Convective heat transfer coefficient with exhaust speed $\dot{m}_e = 25g/s$.

2. Experimental approach

1) Experimental set-up

A $7.7cm \times 7.7cm$ thin aluminum plate was used in the experiment. Soot was added on the surface by a candle flame to increase the surface absorptivity. The opposite side of the plate was insulated by 4 layers of *Kaowool* blanket to minimize heat loss effects. A small box was made by thin *Kaowool* board to hold aluminum plate and *Kaowool* blanket easily. Three thermocouples were used in the experiments. Two of them are shown in Fig. B.3. One was welded on the back face of the aluminum plate to measure the aluminum temperature. Another thermocouple was inserted into the middle of the *Kaowool* blanket layers to measure the heat loss. The third

thermocouple was used to measure the temperature in the small compartment of the cone. The experimental procedure consisted of exposing a sample, in the horizontal orientation, to a constant external irradiance from the cone heater.

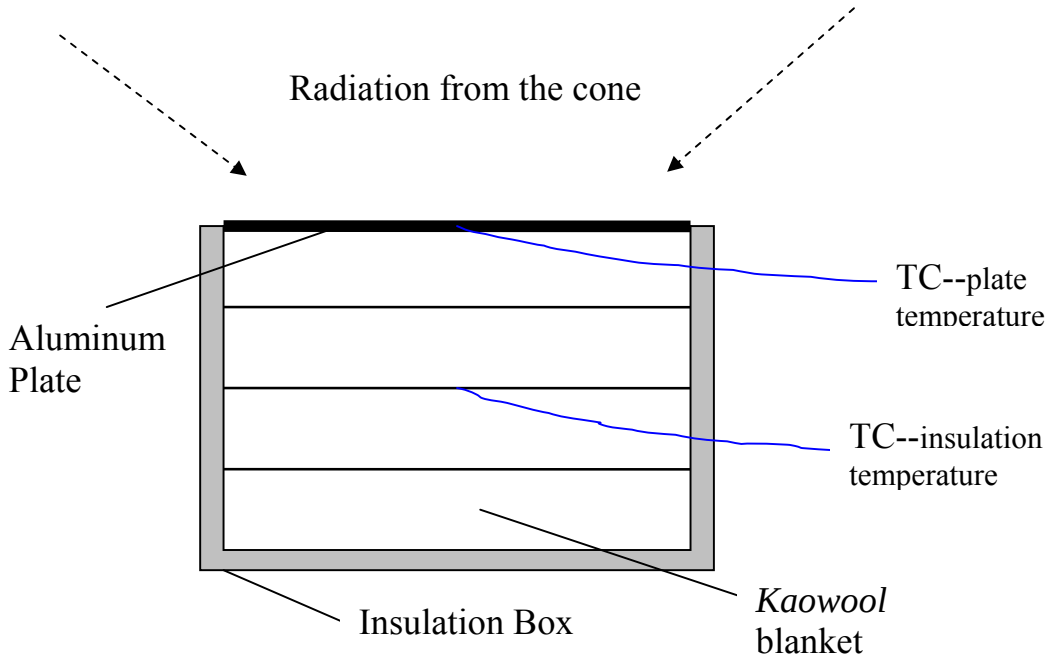

Fig. B.3 Experimental Set-Up of convective heat transfer coefficient

Data from *LabVIEW*:

Time (sec), Ambient temperature (ºC), Insulation temperature (ºC), and Aluminum surface temperature (º C)

2) Data Analysis

- Energy Conservation

Considering the conductive heat loss from the back side (insulation) of the aluminum plate

$$\dot{m}'' c \frac{dT}{dt} = \alpha \dot{q}''_{ext} - \varepsilon\sigma(T^4 - T_o^4) - h(T - T_\infty) - k\frac{T - T_{insulaion}}{l}$$

T is the temperature of the Aluminum plate

T_o in the $\varepsilon\sigma(T^4 - T_o^4)$ term is the room temperature (about 25ºC)

T_∞ in the $h(T - T_\infty)$ term is the temperature around the sample holder in the small compartment of the cone. It is higher than room temperature.

l is the thickness of the insulation

k is the thermal conductivity of the *Kaowool* (insulation)

α is the absorptivity of the hot surface

ε is the emissivity of the hot surface

Without considering the conductive heat loss from the back side

$$\dot{m}'' c \frac{dT}{dt} = \alpha \dot{q}''_{ext} - \varepsilon\sigma(T^4 - T_o^4) - h(T - T_\infty)$$

- Heat capacity of aluminum

Heat capacity of aluminum increases as a function of temperature.

$c_p = -0.0005T^2 + 0.6099T + 884$, T in ºC

- Surface absorptivity α

In order to find α , use the energy equation at the beginning, when all the temperatures are nearly the same.

$$\dot{m}'' c_p \frac{dT}{dt} = \alpha \dot{q}''_{ext}$$

$\frac{dT}{dt}$ is the initial slope value read from the time-temperature curve

$$\alpha = \frac{\dot{m}'' c_p \frac{dT}{dt}}{\dot{q}''_{ext}}$$

The average value of α under different external heat flux tests is 0.93

Assume the surface emissivity is equal to the absorptivity.

- Convective heat transfer coefficient

In the energy equations with or without the consideration of back face conduction heat loss, all of the values are known except for *h*. An average value of α =0.93 is used and all temperatures are measured with time by the thermocouples and recorded by the data acquisition program. The derivative is calculated as:

$$\frac{dT}{dt} \approx \frac{\Delta T}{\Delta t} = \frac{T_{i+4} - T_i}{4 \times \text{interval}}.$$

Then *h* is easily calculated.

Without conduction:

$$\dot{m}'' c \frac{dT}{dt} = \alpha \dot{q}''_{ext} - \varepsilon\sigma(T^4 - T_o^4) - h(T - T_\infty) - k\frac{T - T_{insulaion}}{l}$$

With conduction:

$$\dot{m}'' c \frac{dT}{dt} = \alpha \dot{q}''_{ext} - \varepsilon\sigma(T^4 - T_o^4) - h(T - T_\infty)$$

The definition of ambient temperature is of great importance in this analysis. Although it is common practice to define the ambient temperature as the room temperature, one must recognize that when heater is on, the temperature in the small compartment of the cone is much higher than room temperature. Therefore this elevated temperature should be used as the real ambient temperature around the heated sample.

In these calculations, the temperature underneath the sample in the compartment is defined as T_∞ when in steady state. It is about 50 ºC.

Fig. B.4 shows that the conductive heat loss is not small. The curve with conductive heat loss is closer to the theoretical value. The conductive heat loss can't be neglected. Therefore all values for the convective coefficient h were determined based on the consideration of this heat loss.

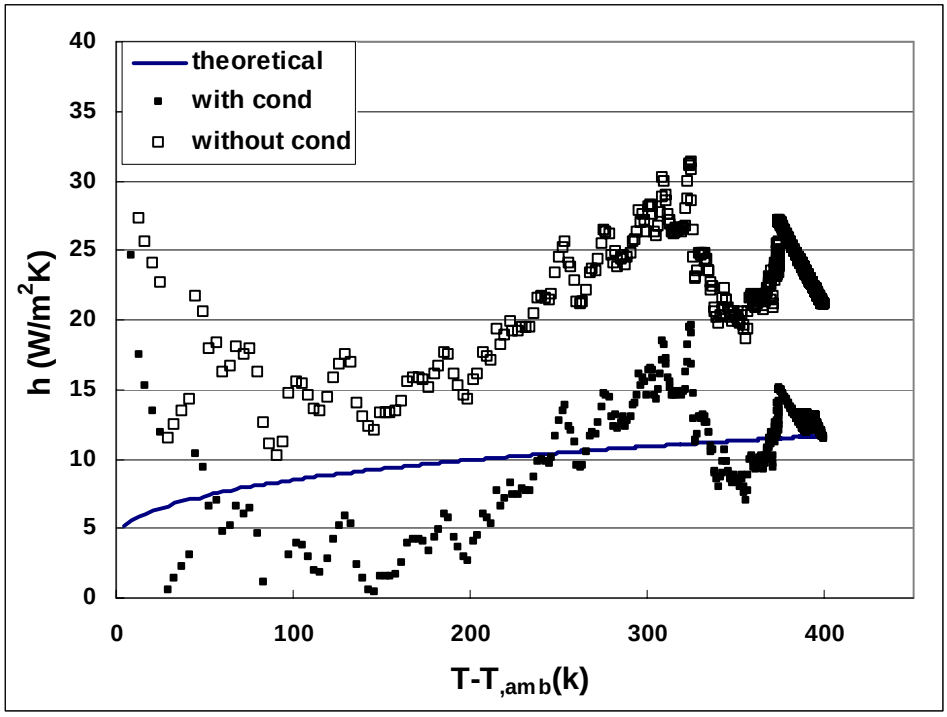

Fig. B.4 h vs. ΔT
20.5 kW/m^2 External Heat Flux, 25 g/s Exhaust Flow

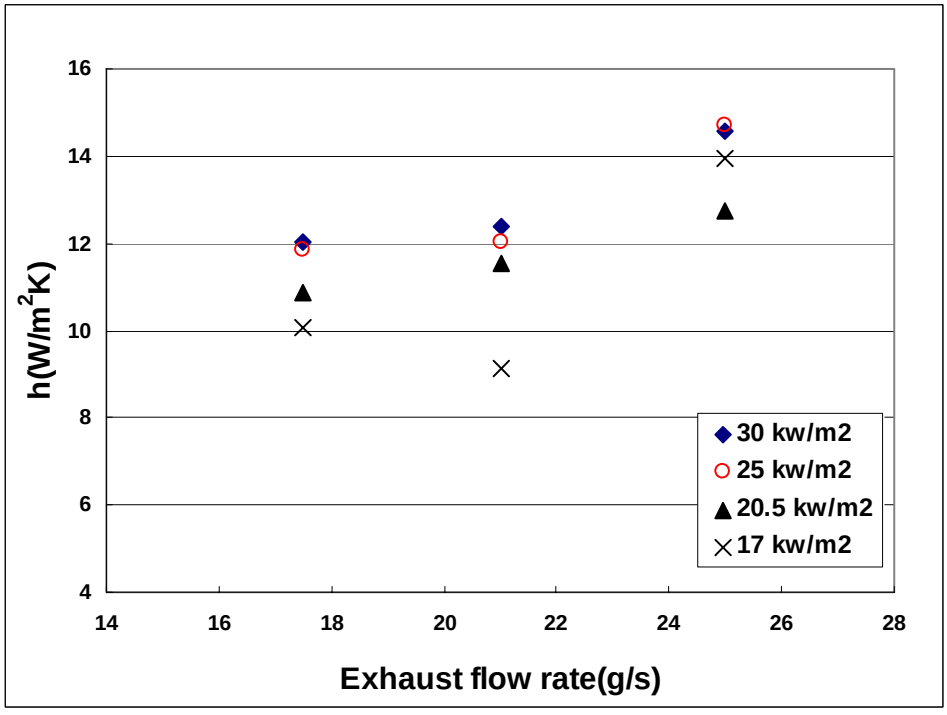

Fig. B.5 h vs. Exhaust Flow Rate under different external heat flow

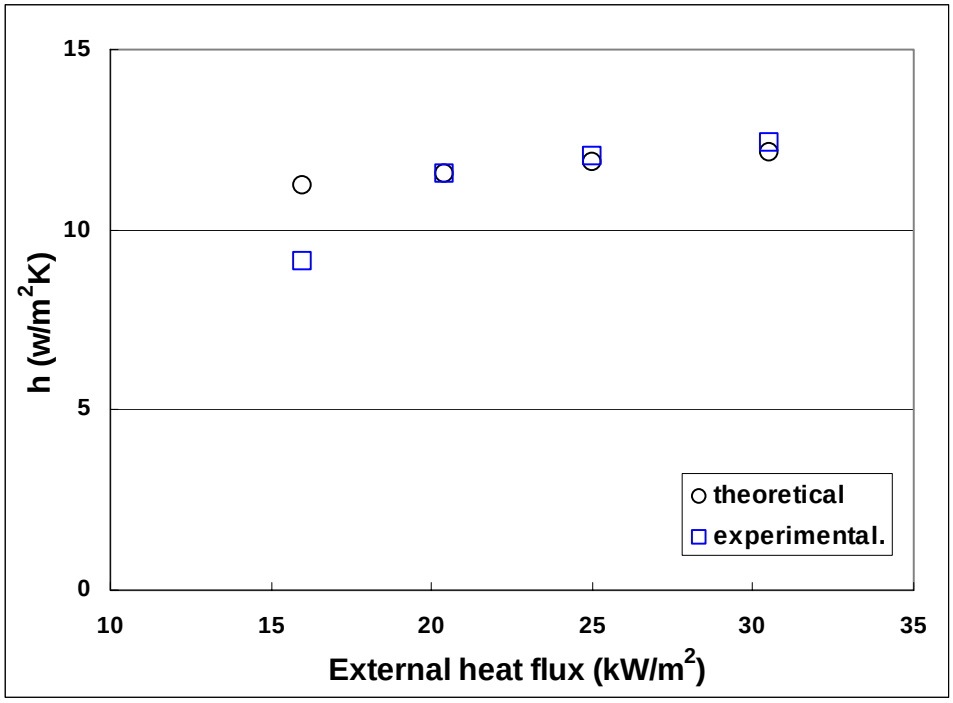

Fig. B.6 h vs. External Heat Flux
Exhaust Flow = 21 g/s

As shown in Figures B.4, B.5 and B.6, the average value of the convective heat transfer coefficient is about 11 W/m^{2}K, which is also close to the theoretical value (shown in Fig.B.2). In the literature, h=10 W/m^{2}K is always used as an average value for the cone. This value is indeed very close to the results of this analysis. Therefore, h=10 W/m^{2}K is used in the analysis in order to maintain consistency between other literature results and this data analysis.

Appendix C FORTRAN Program for Kinetic Modeling

```
      Program Nylon
c     This program aims to solve heat and mass transfer during the decompositoin
c     process of Nylon.
c     The output file is in "dat" format which can be opened by matlab M-file

      implicit none
      integer i,j,npmax,nt_prof
      parameter (npmax = 1600)
      parameter (nt_prof = 100)
      integer nt,npx,itermax,ntmax

      real*8 errTnorm,Ts2
      real*8 Tinf,kwd,cpwd,L,rhowd,timec,Mgc,tol,dtime
      real*8 timed,rhofd,Qpd,Ead,apd,qd,hd,epsilon
      real*8 time,rhof,Qp,q,H,Sigma,ap,Te,dx,Ts1,Mgs,dTs1,ks
      real*8 qflamed,qflame,qnet
      real*8  sumha,sumhc,sumhg,sumQp,SumT
      real*8 rho1(npmax+2),rho2(npmax+2),T1(npmax+2),T2(npmax+2)
      real*8 T1d(npmax+2),T2prim(npmax+2)
      real*8 Mg(npmax+2),A(npmax+2),xc(npmax+2),x(npmax+2)
      real*8 dT(npmax+2)
      real*8 D1(npmax+2),D2(npmax+2),D3(npmax+2),RHS(npmax+2)
      real*8 cpcd1(npmax+2),cpad1(npmax+2),cpgd1(npmax+2)
      real*8 cpc1(npmax+2),cpa1(npmax+2),cpg1(npmax+2)
      real*8 hcd1(npmax+2),had1(npmax+2),hgd1(npmax+2)
      real*8 hc1(npmax+2),ha1(npmax+2),hg1(npmax+2),hall1(npmax+2)
      real*8 ka(npmax+2),kc(npmax+2),kad(npmax+2),kcd(npmax+2)
      real*8 k(npmax+2),rhocps(npmax+2)
      real*8 errT(npmax+2)
```

```
      real*8 drhodt(npmax+2)

      character(50) filename
      character(4) order
      open (file = 'Nylon_characters.dat',unit = 200)
      npx = 500
      dtime = 1.0e-4
      tol = 1.0e-6
      itermax = 500

C     Characteristic variables
      Tinf = 298.d0                    ! K          ambient temperature
      kwd = 3.054e-4*Tinf + 0.0362     ! J/m.s.K    solid virgin conductivity
      cpwd = 10.d0 + 3.7d0*Tinf        ! J/kg.K     solid virgin heat capacity
      L = 8.0e-3                       ! m          solid thickness
      rhowd = 1136.d0                  ! kg/m3      solid virgin density
      timec = cpwd*rhowd*(L**2)/kwd    ! s          characteristic time
      Mgc = kwd/(cpwd*L)               ! kg/s-m2    characteristic massflux

C     Input varialbles
      timed = 500.d0                   ! s          total physical time
      rhofd = 0.017*rhowd              ! kg/m3      solid final density
      Qpd = 0.d0                       ! J/kg       solid heat of pyrolysis
                                       ! + Endothermic and - Exothermic
      Ead = 2.4e5                      ! J/mole     solid activation energy
      apd = 1.0e19                     ! 1/s        solid pre-exponential
                                                    factor
      qd = 50.e3                       ! W/m2       incident heat flux
      qflamed = 5.e3                   ! W/m2       flame heat flux
      hd = 10.d0                       ! W/m2.K     heat transfer coefficient
      epsilon = 1.d0                   ! emissivity
```

```
C       Calculate Dimensionless Parameters
        time = timed/timec
        rhof = rhofd/rhowd
        Qp = Qpd/(cpwd*Tinf)
        q = qd*L/(kwd*Tinf)
        qflame = qflamed*L/(kwd*Tinf)
        H = hd*L/kwd
        Sigma = epsilon*(5.67e-8)*(Tinf**3)*(L)/kwd
        ap = apd*cpwd*rhowd*(L**2)/(kwd*(1-rhof))
        Te = Ead/(8.314*Tinf)

C       Generate Grid
        dx = 1.d0/npx
        do i=1,npx+3
        x(i) = (i-2)*dx
        enddo

        do i = 1,npx+2
        xc(i) = 0.5d0*(x(i+1)+x(i))
        enddo

C       Initialize Solution
        do i = 1,npx+2
                T1(i) = 1.d0
                T2(i) = 1.d0
                dT(i) = 0.d0
                rho1(i) = 1.d0
                rho2(i) = 0.d0
                Mg(i) = 0.d0
        enddo
```

```
      Ts1 = 1.d0
      Mgs = 0.d0
      dTs1 = 0.d0
      ntmax = ceiling(time/dtime)
      write(200,1000) timec,Mgc,Tinf,dtime,L,rhowd,cpwd,kwd,Qpd,apd,Ead
      close (200)
1000  format(11e15.3)
      open (file= 'Nylon_mass_temp.dat', unit = 100)

C     Start Advance in Time
      do nt = 1,ntmax
100   continue
      write(6,*) nt,ntmax
C     Arrhernius Kinetic Decomposition Rate
            do i = 1,npx+2                    ! include ghost points
            A(i) = -ap*dtime*exp(-2.d0*Te/(T2(i)+T1(i)))
            rho2(i) = (2.d0/(2.d0-A(i)))
     &      *(rho1(i)+A(i)*(0.5*rho1(i)-rhof))
            enddo

C     Mass Transfer Equation
C     Mg(L)-Mg(x) = integrate (drho/dtime)dx from x = x to x = L
                  do i = npx+1,2,-1
       Mg(i) = Mg(i+1)-((rho2(i)-rho1(i))/dtime)*dx
                  enddo

C     Calculate cp-heat capacity and h-enthalpy for active wood, char
C     ,and gas base on T1d (nth + dtime time step)
                  do i = 1,npx+2
                  T1d(i) = (T1(i)+dT(i))*Tinf
                  enddo
```

```
                do i = 1,npx+2                    ! include ghost points

                cpcd1(i) = 1430.d0 + 0.355*T1d(i)-0.732*(T1d(i)**(-2.d0))
                cpad1(i) = 10.d0 + 3.7*T1d(i)
                cpgd1(i) = 66.8*(T1d(i)**(1.d0/2.d0)) - 136.d0

                hcd1(i) = (5.0e-4)*(2.86*1.e6*Tinf*(T1d(i)**2.d0)
     &          + 355.d0*Tinf*(T1d(i)**3.d0) + 1464.d0*Tinf -
     &          2.86e6*T1d(i)*(Tinf**2.d0)-355.d0*T1d(i)*(Tinf**3.d0)-
     &          1464.d0*T1d(i))/(T1d(i)*Tinf)

                had1(i) = 1.85*(T1d(i)**2.d0) - 1.85*(Tinf**2.d0)
     &          + 10.d0*(T1d(i)-Tinf)

                hgd1(i) = 44.53*(T1d(i)**(3.d0/2.d0)) - 136.d0*T1d(i) -
     &          44.53*(Tinf**(3.d0/2.d0)) + 136.d0*Tinf

c       None-dimensionalize cp and h
                do i = 1,npx+2
                cpc1(i) = cpcd1(i)/cpwd
                cpa1(i) = cpad1(i)/cpwd
                cpg1(i) = cpgd1(i)/cpwd

                hc1(i) = hcd1(i)/(cpwd*Tinf)
                ha1(i) = had1(i)/(cpwd*Tinf)
                hg1(i) = hgd1(i)/(cpwd*Tinf)
                enddo

                do i = 2,npx+1
                hall1(i) = (1.d0/(1.d0-rhof))*ha1(i)
     &           - (rhof/(1.d0-rhof))*hc1(i) - hg1(i)
```

```
                    enddo

C       Calculate k-thermal conductivity for active wood, char base on T1d (nth +
dtime time step)
                    do i = 1,npx+2
                    kcd(i) = ((9.46e-5)*T1d(i) + 4.88e-2)          ! W/m.K
                    kad(i) = 0.9d0*((3.054e-4)*T1d(i) + 3.62e-2)   ! W/m.K
                                                          !Nylon conductivity
                    enddo

C       Non-dimensionalize k
                    do i = 1,npx+2
                    ka(i) = kad(i)/kwd
                    kc(i) = kcd(i)/kwd
                    enddo

C       Calculate k(i),rhocps and dk/dx base on average value between rho2 and rho1
                do i = 2,npx+1
                k(i) = ((0.5d0*(rho2(i)+rho1(i))-rhof)*ka(i))
    &            /(1.d0-rhof) + ((1.d0-0.5d0*(rho2(i)+rho1(i)))*kc(i))/(1.d0-rhof)

                rhocps(i) = ((0.5d0*(rho2(i)+rho1(i))-rhof)*cpa1(i))/(1.d0-rhof)
    &           + ((1.d0-0.5d0*(rho2(i)+rho1(i)))*cpc1(i))/(1.d0-rhof)
                enddo

C       Energy Eq
C       Calculate D1,D2,D3 (elements of tridiagonal temperature matrix)
        do i = 2,npx+1
        D1(i) =-(0.5d0*dtime/(rhocps(i)*(dx**2)))*0.5d0*(k(i+1)+k(i)) ! One above
        D2(i) = 1.d0+(0.5d0*dtime/(rhocps(i)*(dx**2)))*0.5d0*(k(i+1)+k(i))
    &  +(0.5d0*dtime/(rhocps(i)*(dx**2)))*0.5d0*(k(i)+k(i-1))     ! Diagonal
```

```
      D3(i) = -(0.5d0*dtime/(rhocps(i)*(dx**2)))*0.5d0*(k(i)+k(i-1))! One below
       enddo

C      Back Boundary dT/dx = 0
      D3(npx+2) = -1.d0
      D2(npx+2) = 1.d0

C      Front Boundary q + qflame = -k(dT/dx) + H*(T-1) + Sigma(Ts^4-1).
C      Estimate Ts from Tsn+1 = Tsn + (dTs/dt)*dtime
       ks = 1.5d0*k(2)-0.5d0*k(3)
       D2(1) = 1.d0+ H*dx/(2.d0*ks)
       D1(1) = -1.+ H*dx/(2.d0*ks)

c      Fill in RHS vectior
       RHS(1) = q*dx/ks + H*dx/ks -
     & (dx/ks)*Sigma*(((Ts1+ dTs1)**4)-1.d0) + (dx/ks)*(qflame)
       RHS(npx+2) = 0.d0

       do i = 2,npx+1
       RHS(i)= T1(i) + 0.5d0*(dtime/rhocps(i))*(1.d0/(dx**2))*
     & ((0.5d0*(k(i+1)+k(i)))*(T1(i+1)-T1(i)) -
     & (0.5d0*(k(i)+k(i-1)))*(T1(i)-T1(i-1)))
     & + (1.d0/rhocps(i))*(rho2(i)-rho1(i))*(Qp-hall1(i))
     & + ((Mg(i)*dtime)/rhocps(i))*(hg1(i+1)-hg1(i-1))/(2.d0*dx)
       enddo
       call tridag(D3,D2,D1,RHS,T2prim,npx+2)

C      check errT  relative error
       do i = 2,npx+1
       errT(i) = abs((T2(i)-T2prim(i))/T2(i))
       enddo
```

```
      errTnorm = 0.d0
      do i = 2,npx+1
      if (errTnorm.lt.errT(i)) errTnorm = errT(i)
      enddo

C     write (6,1500) nt,errTnorm
      do i = 1,npx+2
      T2(i)=T2prim(i)
      Ts2 = 1.5d0*T2(2)-0.5d0*T2(3)
c     Ts2 = 0.5d0*(T2(1)+T2(2))
      dTs1 = Ts2-Ts1
      enddo

      if (errTnorm.gt.tol) goto 100
      if (errTnorm.lt.tol) then

c     Calculate Temperature (Ts) and Mass flux (Mgs) at surface for each time step
by linear interpolation
      do i = 2,npx+1
      drhodt(i) = (rho2(i)-rho1(i))/dtime
      enddo

     Mgs = 1.5d0*Mg(2)-0.5d0*Mg(3)

c     Setup T1 for the next time step
      do i = 1,npx+2
      dT(i) = T2(i)-T1(i)
      enddo
      Ts1 = Ts2
      do i = 1,npx+2
      T1(i) = T2(i)
```

```
      rho1(i) = rho2(i)
      enddo
      endif

c     Check Magnitude of energy term of time step nt
      sumha = 0.d0
      sumhc = 0.d0
      sumhg = 0.d0
      sumQp = 0.d0
      sumT = 0.d0

      do i = 2,npx+1
      sumha = sumha + cpwd*Tinf*dx*(ha1(i)/(1.d0-rhof))
      sumhc = sumhc + cpwd*Tinf*dx*(rhof*hc1(i)/(1.d0-rhof))
      sumhg = sumhg + cpwd*Tinf*dx*(hg1(i))
      sumQp = sumQp + cpwd*Tinf*dx*(Qp)
      sumT = sumT+Tinf*dx*T1(i)
      enddo

C     calculated qnet
      qnet = q-H*(Ts1-1.d0)-Sigma*((Ts1**4) - 1.d0)
      open (file='Nylon_energy.dat',unit = 500)
      write(500,2000) nt,sumha,sumhc,sumhg,sumQp,sumT,qnet,q,Ts2,Mgs

C     Writing Output File
      write(100,2500) nt,Ts2,Mgs
C     write In-depth profiles every nt_prof time step
      if (mod(nt,nt_prof).eq.0) then
      call int_to_char(order,nt,4)
      filename = 'Nylon_profile_'//order//'.dat'
      open (file = trim(filename) ,unit=150)
```

```
      do i = 2,npx+1
      write(150,3000) nt,xc(i),rho2(i),T2(i),drhodt(i)
      enddo
      close (150)
      endif
      Enddo ! Enddo of advancing in time
      close (100)
      close (500)

1500  format(i9,1e15.3)
2000  format(i9,9e18.8)
2500  format(i9,2e18.8)
3000  format(i9,9e18.8)
      End

c     ****************************************************************
      subroutine tridag(a,b,c,r,u,n)
      integer n,nmax
      real*8 a(n),b(n),c(n),r(n),u(n)
      parameter (nmax = 1600)
      integer j
      real*8 bet,gam(nmax)
      if(b(1).eq.0) pause 'tridag:rewrite equations'
      bet = b(1)
      u(1) = r(1)/bet
      do j = 2,n
            gam(j) = c(j-1)/bet
            bet = b(j)-a(j)*gam(j)
            if(bet.eq.0) pause 'tridag failed'
            u(j) = (r(j)-a(j)*u(j-1))/bet
```

```
      enddo
      do j = n-1,1,-1
      u(j) = u(j)-gam(j+1)*u(j+1)
      enddo
      return
      end

      subroutine int_to_char(file_ext,num,max)
      ! converts a positive integer (num) to character (file_ext) of length max
      ! in other words, 0 < num < (10**max)-1
      ! routine uses function getchar (see below)
      ! note: this routine takes advantage of the fortran convention for passing
arrays
      !   through argument lists; in particular, in this routine file_ext is delcared
      !   as a character array of length equal to the length of the single character
      !   declaration of the calling routine; i'm sorry to have to do this, but it
      !   made things very nice in this routine; in short:
      !   character*max file_ext => character file_ext(max)
      !-----------------------------------------------------------------------------
        implicit none
      ! declarations passed in
        character(*) file_ext
        integer num, max
      ! other declarations
        integer i, m, n, temp
        character getchar
      !-----------------------------------------------------------------------------
      ! check for postiveness
        if(num.lt.0) then
        write(6,*) 'num passed into routine'
         write(6,*) 'set_file_extension_string is negative'
```

```
  stop
  endif

! check for maximum value of num
  if(num.gt.(10**max)-1) then
  write(6,*) 'num passed into routine set_file_extension_string'
  write(6,*) 'is greater than the character file_ext will allow'
  stop
  endif
!-------------------------------------------------------------------------------
! zero stuff (must do this!)
  n=0; temp=0
  do i=1,max,1
  file_ext(i:i)='0'
  enddo
! set file extension
  do i=max,1,-1
  temp=n
  n=(num/10**(i-1))
  m=max-i+1
  file_ext(m:m)=getchar(int(n-(temp*10)))
  enddo
!-------------------------------------------------------------------------------
  return
  end subroutine int_to_char
!===============================================================
  function getchar(n)
!===============================================================
! getchar returns a character corresponding to n
!-------------------------------------------------------------------------------
  implicit none
```

```
!-------------------------------------------------------------------------------
! declarations passed in
  character getchar
  integer n
!-------------------------------------------------------------------------------
  if(n.eq.0) getchar = '0'
  if(n.eq.1) getchar = '1'
  if(n.eq.2) getchar = '2'
  if(n.eq.3) getchar = '3'
  if(n.eq.4) getchar = '4'
  if(n.eq.5) getchar = '5'
  if(n.eq.6) getchar = '6'
  if(n.eq.7) getchar = '7'
  if(n.eq.8) getchar = '8'
  if(n.eq.9) getchar = '9'
!-------------------------------------------------------------------------------
  return
  end function getchar
```

Appendix D Experimental Data of Nanocomposites

Nylon under different external heat flux
(Thickness 8 mm, Diameter 74 mm)

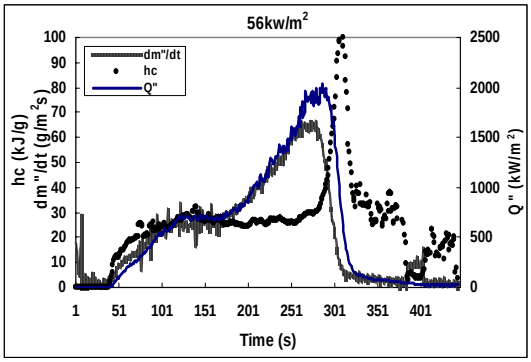

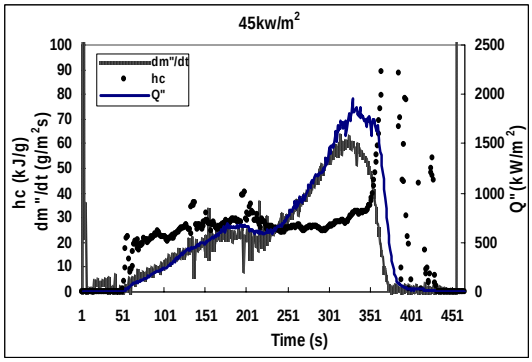

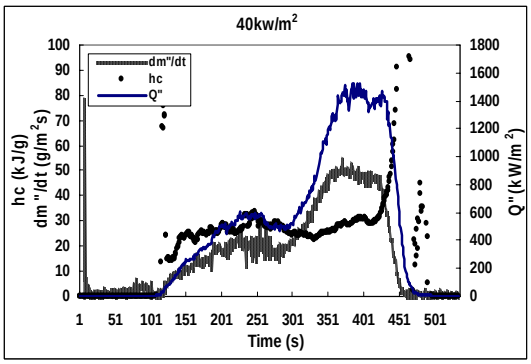

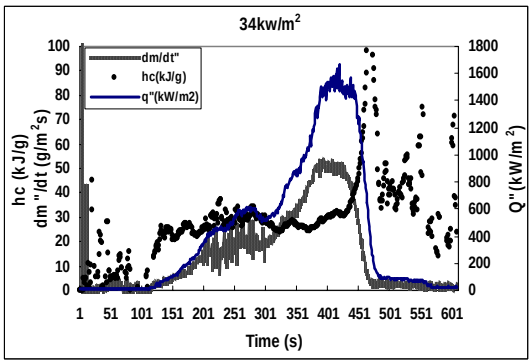

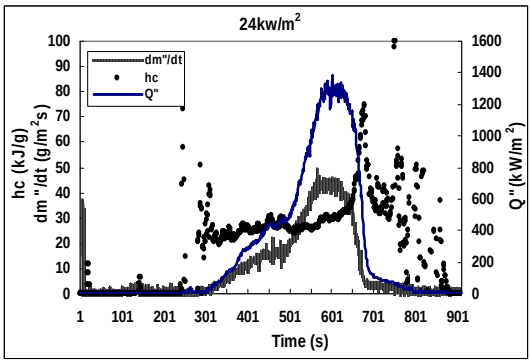

Summary of 8 mm Nylon

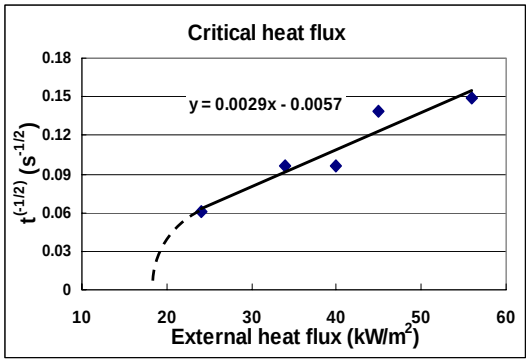

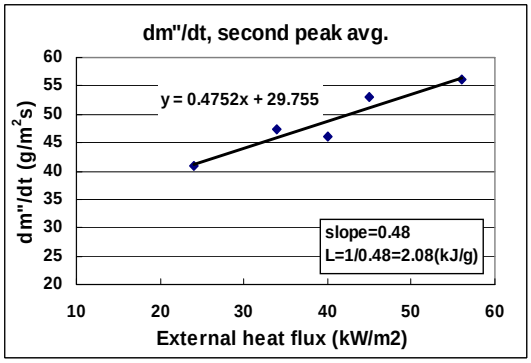

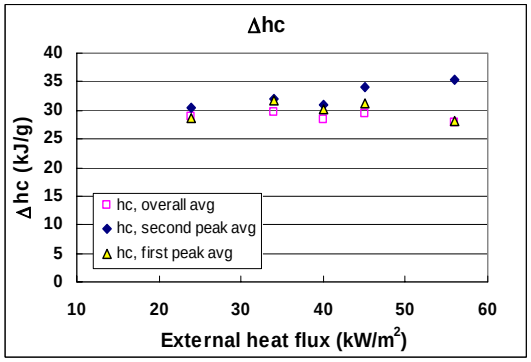

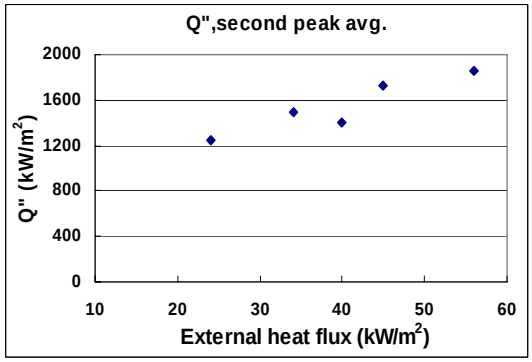

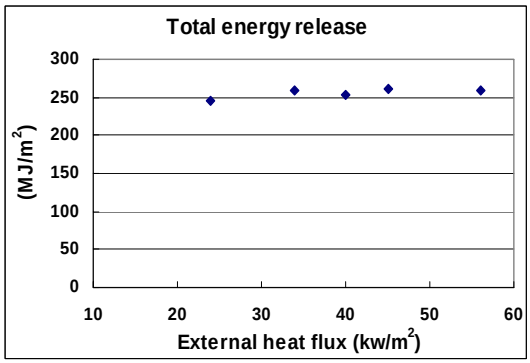

Heat Flux (kW/m^2)	Ignition Time (s)	Char/Mass (g)
56	45	0/38.2
45	52	0/38.2
40	108	0/38.2
34	109	0/38.2
24	270	0.1/38

Nylon under different external heat flux
(Thickness 4 mm, Diameter 74 mm)

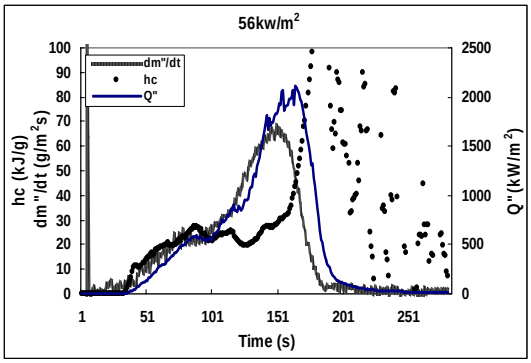

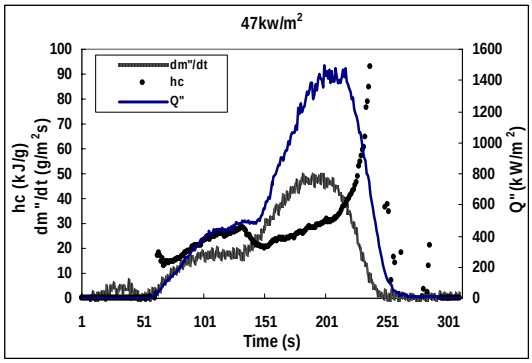

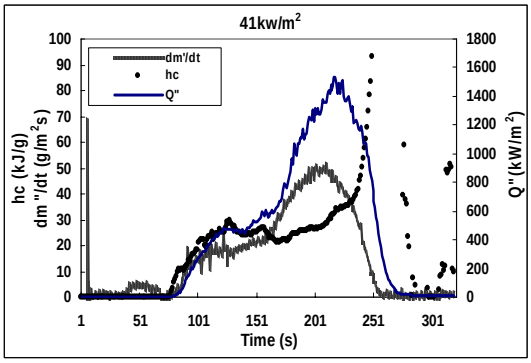

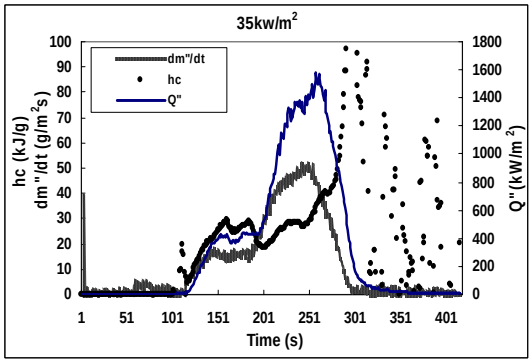

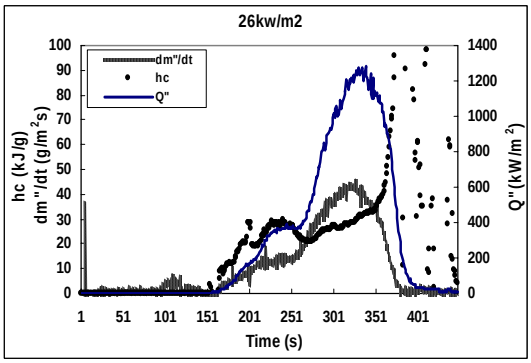

Summary of 4 mm Nylon

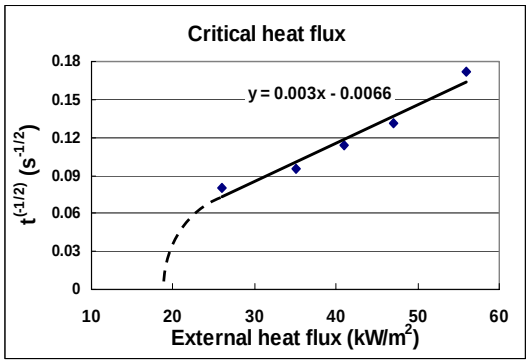

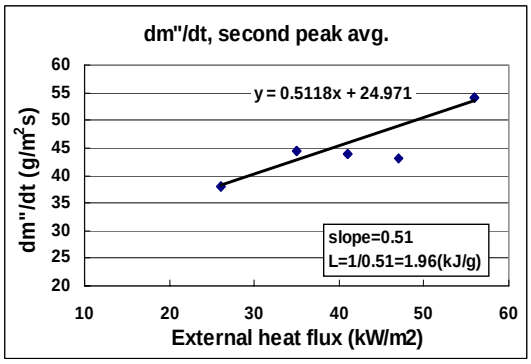

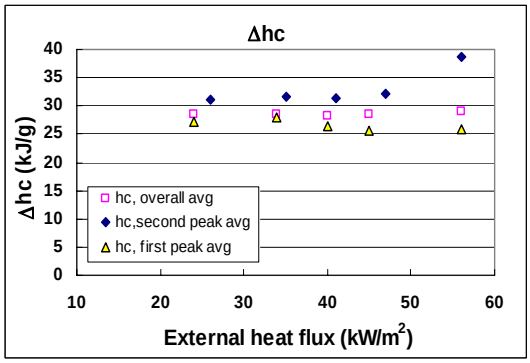

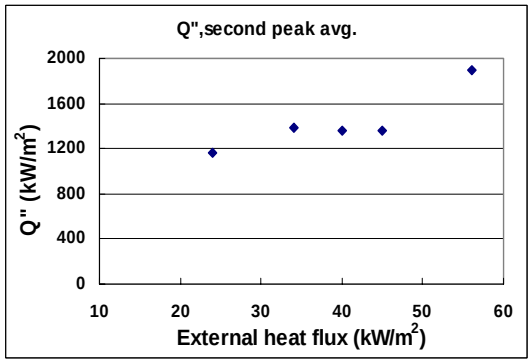

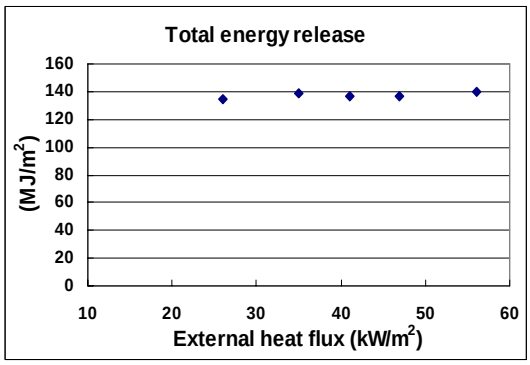

Heat Flux (kW/m^2)	Ignition Time (s)	Char/Mass (g)
56	34	0/20.7
47	58	0/20.6
41	77	0/20.5
35	110	0~0.1/21
26	157	0.1/20.5

Nylon under different external heat flux
(Thickness 3.2 mm, Diameter 75 mm)

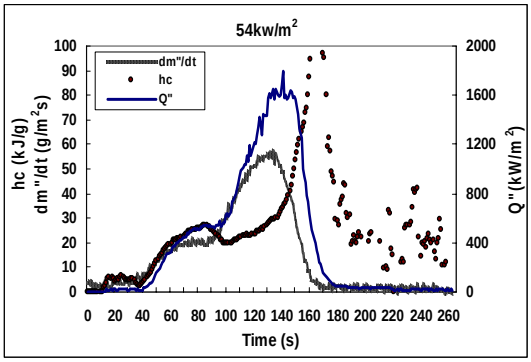

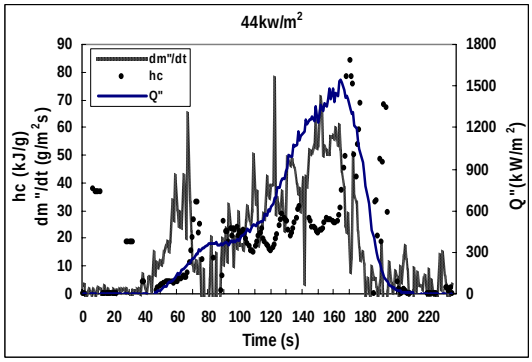

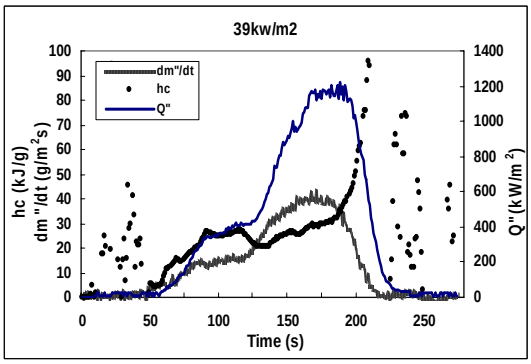

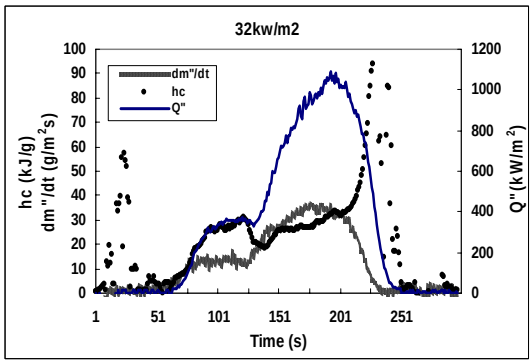

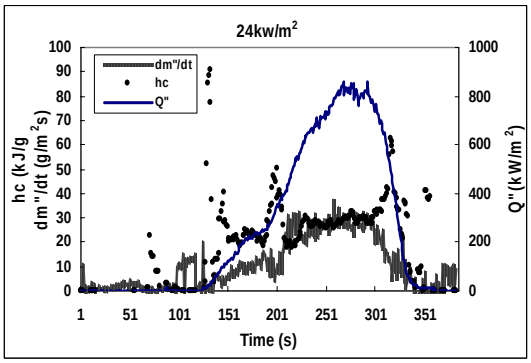

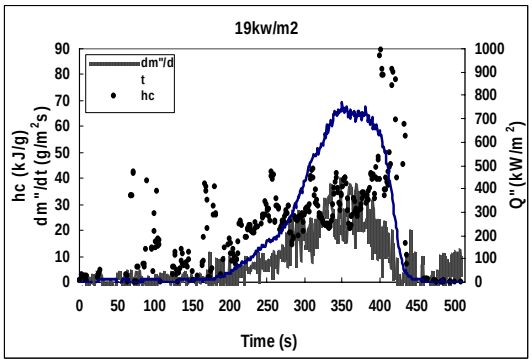

Summary of 3.2 mm Nylon

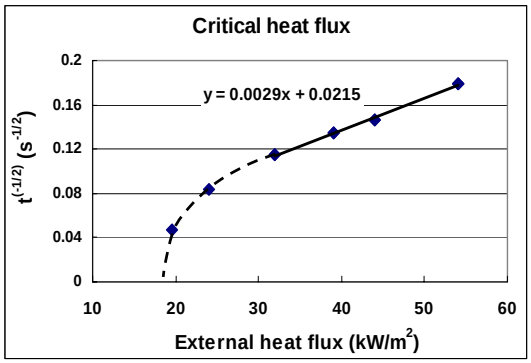

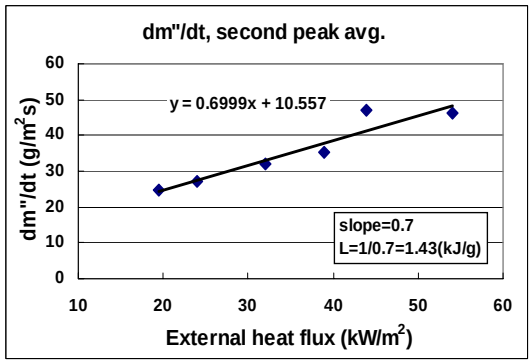

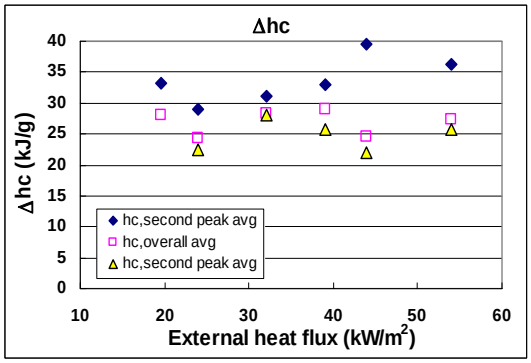

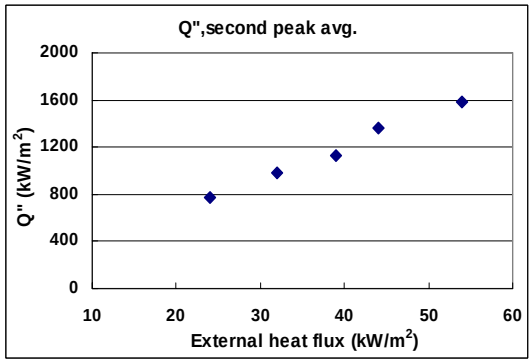

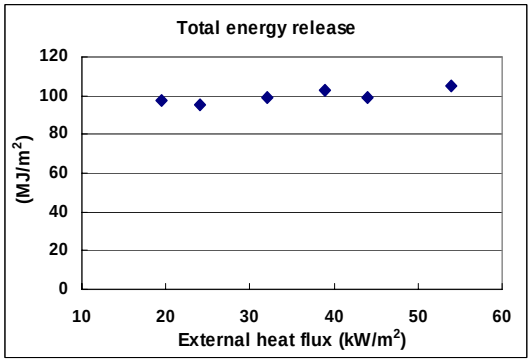

Heat Flux (kW/m^2)	Ignition Time (s)	Char/Mass (g)
54	31	0/15.5
44	47	0/15.4
39	55	0/15.5
32	75	0~0.1/15.5
24	144	0~0.1/15.4
19.5	459	0.2/15.7

Nylon under different external heat flux
(Thickness 1.6 mm, Diameter 76 mm)

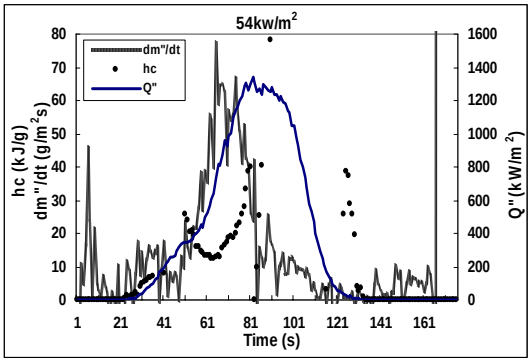

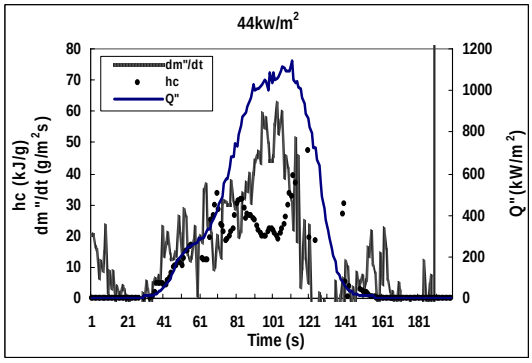

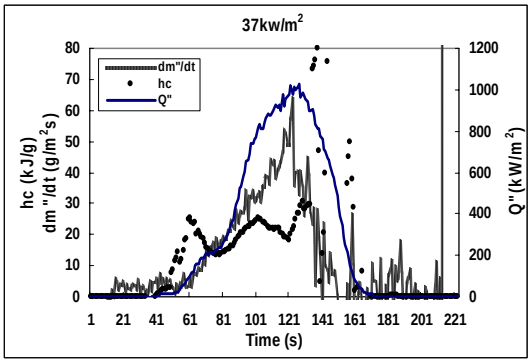

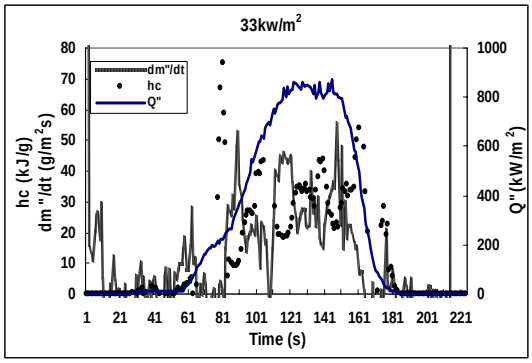

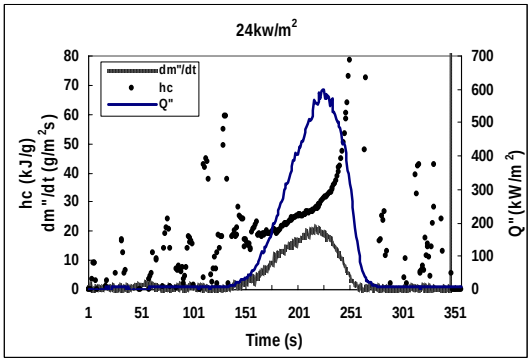

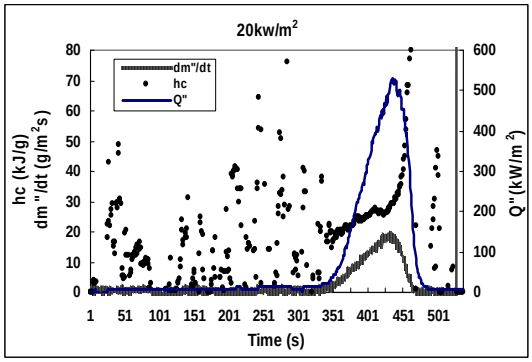

Summary of 1.6 mm Nylon

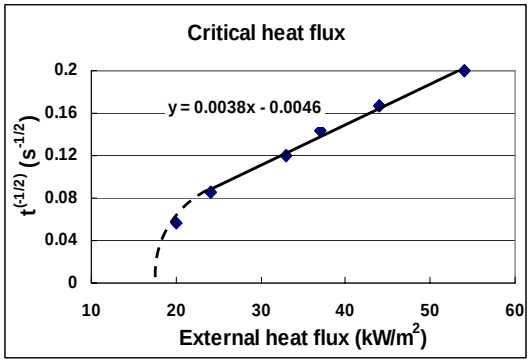

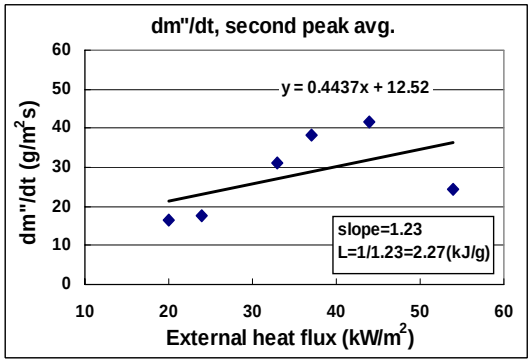

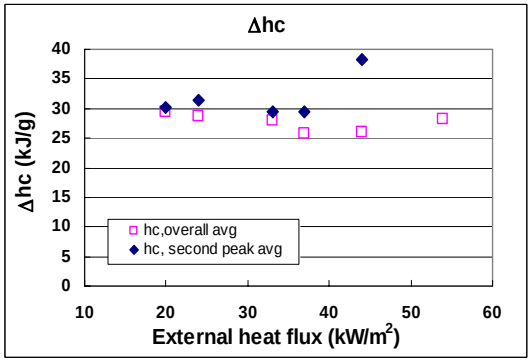

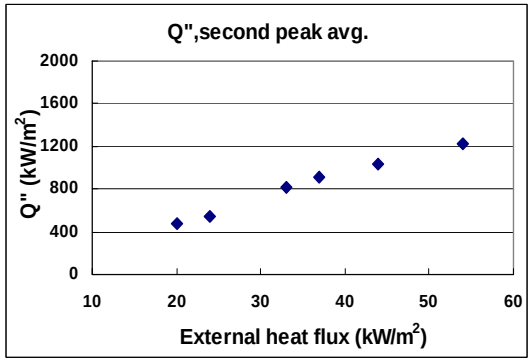

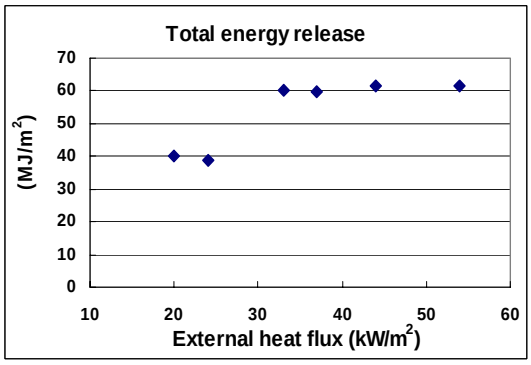

Heat Flux (kW/m^2)	Ignition Time (s)	Char/Mass (g)
54	25	0/9.7
44	36	0/9.9
37	49	0/9.7
33	69	0/9.8
24	137	0.1/9.6
20	314	0.1/9.6
19	465	8.7/9.6

Nylon+2%Clay under different external heat flux
(Thickness 8 mm, Diameter 75 mm)

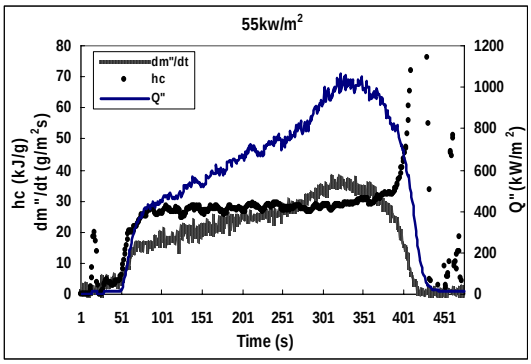

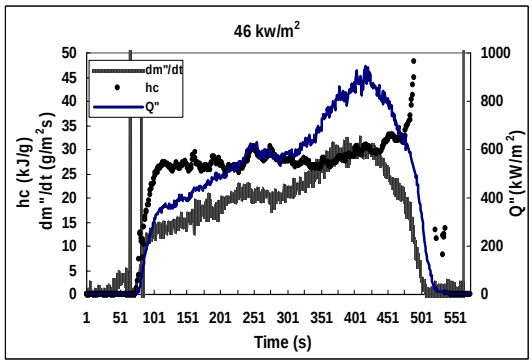

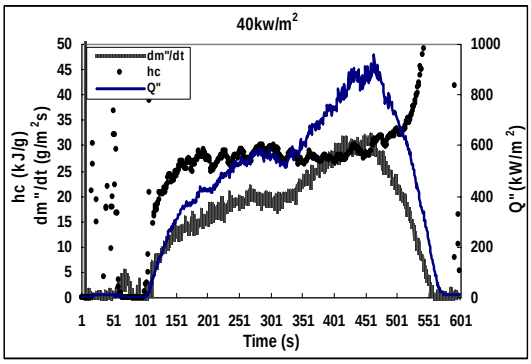

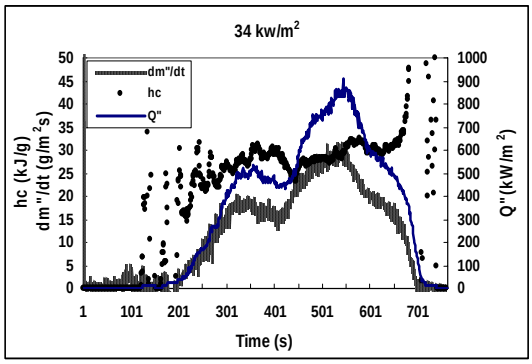

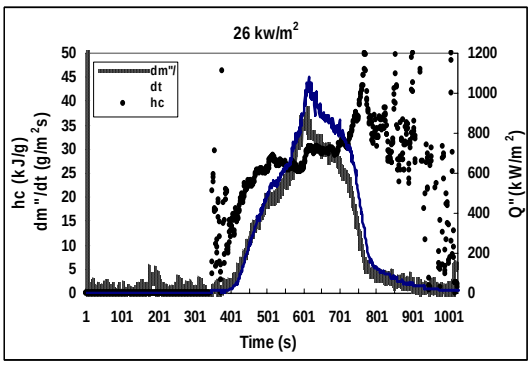

Summary of 8 mm Nylon＋2％Clay

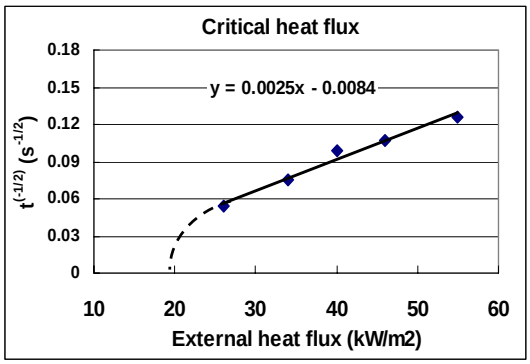

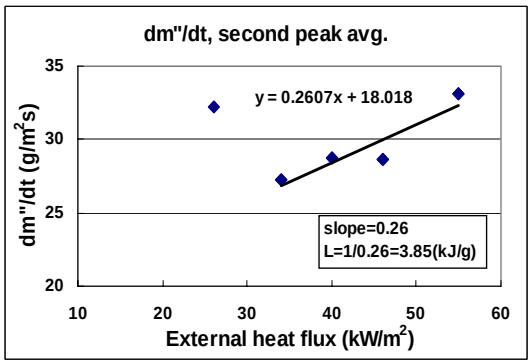

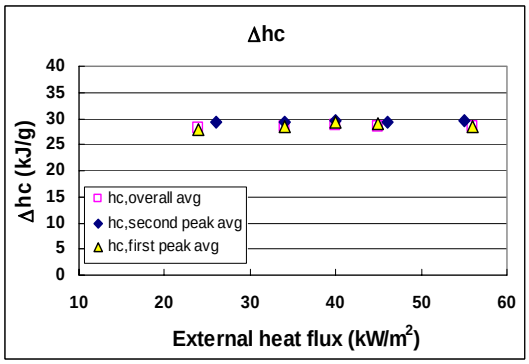

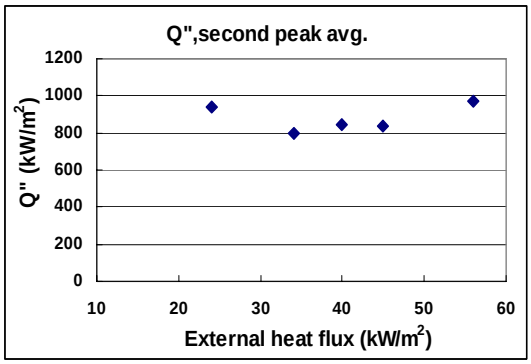

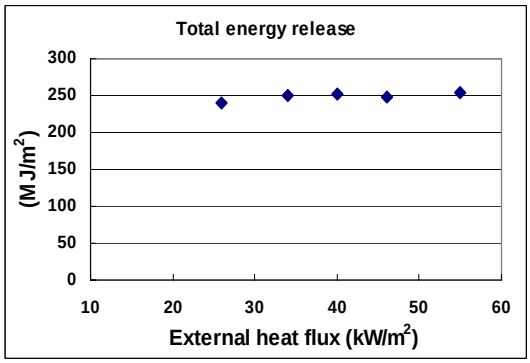

Heat Flux (kW/m^2)	Ignition Time (s)	Char/Mass (g)
55	63	0.8/38.1
46	87	0.7/38.1
40	102	0.7/38.2
34	177	0.8/38.1
26	343	/38.1

Nylon+2%Clay under different external heat flux
(Thickness 4 mm, Diameter 75 mm)

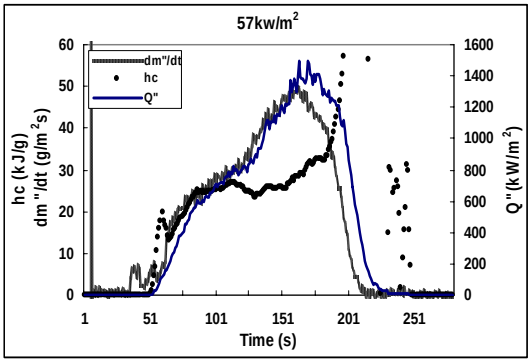

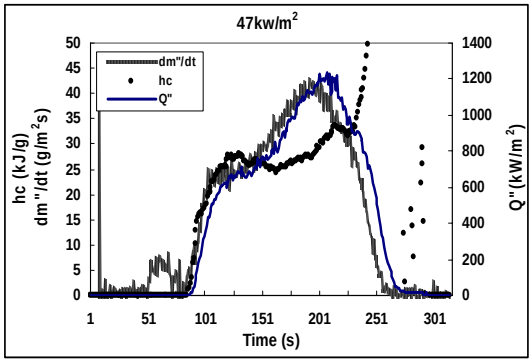

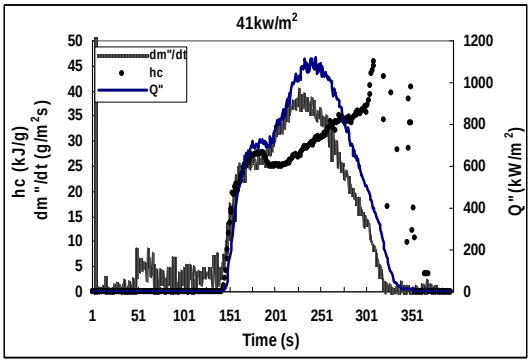

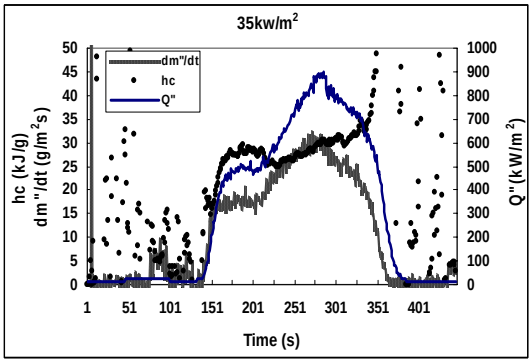

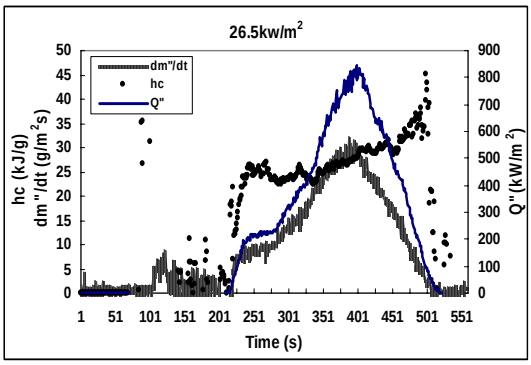

Summary of 4 mm Nylon＋2％Clay

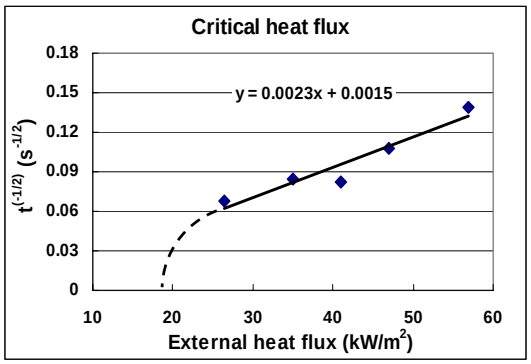

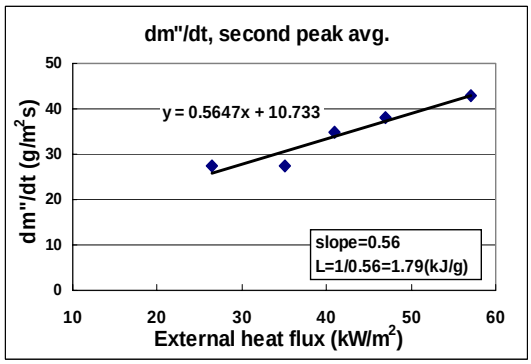

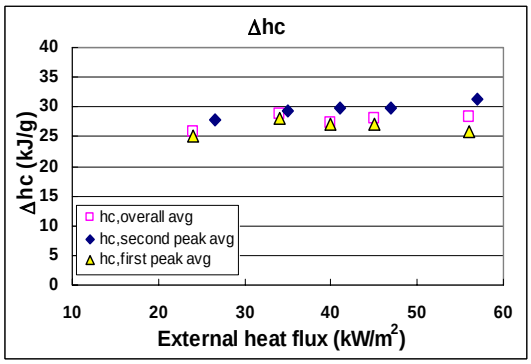

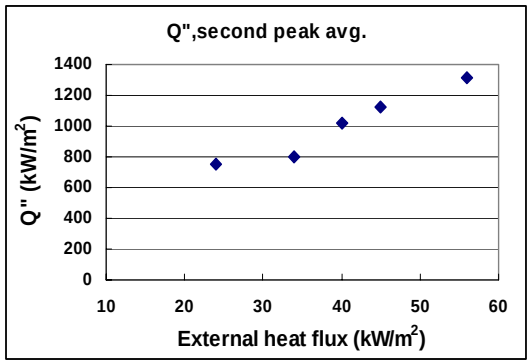

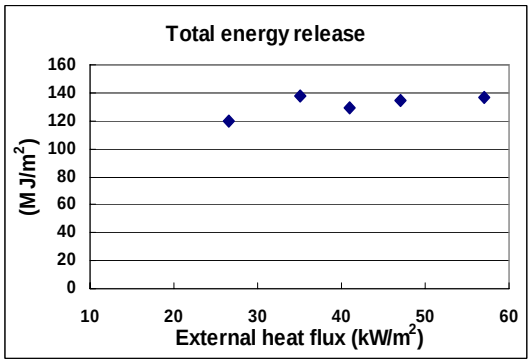

Heat Flux (kW/m^2)	Ignition Time (s)	Char/Mass (g)
57	52	0.3/20.8
47	86	0.4/20.8
41	149	0.4/20.7
35	139	0.3/20.7
26.5	219	0.4/20.9

Nylon+2%Clay under different external heat flux
(Thickness 3.2 mm, Diameter 75 mm)

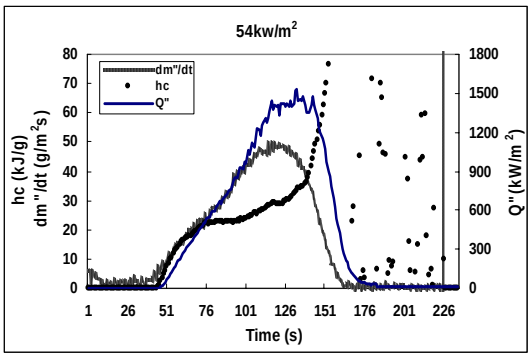

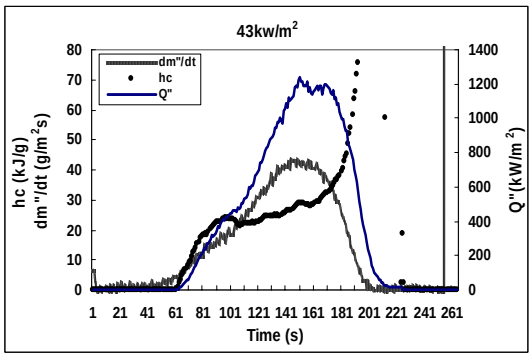

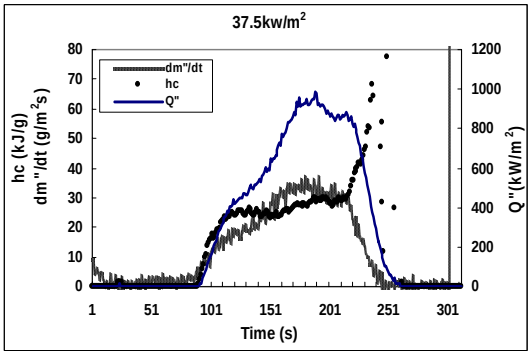

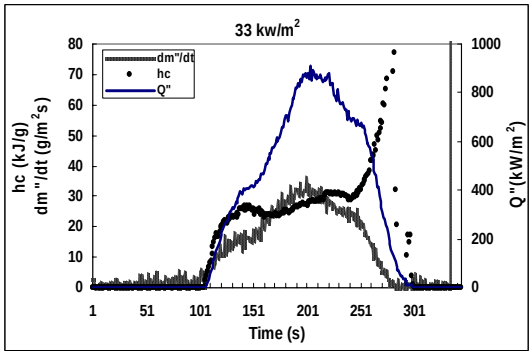

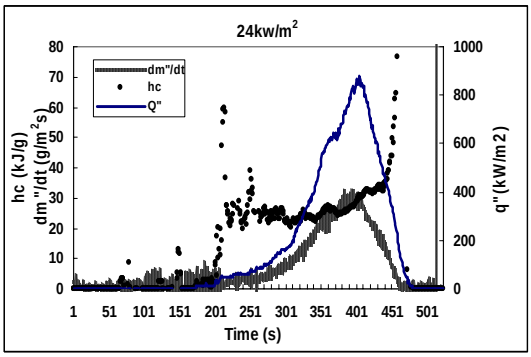

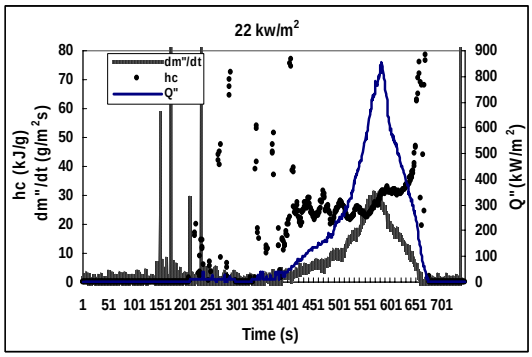

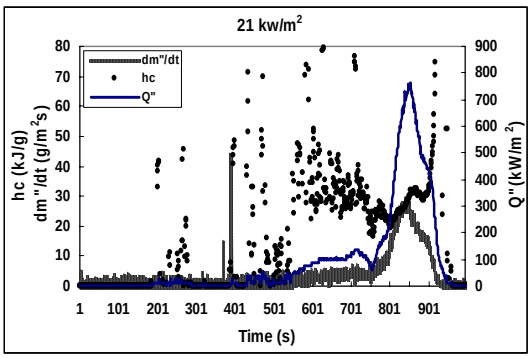

Summary of 3.2 mm Nylon＋2％Clay

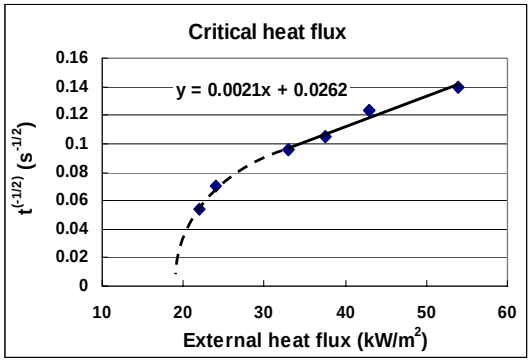

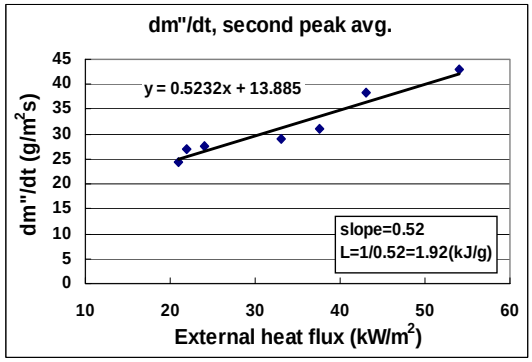

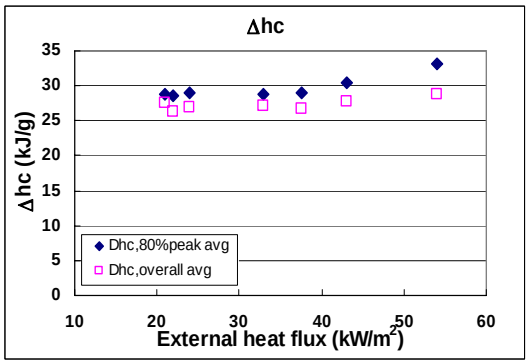

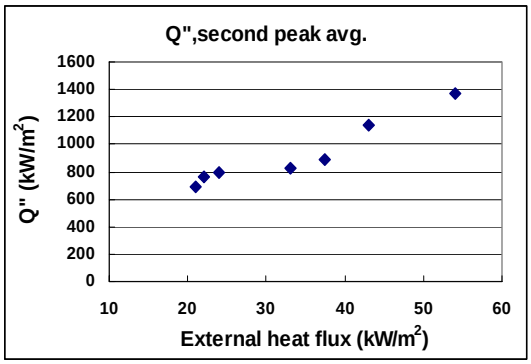

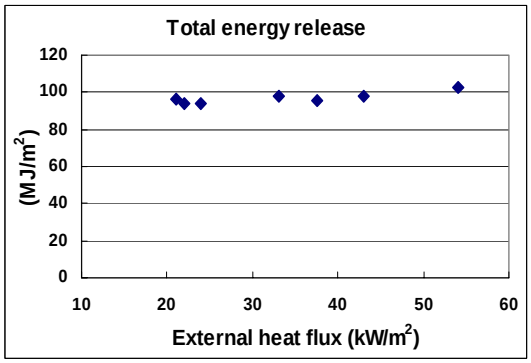

Heat Flux (kW/m^2)	Ignition Time (s)	Char/Mass (g)
54	51	0.1/15.6
43	66	0.3/15.7
37.5	91	0.3/15.5
33	109	0.3/15.9
24	203	0.3/15.4
22	338	0.3/15.7
21	568	0.4/15.5

Nylon+2%Clay under different external heat flux
(Thickness 1.6 mm, Diameter 76 mm)

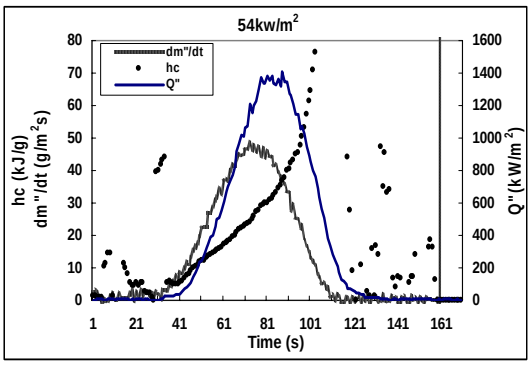

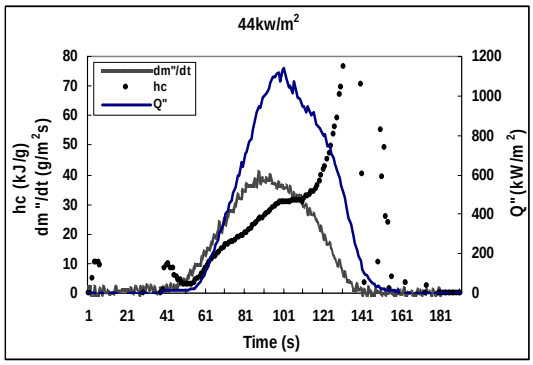

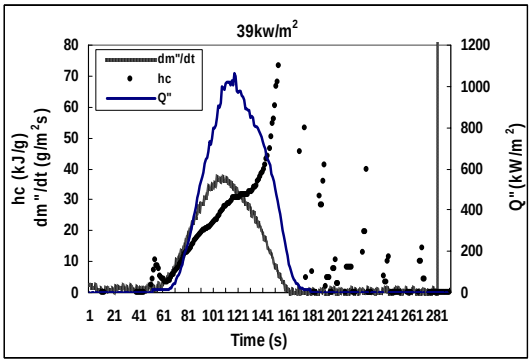

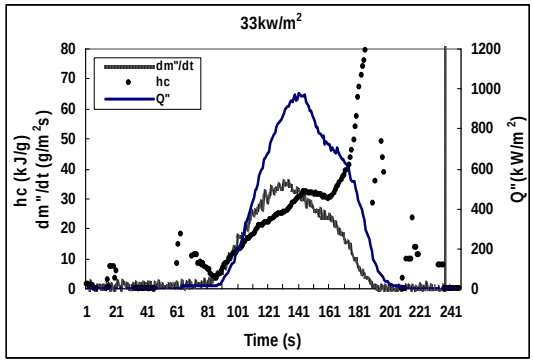

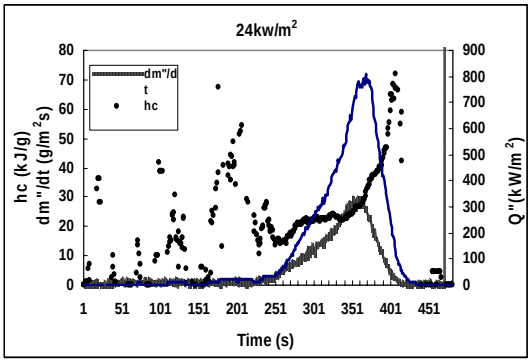

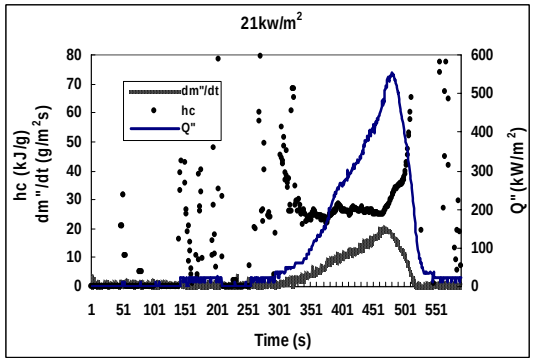

Summary of 1.6 mm Nylon＋2％Clay

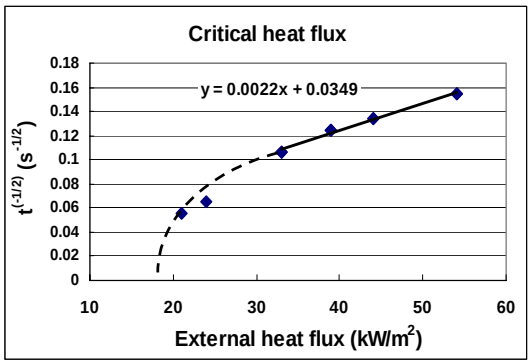

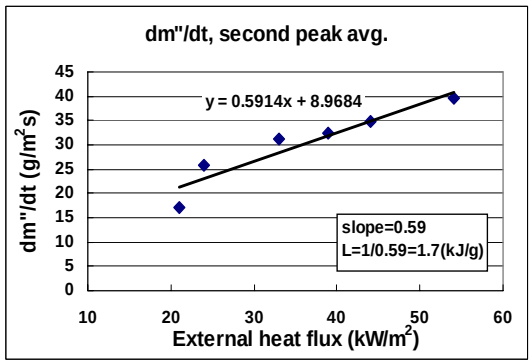

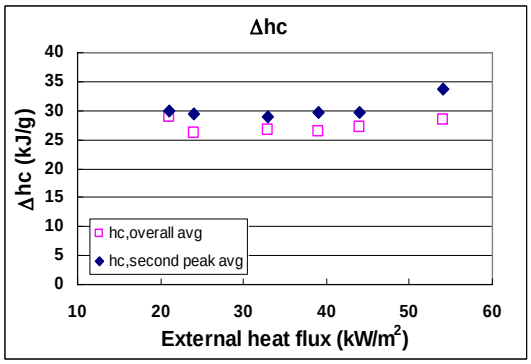

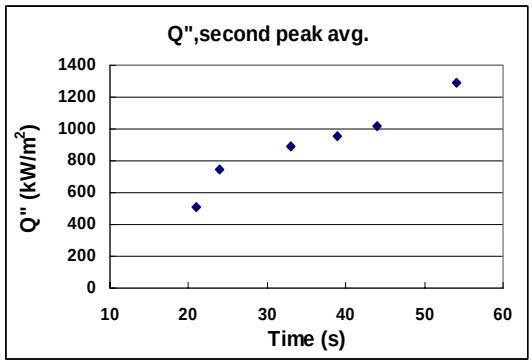

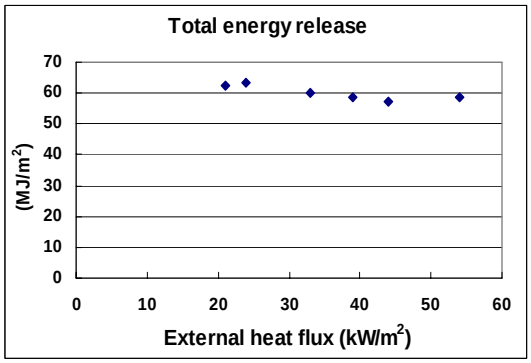

Heat Flux (kW/m^2)	Ignition Time (s)	Char/Mass (g)
54	42	0.1/9.4
44	56	0.1/9.5
39	65	0.1/9.9
33	88	0.1/10.2
24	236	0.3/11.1
21	324	0.3/9.7

Nylon+5%Clay under different external heat flux
(Thickness 8 mm, Diameter 74 mm)

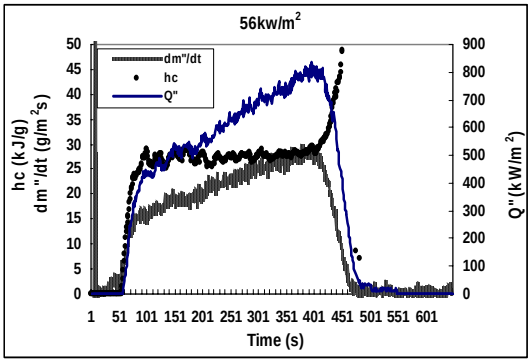

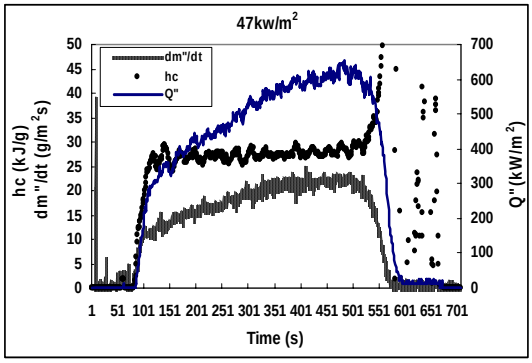

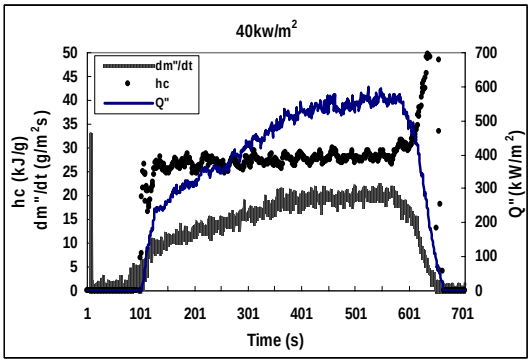

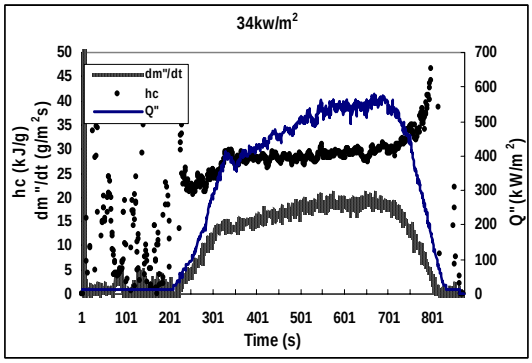

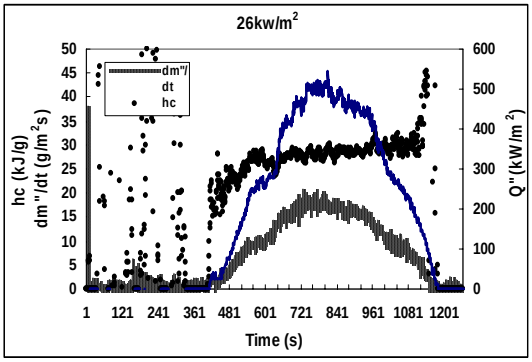

Summary of 8 mm Nylon＋5％Clay

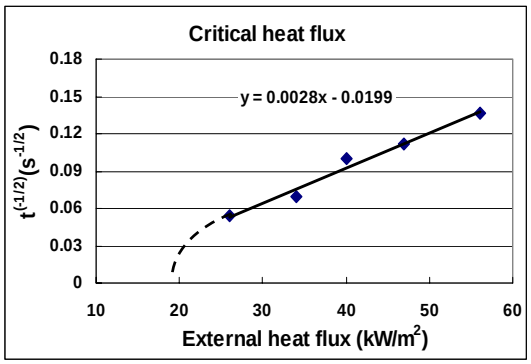

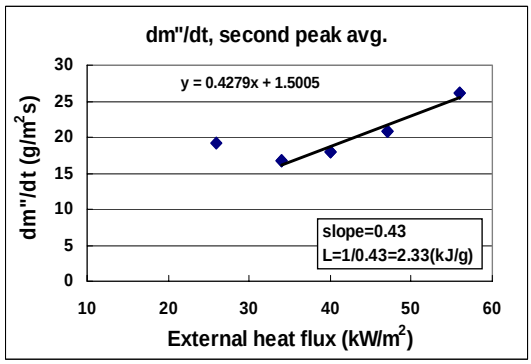

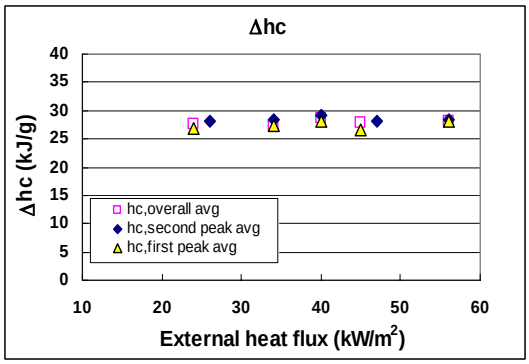

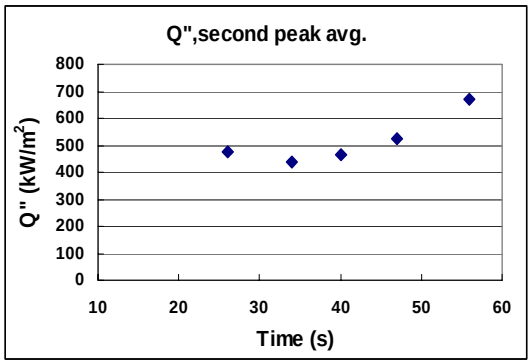

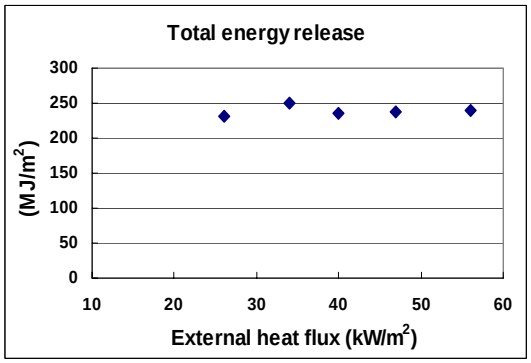

Heat Flux (kW/m^2)	Ignition Time (s)	Char/Mass (g)
56	54	1.6/38.2
47	80	1.7/38.2
40	100	1.7/38.2
34	211	1.9/38.3
26	339	1.8/38

Nylon+5%Clay under different external heat flux
(Thickness 4 mm, Diameter 74 mm)

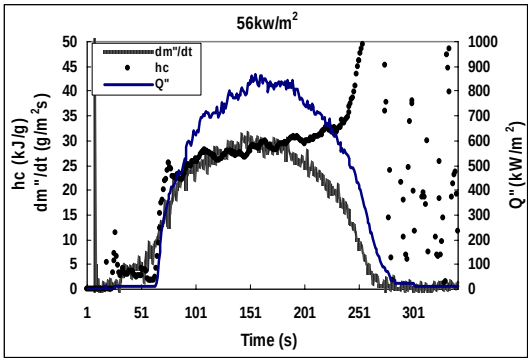

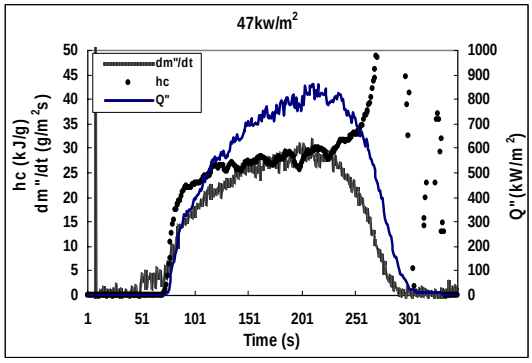

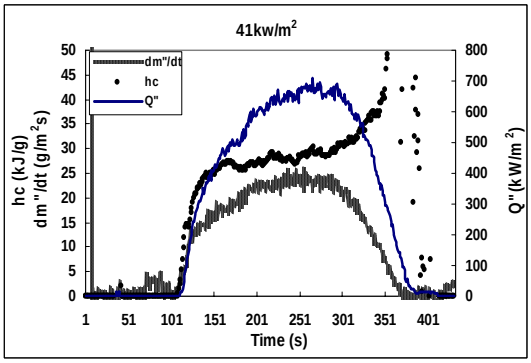

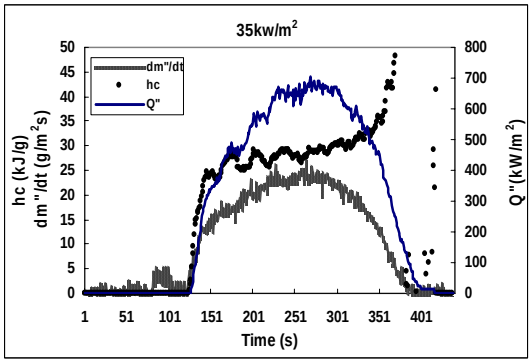

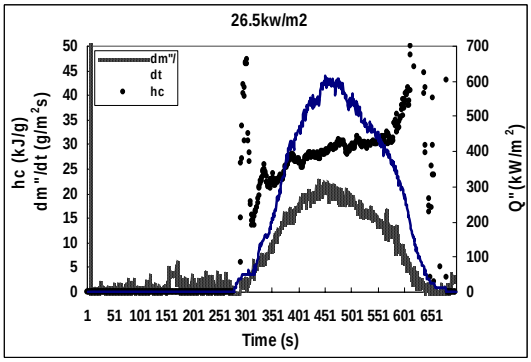

Summary of 4 mm Nylon＋5％Clay

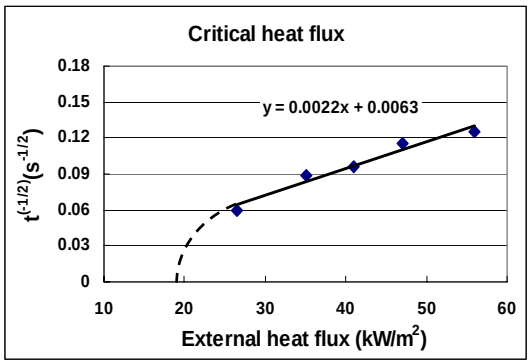

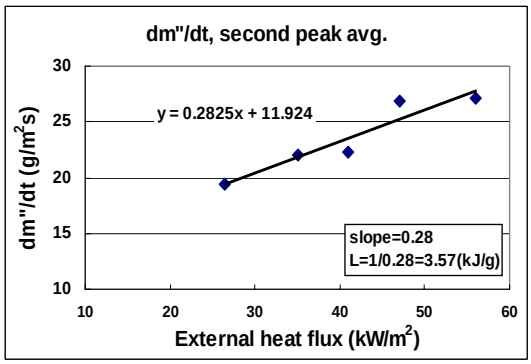

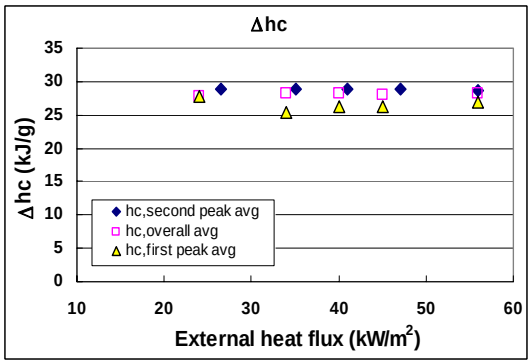

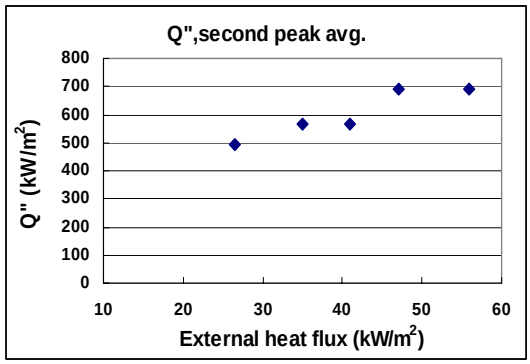

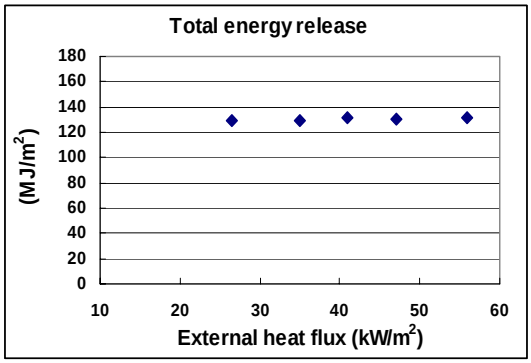

Heat Flux (kW/m^2)	Ignition Time (s)	Char/Mass (g)
56	64	0.8/20.7
47	75	0.9/20.6
41	109	0.9/20.7
35	127	0.9/20.6
26.5	279	1/20.8

Nylon+5%Clay under different external heat flux
(Thickness 3.2 mm, Diameter 75 mm)

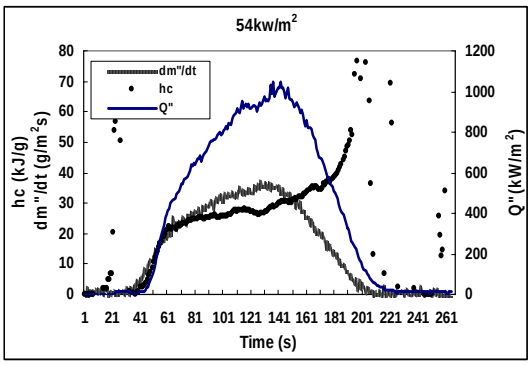

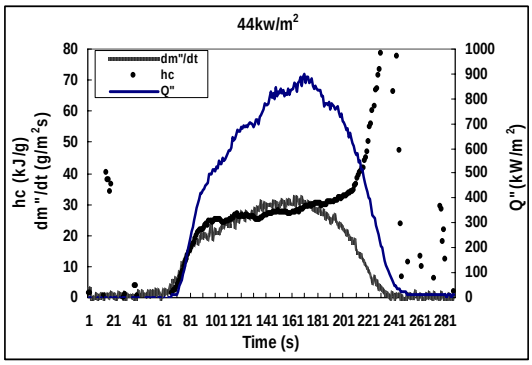

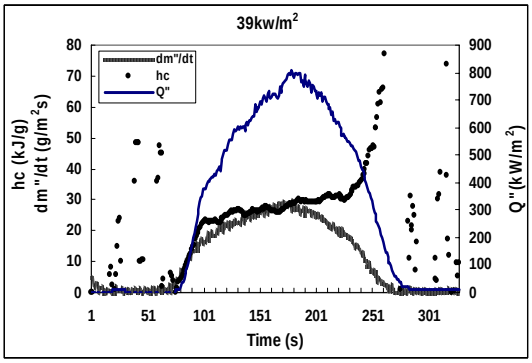

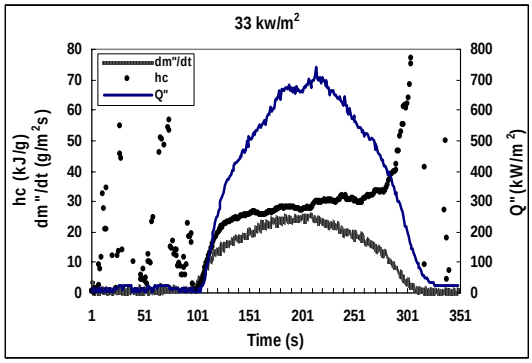

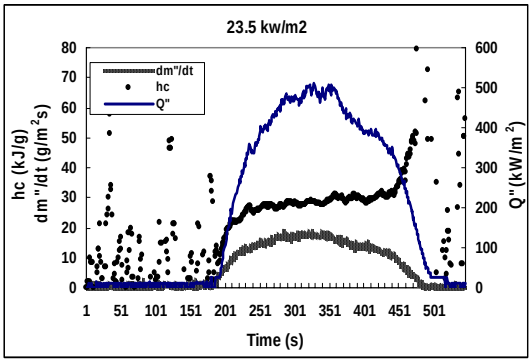

Summary of 3.2 mm Nylon＋5％Clay

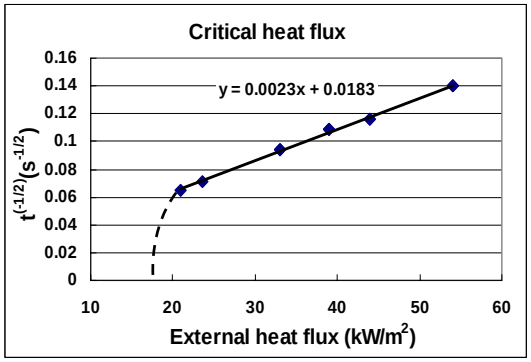

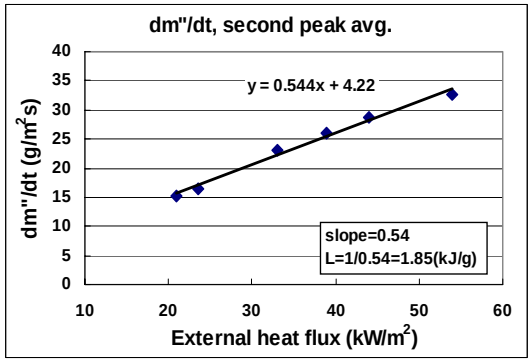

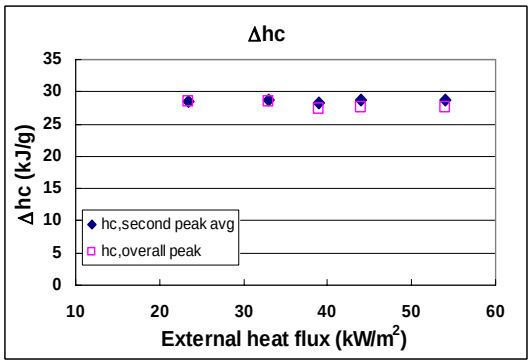

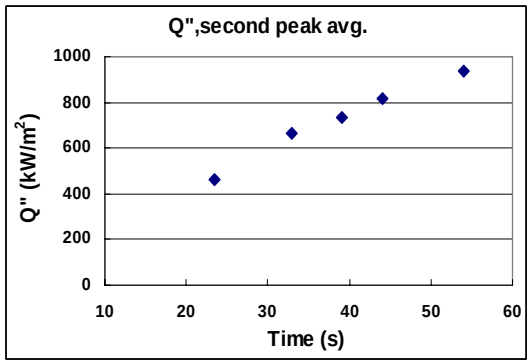

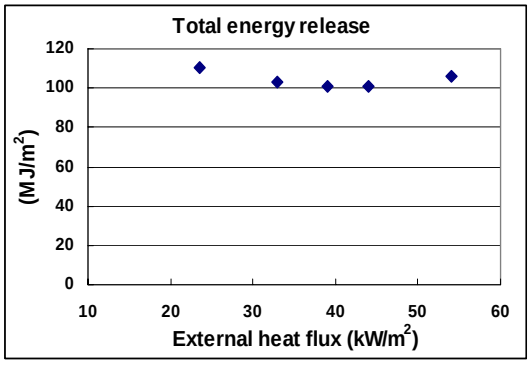

Heat Flux (kW/m^2)	Ignition Time (s)	Char/Mass (g)
54	51	0.7/17.3
44	74	0.8/16.7
39	84	0.8/16.7
33	112	0.7/16.5
23.5	197	0.8/17.7
21	239	0.8/16.5

Nylon+5%Clay under different external heat flux
(Thickness 1.6 mm, Diameter 76 mm)

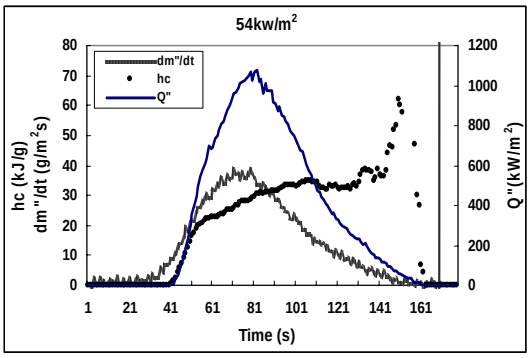

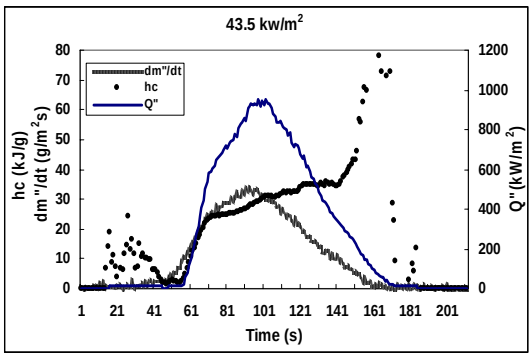

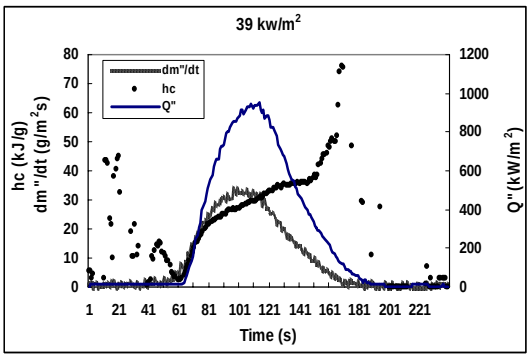

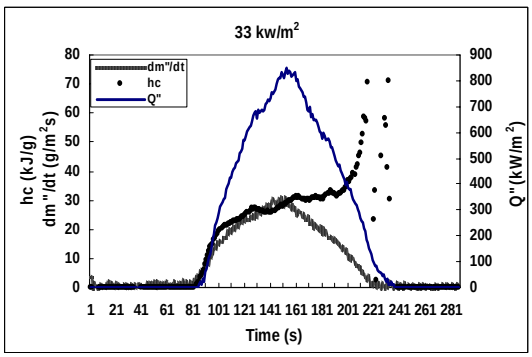

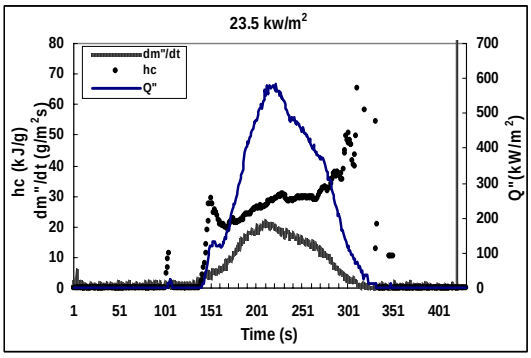

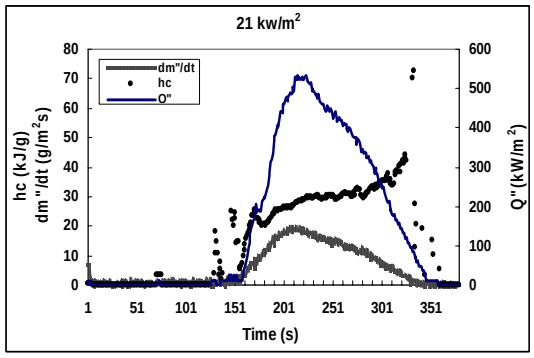

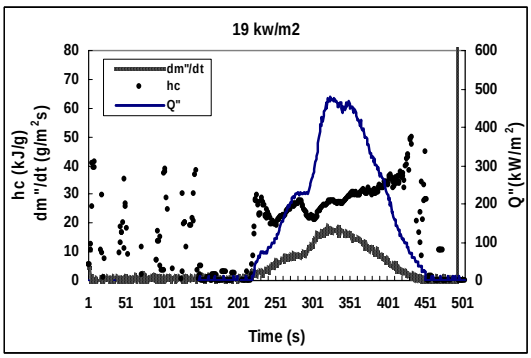

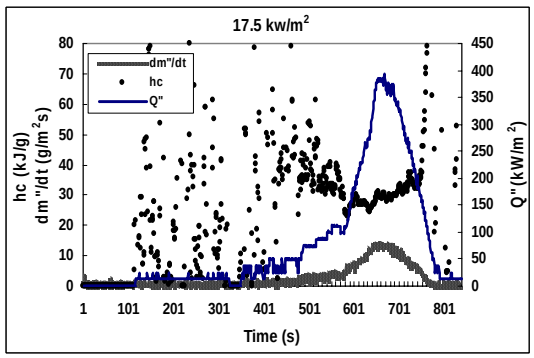

Summary of 1.6 mm Nylon＋5％Clay

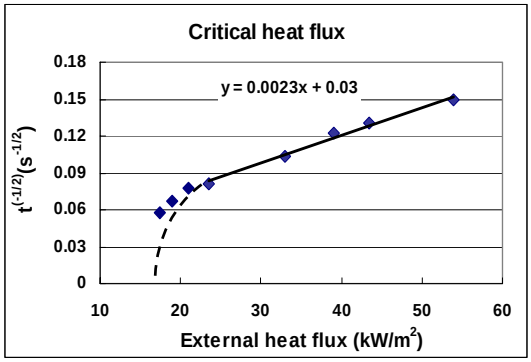

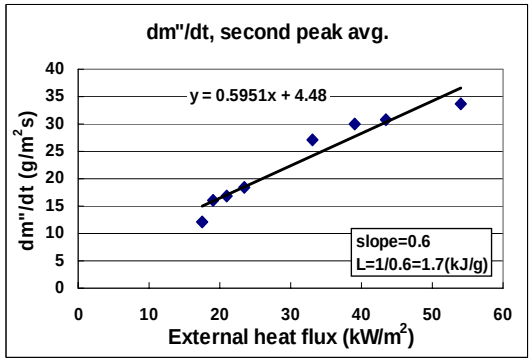

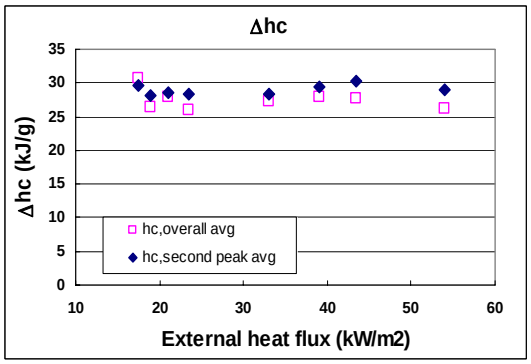

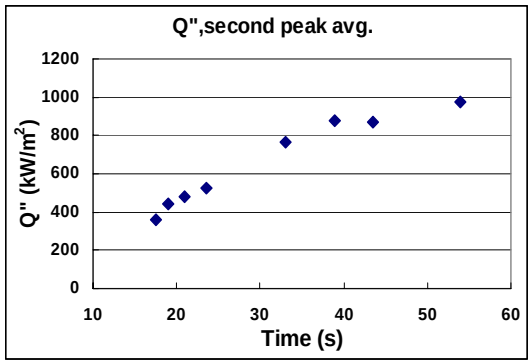

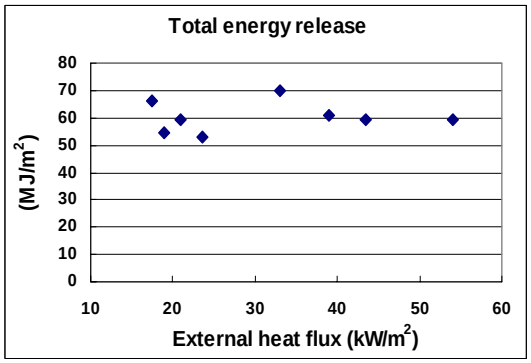

Heat Flux (kW/m^2)	Ignition Time (s)	Char/Mass (g)
54	45	0.4/9.9
43.5	59	0.5/10
39	67	0.5/10.2
33	93	0.6/12
23.5	152	0.5/10
21	166	0.5/10
19	223	0.5/10
17.5	303	0.5/10.1

24 mm samples under 50 kW/m^2 external heat flux (Diameter 74 mm)

24 mm samples were made by 3 pieces of 8 mm samples, overlapped. The sample surface was smoothed by a sand paper in order to minimize the gap between the connection of two surface. If they were not perfectly contacted, it is still ok. During the test, the sample will be melted by the heat. The soft sample can seal the gap itself.

24 mm Nylon under 50 kW/m^2 external heat flux

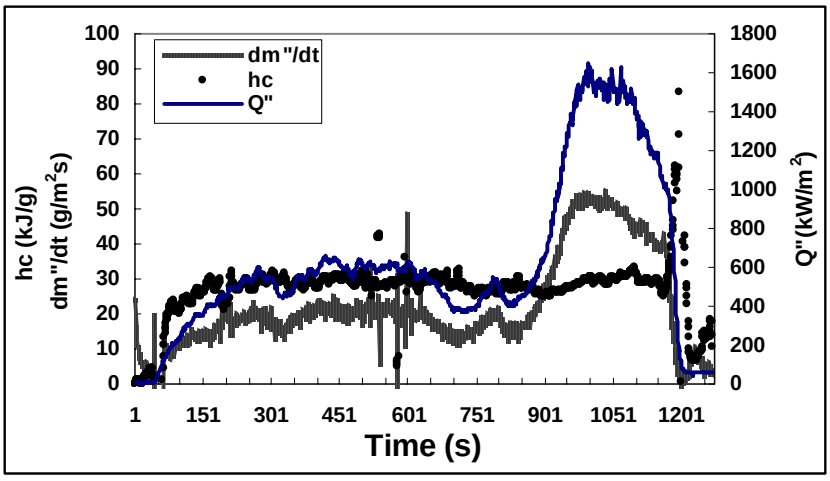

24 mm Nylon+2%Clay under 50 kW/m^2 external heat flux

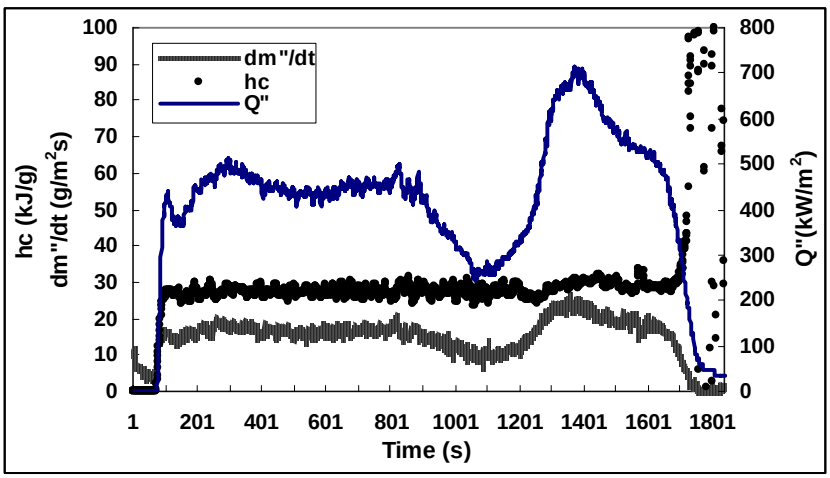

24 mm Nylon+5%Clay under 50 kW/m^2 external heat flux

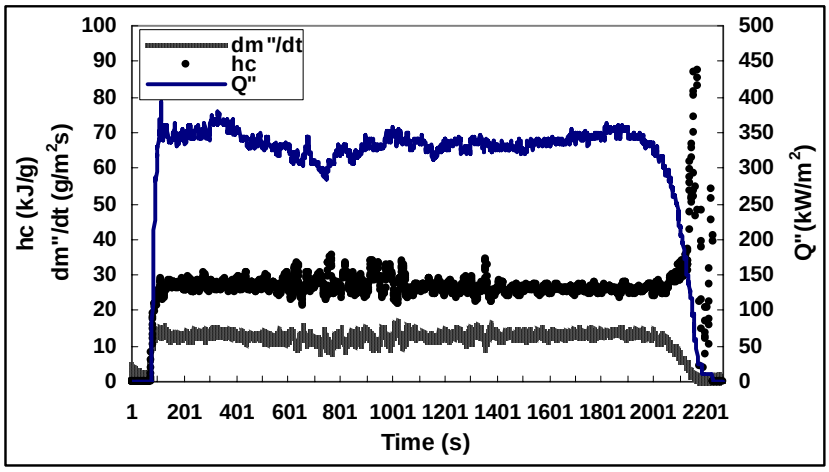

Sample	Ignition Time (s)	Char/Mass (g)
Nylon	47	0/113.8
Nylon+2%Clay	57	7/114.4
Nylon+5%Clay	75	8.6/114.4

Appendix E Experimental Results of convective heat transfer coefficient

Properties:

- **Air**:

T_S =500 ° C $T_o = 25$ºC $T = \frac{T_S + T_o}{2} = 263$ºC=536 K

So use air properties @ 550 K

$\rho = 0.6329 kg/m^2$ $\nu = 45.57 \times 10^{-6} m^2/s$

$\Pr = 0.683$ $k = 43.9 \times 10^{-3} w/mK$

- **Aluminum plate**:

Area= $7.7cm \times 7.7cm$

Mass=7.4 g

c_p=0.896 *J/g ºC*

- **Kaowool blanket**:

Conductivity=0.15 *W/mºC*

Total thickness=1/2 inch=0.0127m

- **Exhaust duct**

Dia. =0.1106m

Energy conservation

With considering the conductive heat loss from the back side (insulation) of the aluminum plate

$$\dot{m}'' c \frac{dT}{dt} = \alpha \dot{q}''_{ext} - \varepsilon\sigma(T^4 - T_o^4) - h(T - T_\infty) - k_{ins} \frac{T - T_{ins}}{\delta_{ins}}$$

Without conductive heat loss:

$$\dot{m}''c\frac{dT}{dt} = \alpha\dot{q}''_{ext} - \varepsilon\sigma(T^4 - T_o^4) - h(T - T_\infty)$$

✶ **Surface absorptivity** α

Energy conservation at initial status: $\dot{m}''c_p\frac{dT}{dt} = \alpha\dot{q}''_{ext}$

Read the initial slope from temperature-time curve, then calculate α from above equation.

Surface made:

Soot was added by a candle flame, and then painted by several layers of high temperature resistant paint. If the soot was deposited by a burner burning under the plate for one hour and a half, the soot will be thicker and even, the absorptivity is higher.

The following figures show the comparison of convective heat transfer coefficient under different exhaust fan speed.

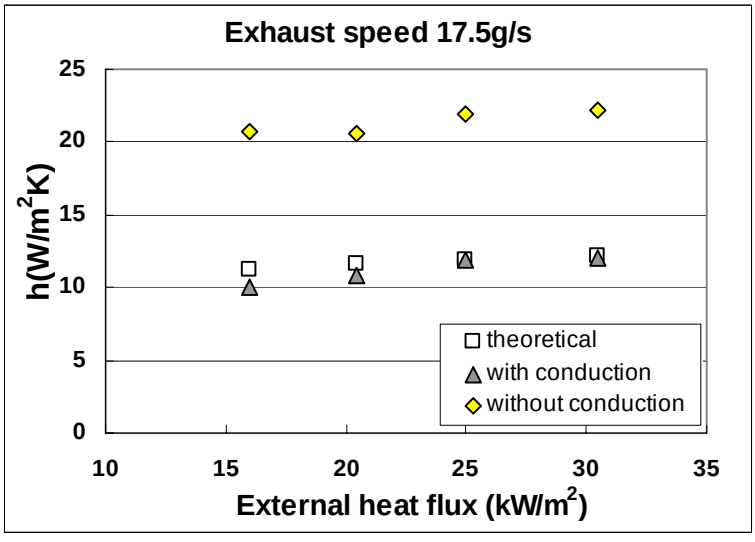

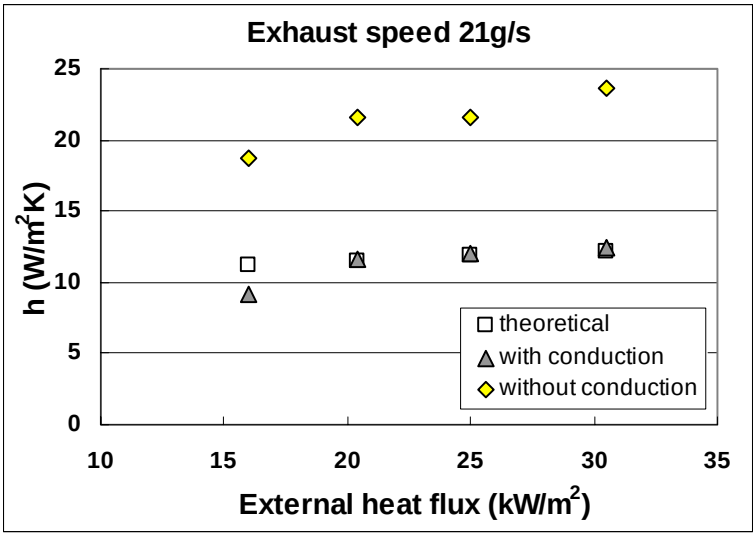
Exhaust speed 21g/s
25
20
15
10
5
0
h (W/m2K)
10
15
20
25
30
35
External heat flux (kW/m2)
theoretical
with conduction
without conduction

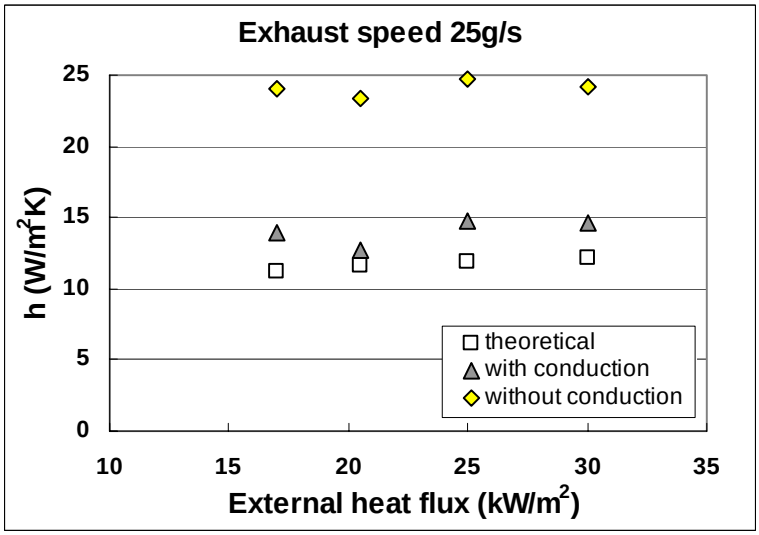
Exhaust speed 25g/s
25
20
15
10
5
0
h (W/m2K)
10
15
20
25
30
35
External heat flux (kW/m2)
theoretical
with conduction
without conduction